

Synthesis of Novel Unsymmetrical Zinc(II) Phthalocyanines for Photodynamic Therapy

DUAN Lei

**A Thesis Submitted in Partial Fulfillment
of the Requirements for the Degree of
Master of Philosophy
in
Chemistry**

©The Chinese University of Hong Kong

July 2005

The Chinese University of Hong Kong holds the copyright of this thesis. Any person(s) intending to use a part or whole of the materials in the thesis in a proposed publication must seek copyright release from the Dean of the Graduate School.



Abstract

This thesis reports the synthesis, spectroscopic characterization, and *in vitro* photodynamic activities of a series of unsymmetrical zinc(II) phthalocyanines, focusing on the amphiphilic analogues.

Chapter 1 gives an overview of unsymmetrical phthalocyanines including their general synthetic methods and applications. Special emphasis has been placed on amphiphilic and non-aggregated analogues and their applications as efficient photosensitizers for photodynamic therapy.

Chapter 2 reports a simplified procedure to prepare a series of unsymmetrical zinc(II) phthalocyanines. By using the phthalonitrile substituted with the bulky 3,4,5-tris(dodecyloxy)phenylmethoxy group in mixed cyclization with an excess of unsubstituted phthalonitrile or its halogenated derivatives, the desired “3+1” unsymmetrical phthalocyanines can be separated readily. This bulky group can then be removed to form the mono-hydroxy phthalocyanine. The preparation of these compounds and their spectroscopic properties are reported herein. The *in vitro* photodynamic activities of the amphiphilic mono-hydroxy zinc(II) phthalocyanine against human colorectal adenocarcinoma HT29 and hepatocarcinoma HepG2 are also described in this chapter.

Chapter 3 presents the synthesis, characterization, and photophysical properties of several phthalocyanines substituted with the

2-*N,N*-dimethylaminoethylsulfanyl group. The corresponding *N*-alkylated analogues have also been studied. The *in vitro* photodynamic activities of these phthalocyanines in Cremophor EL emulsions against several cell lines are also described in this chapter.

摘要

本論文報告一系列不對稱鋅(II)酞菁的合成、光譜表徵和離體光動力反應，其中重點介紹具有雙親性質的酞菁。

第一章綜述不對稱酞菁，包括它們的一般合成方法和應用。特別著重描述了具有雙親性質和不聚集性質的酞菁，以及它們在光動力學治療方面作為有效的光敏劑的應用。

第二章報告一種簡單化了的製備一系列不對稱鋅(II)酞菁的合成步驟。通過 3, 4, 5-三(十二烷氧基)苯基甲氧基取代的鄰苯二甲腈和過量的無取代鄰苯二甲腈的混合環化，得到的“3+1”不對稱酞菁很容易被分離。這種酞菁上的大基團繼而被脫離，生成單經基酞菁。這兩種酞菁的製備和光譜性質均報告在這裏。本章還描述了這種具有雙親性質的單經基酞菁對人體的結腸直腸腺癌細胞和肝癌細胞的離體光動力反應。

第三章介紹一些帶有 2-二甲替氨基乙硫基基團的酞菁的合成和光物理特性。同時，並研究了其對應的 *N*-烷基化的酞菁化合物。在此章節中，還描述了這些酞菁在臨床認可的表面活性劑 Cremophor EL 中對一些人體癌細胞的離體光動力反應。

Acknowledgement

Firstly, I would like to express my greatest thanks to my supervisor, Prof. Dennis K. P. Ng, for his continuous encouragement, support and help during the course of my work, and the preparation of my thesis and seminars.

My sincere thanks are also given to Dr. Wubiao Duan for his help and advice, Dr. Jiandong Huang in Fuzhou University and his group members for the HPLC analysis, and my groupmates, Gigi P. C. Lo, Ming Bai, Bill C. F. Choi, and Xuebing Leng, for their nice encouragement and help. Thanks are also given to all the technical staffs in the Department.

Finally, this research work was made possible by the generous financial support from the Hong Kong Research Grants Council and The Chinese University of Hong Kong.

DUAN Lei

Department of Chemistry

The Chinese University of Hong Kong

July 2005

Table of Contents

Abstract	i
Abstract (in Chinese)	iii
Acknowledgement	iv
Table of Contents	v
List of Figures	viii
List of Tables	xii
List of Schemes	xiii
Abbreviations	xvi

Chapter 1 Unsymmetrical Phthalocyanines – An Overview

1.1 Introduction	1
1.2 Synthesis of A ₃ B Phthalocyanines	7
1.2.1 Statistical Condensation	7
1.2.2 The Subphthalocyanine Approach	13
1.2.3 Synthesis on Polymer Support	16
1.3 Synthesis of A ₂ B ₂ Phthalocyanines	18
1.3.1 Preparation of Cross-Substituted Phthalocyanines (ABAB-type)	19
1.3.2 Preparation of “Adjacent” Phthalocyanines (AABB-type)	21

1.4	Objectives of This Thesis	24
1.5	References	25
Chapter 2 Synthesis, Characterization and <i>in vitro</i> Photodynamic		
Activities of Mono-Alkoxy and Hydroxy Zinc(II)		
Phthalocyanines		
2.1	Introduction	29
2.2	Preparation and Characterization of Unsymmetrical Zinc(II) Phthalocyanines Substituted with a 3,4,5- Tris(dodecyloxy)phenylmethoxy Group	30
2.3	Preparation and Characterization of Halogenated Unsymmetrical Zinc(II) Phthalocyanines	35
2.4	Preparation and Characterization of 2-Hydroxy Zinc(II) Phthalocyanine	44
2.5	Introduction of Photodynamic Therapy (PDT)	47
2.6	<i>In vitro</i> Photodynamic Activities of 2-Hydroxy Zinc(II) Phthalocyanine	50
2.7	Conclusion	52
2.8	Experimental Section	52
2.9	References	63

**Chapter 3 Synthesis, Characterization and *in vitro* Photodynamic
Activities of Phthalocyanines Containing *N,N*-Di-
methylaminoethylsulfanyl Substituents**

3.1	Introduction	66
3.2	Preparation and Characterization of Octasubstituted Phthalocyanines	67
3.3	Characterization of Disubstituted Amphiphilic Zinc(II) Phthalocyanines	74
3.4	<i>In vitro</i> Photodynamic Activities	80
3.5	Conclusion	83
3.6	References	90

List of Figures

Figure 1.1	Structures of A ₃ B-type and A ₂ B ₂ -type phthalocyanines.	7
Figure 2.1	HPLC profile of phthalocyanine 4 by monitoring the absorption at 669 nm.	32
Figure 2.2	¹ H NMR spectrum of phthalocyanine 4 in pyridine- <i>d</i> ₅ .	33
Figure 2.3	Electronic absorption spectra of 4 in THF in different concentrations. The plot of the absorbance of the Q-band at 669 nm versus the concentration of 4 is given in the inset.	34
Figure 2.4	HPLC profiles of the halogenated unsymmetrical phthalocyanines 17-19 .	39
Figure 2.5	UV-visible spectra of unsymmetrical phthalocyanines 17-19 in THF.	40
Figure 2.6	¹ H NMR spectrum of compound 18 in pyridine- <i>d</i> ₅ .	41
Figure 2.7	Molecular ion cluster of 19 shown in the MALDI-TOF mass spectrum (left). The corresponding simulated isotopic pattern is shown on the right.	42
Figure 2.8	¹ H NMR spectrum of compound 20 in DMSO- <i>d</i> ₆ .	45
Figure 2.9	UV-visible (---) and fluorescence (—) spectra of 2-hydroxy zinc(II) phthalocyanine (20) in THF.	46

- Figure 2.10** The MALDI-TOF mass spectrum of 2-hydroxy zinc(II) phthalocyanine (**20**). The simulated spectrum of the molecular ion is shown in the inset. 47
- Figure 2.11** General photophysical mechanisms involved in photodynamic therapy. 49
- Figure 2.12** Effect of compound **20** against HT29 colon cells in the absence (◆) and presence (■) of light. For the latter, the cells were illuminated with a red light ($\lambda > 610$ nm, 40 mW cm^{-2} , 48 J cm^{-2}). Data are expressed as mean \pm SD ($n = 3$). 51
- Figure 2.13** Effect of compound **20** against HepG2 human hepatocarcinoma cells in the absence (◆) and presence (■) of light. For the latter, the cells were illuminated with a red light ($\lambda > 610$ nm, 40 mW cm^{-2} , 48 J cm^{-2}). Data are expressed as mean \pm SD ($n = 3$). 51
- Figure 3.1** ^1H NMR spectrum of compound **22** in CDCl_3 . 69
- Figure 3.2** Electronic absorption spectra of **22** in CHCl_3 in different concentrations. The plot of the absorbance of the Q-band at 731 nm versus the concentration of **22** is given in the inset. 70
- Figure 3.3** ^1H NMR spectrum of compound **23** in CDCl_3 with a drop 72

of pyridine- d_5 . The asterisk indicates the signals of pyridine- d_5 .

- Figure 3.4** Electronic absorption spectra of **23** in DMF in different concentrations. The plot of the absorbance of the Q-band at 706 nm versus the concentration of **23** is given in the inset. 73
- Figure 3.5** ^1H NMR spectrum of **25** in DMSO- d_6 . 76
- Figure 3.6** Electronic absorption spectra of **25** in DMF in different concentrations. The plot of the absorbance of the Q-band at 680 nm versus the concentration of **25** is given in the inset. 77
- Figure 3.7** ^1H NMR spectrum of **27** in DMSO- d_6 . 78
- Figure 3.8** Effect of compound **23** against HepG2 human hepatocarcinoma cells in the absence (\blacklozenge) and presence (\blacksquare) of light. For the latter, the cells were illuminated with a red light ($\lambda > 610$ nm, 40 mW cm $^{-2}$, 48 J cm $^{-2}$). Data are expressed as mean \pm SD ($n = 1$). 81
- Figure 3.9** Effect of compound **24** against HepG2 human hepatocarcinoma cells in the absence (\blacklozenge) and presence (\blacksquare) of light. For the latter, the cells were illuminated with a red light ($\lambda > 610$ nm, 40 mW cm $^{-2}$, 48 J cm $^{-2}$). 81

Data are expressed as mean \pm SD ($n = 1$).

Figure 3.10 Effect of compound **25** against HepG2 human 82 hepatocarcinoma cells in the absence (\blacklozenge) and presence (\blacksquare) of light. For the latter, the cells were illuminated with a red light ($\lambda > 610$ nm, 40 mW cm⁻², 48 J cm⁻²).

Data are expressed as mean \pm SD ($n = 1$).

List of Tables

- Table 3.1** Electronic absorption and photophysical data for zinc(II) 79
phthalocyanines **23-27** in DMF.
- Table 3.2** Comparison of the IC_{50} values of zinc(II) 83
phthalocyanines **23-27** against HepG2, HT29 and T84.

List of Schemes

Scheme 1.1	Statistical condensation of two different phthalonitriles to give a mixture of six products.	8
Scheme 1.2	Synthesis of zinc diphenylmethoxy phthalocyanine.	9
Scheme 1.3	Synthesis of <i>bis</i> vinylene-phenylene-bridged <i>bis</i> -phthalocyanine 1.19 .	10
Scheme 1.4	Preparation of dihydroxy zinc phthalocyanine 1.12 .	11
Scheme 1.5	Synthesis of nickel unsymmetrical phthalocyanine having a crown ether moiety for the formation of self-assembled supramolecular dimer.	12
Scheme 1.6	Synthesis of a chloro-subphthalocyanine.	13
Scheme 1.7	Selective synthesis of A ₃ B phthalocyanines via subphthalocyanines.	14
Scheme 1.8	Synthesis of an A ₃ B phthalocyanine on polymeric support.	16
Scheme 1.9	Synthesis of an A ₃ B phthalocyanine on silica gel support.	17
Scheme 1.10	Selective synthesis of ABAB-type phthalocyanines via 1,3,3-trichloroisindoline.	19
Scheme 1.11	Synthesis of a ladder-type trimer 1.33 based on	21

*bis*diene- and *bis*dienophile-type phthalocyanines.

Scheme 1.12	Preparation of zinc “adjacent” AABB phthalocyanines including “half-Pc” intermediate.	22
Scheme 1.13	Synthesis of adjacently-fused donor-acceptor phthalocyanine.	22
Scheme 1.14	Preparation of a cobalt AABB phthalocyanine using a biphenyl-linked <i>bis</i> (phthalonitrile).	24
Scheme 2.1	Synthesis of phthalonitrile 3 bearing a bulky 3,4,5-tris(dodecyloxy)phenylmethoxy group.	30
Scheme 2.2	Mixed cyclization between phthalonitrile 3 and the unsubstituted phthalonitrile.	31
Scheme 2.3	Preparation of 4,5-dichlorophthalonitrile (10).	36
Scheme 2.4	Preparation of 4,5-dibromophthalonitrile (13).	37
Scheme 2.5	Preparation of 4,5-diiodophthalonitrile (16).	37
Scheme 2.6	Preparation of halogenated unsymmetrical phthalocyanines 17-19 .	38
Scheme 2.7	Mixed cyclization of 3 and tetrafluorophthalonitrile.	43
Scheme 2.8	Preparation of 2-hydroxy zinc(II) phthalocyanine (20).	44
Scheme 3.1	Preparation of 4,5- <i>bis</i> -(2-dimethylaminoethylsulfanyl)-phthalonitrile (21).	67
Scheme 3.2	Synthesis of octakis(2-dimethylaminoethylsulfanyl)-	68

phthalocyanine (**22**).

Scheme 3.3 Synthesis of octakis(2-dimethylaminoethylsulfanyl) 71

zinc(II) phthalocyanine (**23**).

Scheme 3.4 Synthesis of octacationic phthalocyanine **24**. 74

Abbreviations

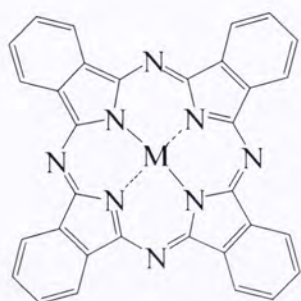
δ	Chemical shift
ε	Molar absorptivity
Φ_{Δ}	Singlet oxygen quantum yield
Φ_f	Fluorescence quantum yield
λ_{em}	Emission maximum
λ_{max}	Absorption maximum
ca.	Coarse approximation
$CDCl_3$	Deuterated chloroform
conc.	Concentration
d	Doublet
DBU	1,8-diazabicyclo[5.4.0]undec-7-ene
dd	Doublet of doublet
DMAE	<i>N,N</i> -Dimethylaminoethanol
DMF	<i>N,N</i> -Dimethylformamide
DMSO	Dimethylsulfoxide
h	Hour
HPLC	High performance liquid chromatography
m	Multiplet
NMR	Nuclear magnetic resonance
<i>n</i> -Bu	<i>n</i> -Butyl group

<i>n</i> -Pr	<i>n</i> -Propanyl group
ppm	Part per million
s	Singlet
t	Triplet
TEA	Triethylamine
THF	Tetrahydrofuran
TLC	Thin layer chromatography
UV	Ultraviolet
Vis	Visible

Chapter 1 Unsymmetrical Phthalocyanines – An Overview

1.1 Introduction

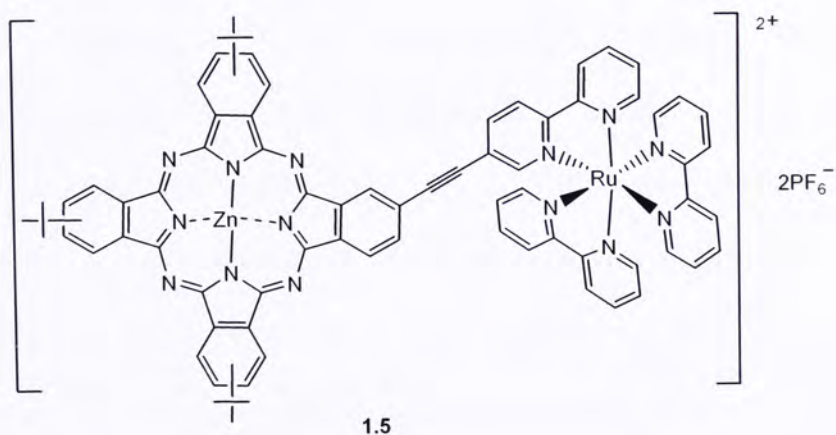
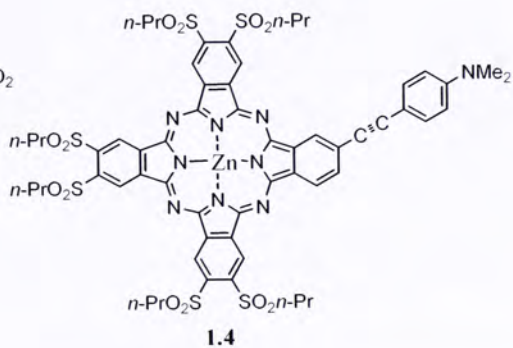
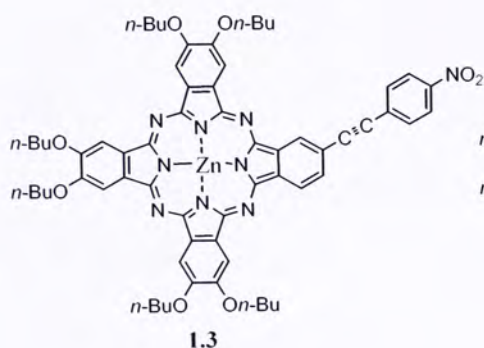
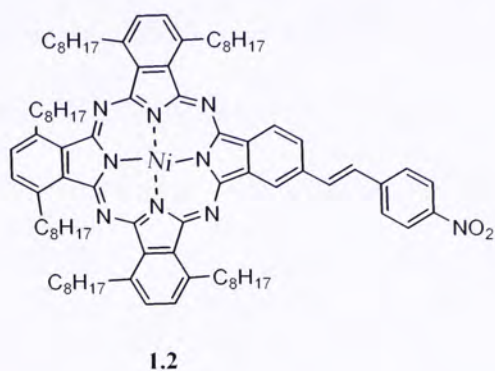
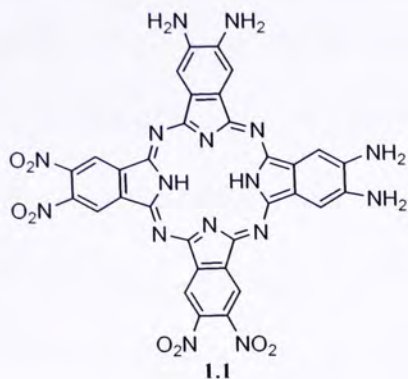
Phthalocyanines contain a highly conjugated two-dimensional π system. They absorb strongly in the red visible region, giving a characteristic greenish blue color. The compounds are thermally and chemically stable. Because of the intriguing electronic and optical properties, phthalocyanines are versatile functional dyes showing a wide range of applications in various disciplines.¹ To name a few, they can be used as photoconductors, optical recording materials, and sensors. They can also be used as catalysis, for example, in the oxidative degradation of pollutants. Apart from these applications, they are promising photosensitizers in photodynamic therapy in the treatment of cancer and age-related macular degeneration.



M = H₂ or various metals

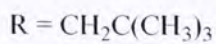
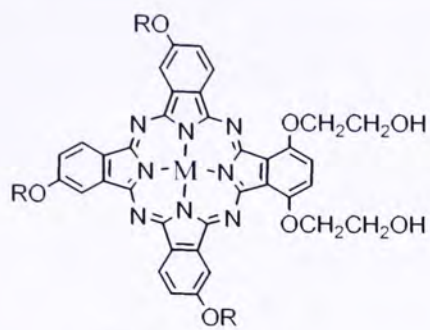
Numerous studies have been carried out to modify these macrocyclic compounds with a view to tailoring their properties for different applications.

Since the compounds are usually prepared by tetramerization of phthalonitriles, unsubstituted, and tetra- and octa-substituted phthalocyanines are most common. However, for some of the applications, unsymmetric phthalocyanines are desirable candidates. For example, push-pull non-centrosymmetric phthalocyanines substituted with suitable donor and acceptor groups can exhibit large second-order nonlinear optical responses,² and are therefore potentially useful for various optoelectronic devices. Compounds **1.1-1.4** are some of the examples which have been reported recently. The non-linear optical characteristic of compound **1.1** has been calculated via perturbation theory and the PPP model Hamiltonian to give a β_{vec} value of $165 \times 10^{-30} \text{ cm}^5 \cdot \text{esu}^{-1}$ and a dipole moment of 19.6 D.^{2a} Compounds **1.2-1.4** show quite high permanent dipole moments and dipolar off-resonant $\beta_{\text{v}}(0)$ coefficients, which have been obtained from capacitance measurements in chloroform solutions by a classical Guggenheim methods.³ Compound **1.2** shows a $\mu \cdot \beta_{\text{v}}(0)$ value of $511 \times 10^{-48} \text{ esu}$ and a dipole moment of 12.6 D.^{2b} The corresponding values for compound **1.3** and **1.4** are $220 \times 10^{-30} \text{ esu}$ and 39 D.^{2c} The unsymmetrical phthalocyanine **1.5** having a *tris*(bipyridyl) ruthenium(II) group has also been prepared. The compound exhibits special photophysical properties due to the electron and/or energy transfer between the two subunits. Excitation of ZnPc leads to faster intersystem crossing kinetics compared with the zinc(II) phthalocyanine reference, while photoexcited $[\text{Ru}(\text{bpy})_3]^{2+}$ undergoes a rapid and efficient transduction of triplet excited-state energy to the phthalocyanine.⁴

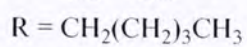
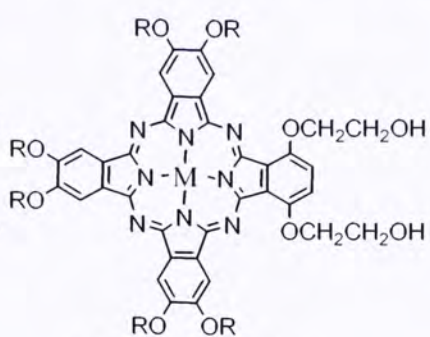


Symmetrical amphiphilic phthalocyanines are also excellent candidates to form well-ordered films by the Langmuir-Blodgett (LB) technique.⁵ Compounds **1.6-1.8** are some examples for this application. Amphiphilic

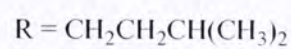
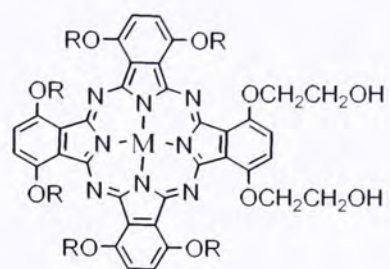
phthalocyanines are also promising photosensitizers for photodynamic therapy. It is believed that the amphiphilic character can facilitate the cellular uptake and therefore the photodynamic activity.⁶ For example, compounds **1.9-1.11** have been found to behave as good photosensitizers in photodynamic activities. An additional remarkable feature of unsymmetrical phthalocyanines is their ability to form a wide range of condensed phases with controlled molecular architectures, such as liquid crystals and other self-organized supermolecules.^{7, 8} Compound **1.12** and its dimeric **1.13** and trimeric **1.14** derivatives display birefringent textures which are consistent with a hexagonal columnar mesophase over a very wide temperature range (between 100 °C and their decomposition temperatures >300 °C).⁷ Compound **1.15** has a supramolecular structure in which two unsymmetrical phthalocyanines having a dibenzo-24-crown-8 unit are linked by a secondary dialkylammonium cation, such as dibenzylammonium (DBA⁺) ions. These two components assemble in solution, forming stable hydrogen-bonded complexes with a pseudorotaxane geometry. The stoichiometry of the complex is determined by the number of ammonium centers that are present in the threadlike component. Furthermore, dethreading can occur by adding a base to solution so that the two reversible states can be switched by controlling the pH.^{8b}



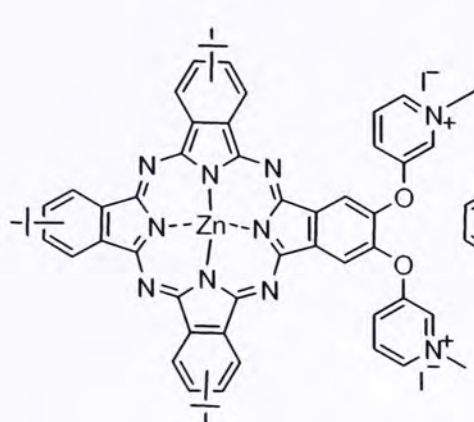
1.6



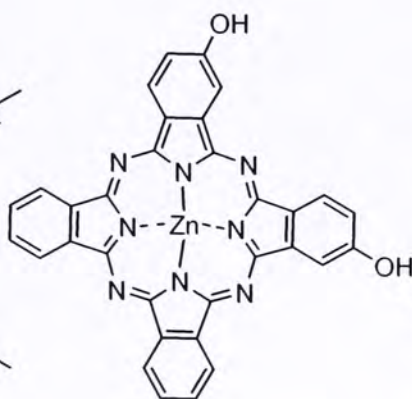
1.7



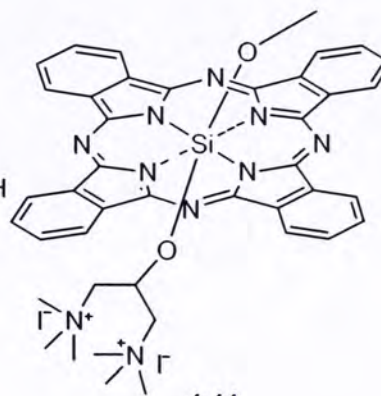
1.8



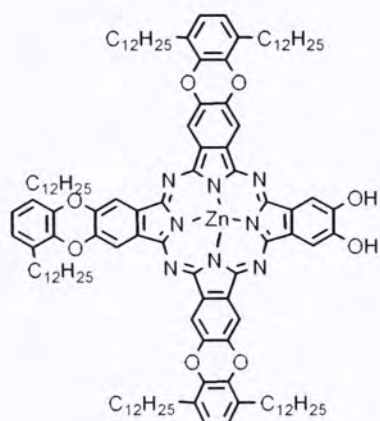
1.9



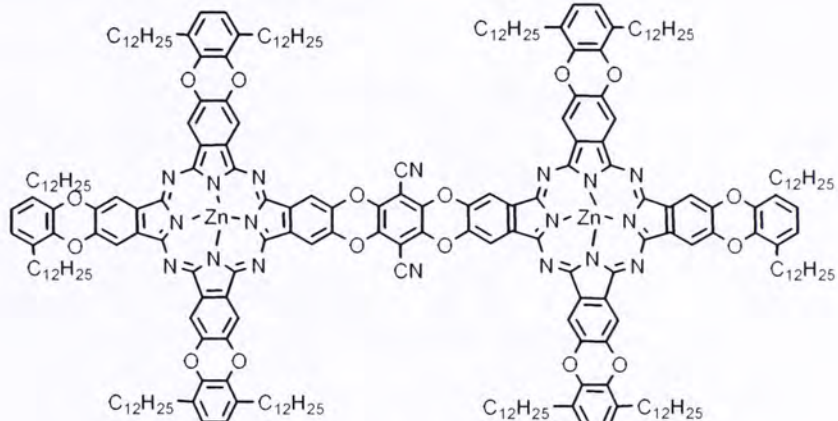
1.10



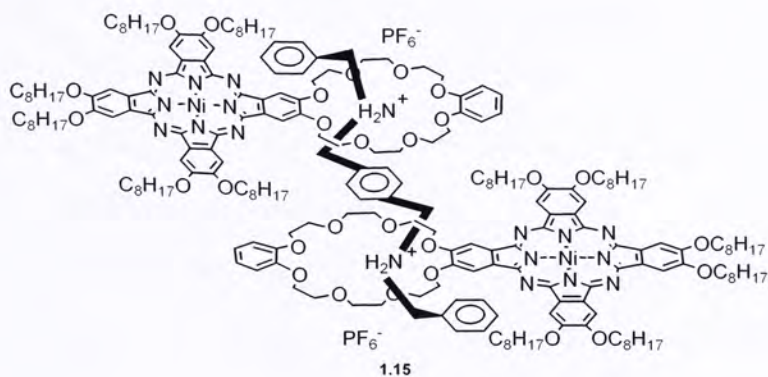
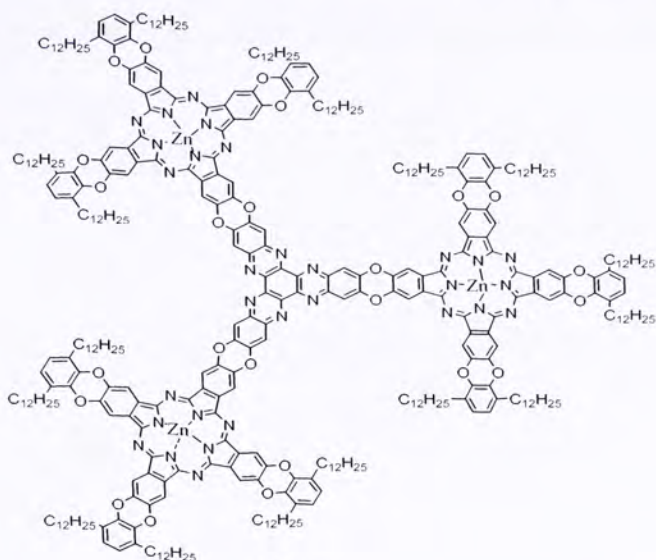
1.11



1.12



1.13



Despite the many potential applications of unsymmetric phthalocyanines, these compounds are difficult to prepare due to the difficulty in separating the many side products formed during mixed cyclization, and also the intrinsic aggregation behavior of these compounds which hinders the chromatographic purification processes. In this chapter, different synthetic pathways to

unsymmetrical phthalocyanines with different substitution patterns (Figure 1.1) will be reviewed. The properties of some of these unsymmetrical phthalocyanines will also be described briefly.

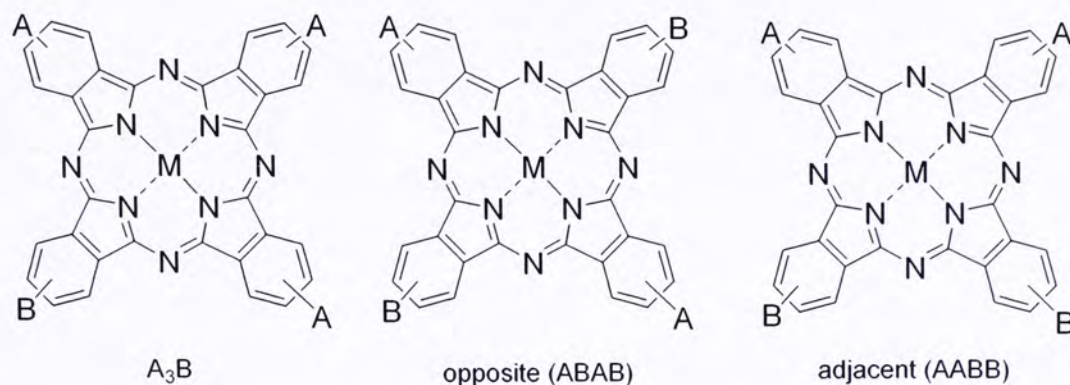
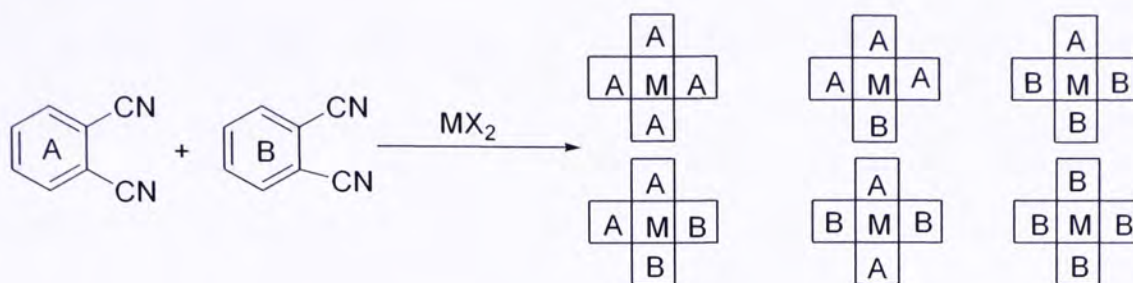


Figure 1.1. Structures of A_3B -type and A_2B_2 -type phthalocyanines.

1.2 Synthesis of A_3B Phthalocyanines

1.2.1 Statistical Condensation

This method is the most widely used strategy to prepare this kind of phthalocyanines. It is based on the statistical reaction of two differently substituted phthalonitriles or 1,3-diiminoisoindolines (A and B), affording in principle a mixture of six compounds as shown in Scheme 1.1. Extensive chromatographic purification is usually required to isolate the desired A_3B macrocycle from the statistical mixture.⁹

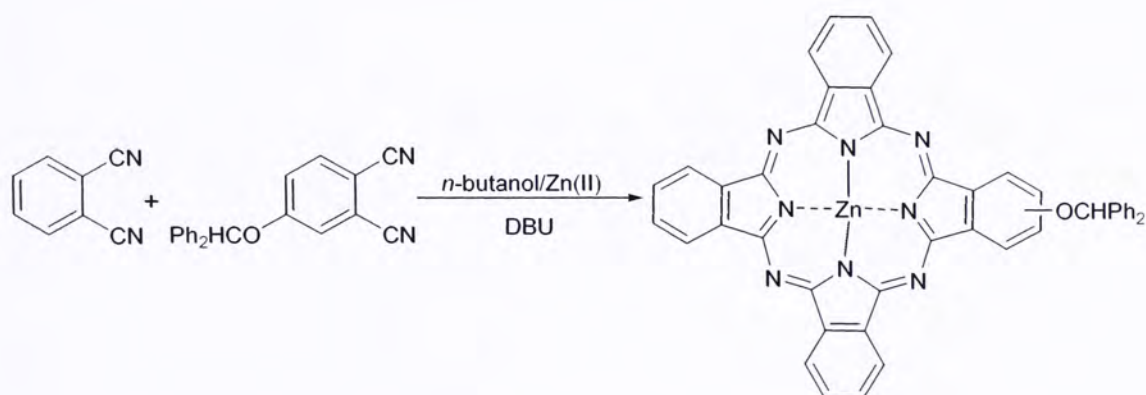


Scheme 1.1. Statistical condensation of two different phthalonitriles to give a mixture of six products.

This approach is a straightforward procedure. The stoichiometry can play an important role in the mixed cyclization. One of the reactants is usually employed in excess, typically in a 3:1 molar ratio, thus favoring the formation of the A_3B phthalocyanine. Under this condition, the theoretical yields of products are as follows: A_4 (33 %), A_3B (44 %), and other condensation products (23 %).¹⁰

The ratio of products obtained will also depend on the electronic character or the position of the substituents in the phthalonitrile precursors. For this reason, the proportion of the reactants may be changed by considering the relative reactivity of the precursors. Therefore, a higher molar ratio of A:B can be used if B is much more reactive than A, while the ratio can be inverted if B is less reactive than A (e.g. 1:5).¹¹ For example, Leznoff *et al.* performed the mixed cyclization of the unsubstituted phthalonitrile and 4-(diphenylmethoxy)-phthalonitrile in 1:1 ratio to give a mixture of all the statistical products.^{4b} By changing the ratio to 10:1, the A_3B phthalocyanine was isolated as the main product in 50% yield (Scheme 1.2). The diphenylmethoxy group of this

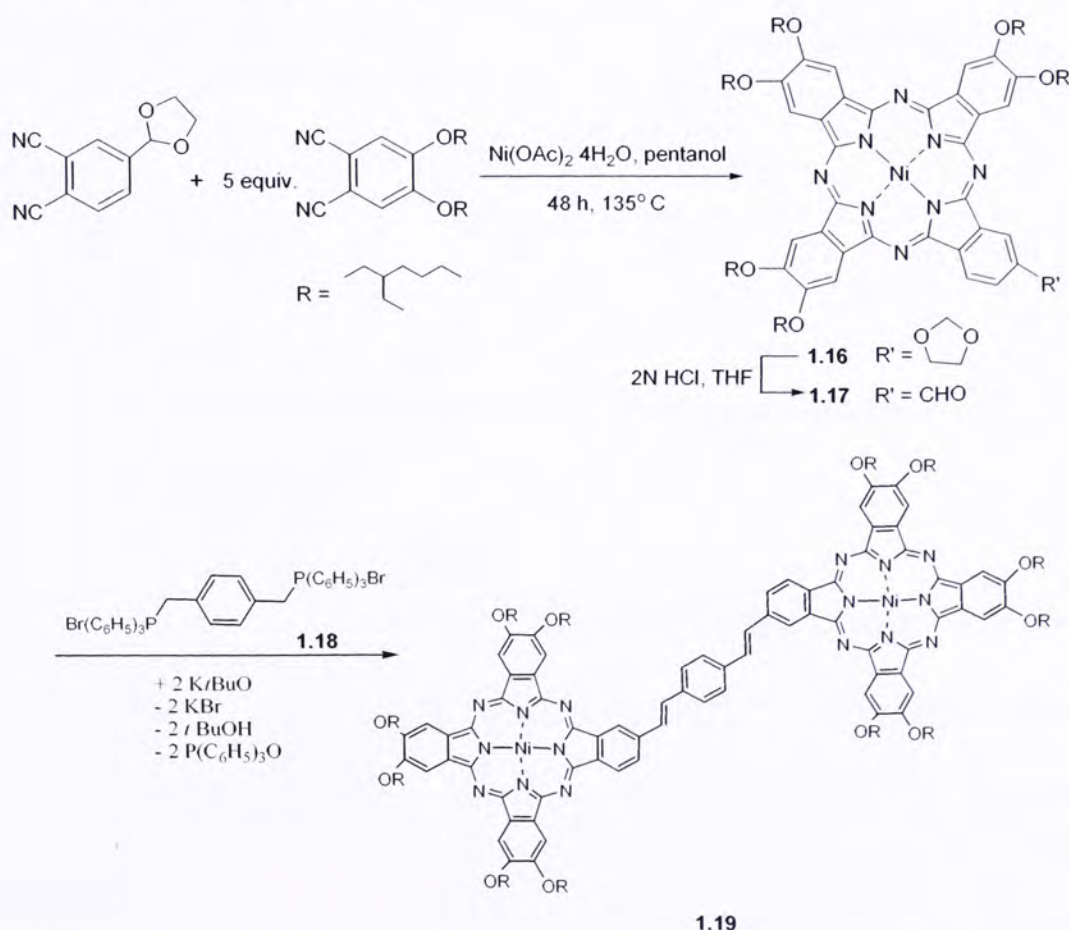
compound was then deprotected to give 2-hydroxyphthalocyanine, which exhibited a high *in vitro* photodynamic activity. Evaluated on the EMT-6 mammary tumor cell line, this compound gave LD₉₀ values of 0.40 and 0.15 J·cm⁻² after 1- and 24-h incubation with a fixed drug concentration of 1 μM, respectively, which were the light dose ($\lambda > 590$ nm, fluence rate 10 mW·cm⁻²) required to kill 90 % of cells. And its LC₉₀ values were 0.25 and 0.12 μM, which were the drug dose required to kill 90 % of cells after 1- and 24-h incubation with a fixed fluence of 2.4 J·cm⁻². It was the most active compared with di- and tri-hydroxy zinc phthalocyanines.



Scheme 1.2. Synthesis of zinc diphenylmethoxy phthalocyanine.

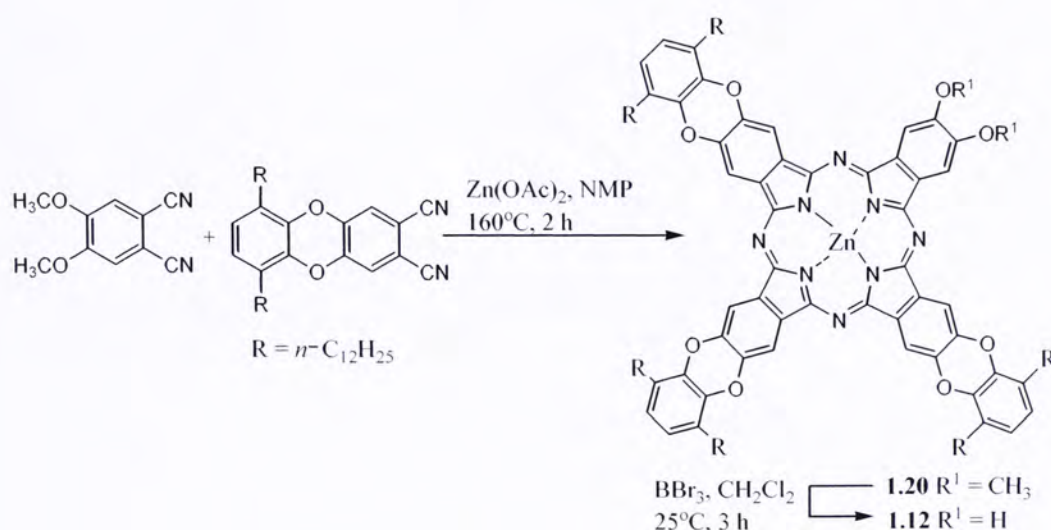
Steric interactions may also influence the composition of the products. Mixed condensation involving phthalonitriles bearing bulk groups in the 3,6-positions with other differently substituted phthalonitriles usually leads to a smaller number of products because the steric hindrance prevents these groups coming in close vicinity.¹²

Purification of unsymmetrical phthalocyanines requires tedious chromatographic separation procedures which are exaggerated by the high aggregation tendency of phthalocyanine molecules. Thus, attachment of bulky groups on the peripheral of phthalocyanines may facilitate the chromatographic process due to their low aggregation tendency.^{6b, 13} For example, Hanack *et al.* performed a statistical condensation of phthalonitriles with two bulky substituents to obtain the “3+1” product **1.16**, which could be isolated readily (Scheme 1.3).^{13a} Removal of the acetal group gave the phthalocyanine aldehyde **1.17**, which was then treated with *p*-xylylene-bis(triphenylphosphonium bromide) (**1.18**) to give the novel *bis*phthalocyanine **1.19**.



Scheme 1.3. Synthesis of *bis*vinylene-phenylene-bridged *bis*phthalocyanine **1.19**.

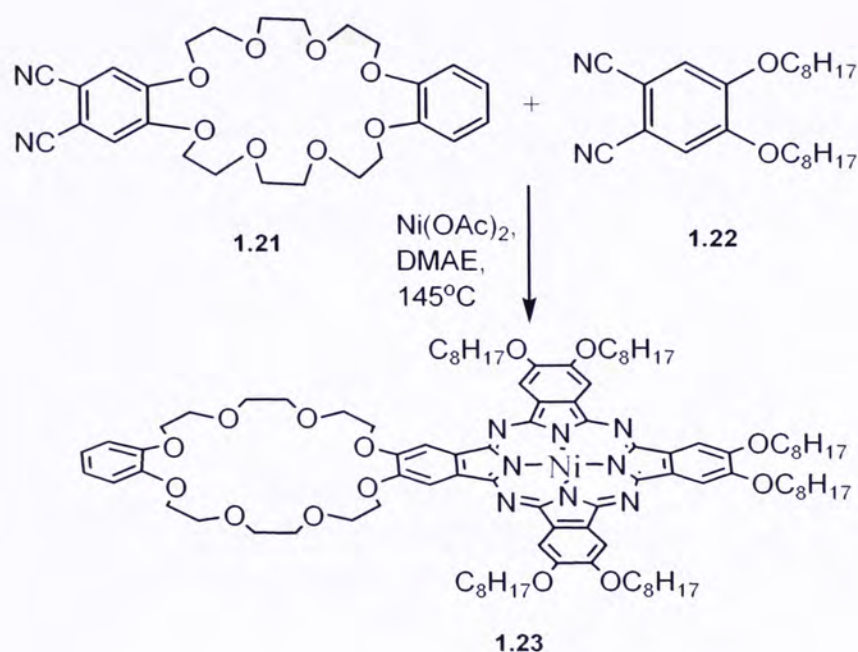
Scheme 1.4 shows the preparation of another unsymmetric phthalocyanine which again involves a mixed condensation of two different phthalonitriles. The dimethoxy groups of **1.20** undergo deprotection upon treatment with BBr_3 in dichloromethane to give compound **1.12**. The *cis*-dihydroxy moiety of **1.12** can couple with different linkers to give the dimer **1.13** and the trimer **1.14**, which display a remarkable liquid crystalline behavior.⁷



Scheme 1.4. Preparation of dihydroxy zinc phthalocyanine **1.12**.

For supramolecular studies, A_3B phthalocyanines bearing bulky groups and crown ether moieties have been widely studied.^{8b, 14} For example, Torres *et al.* performed the mixed cyclization of a dibenzo-24-crown-8 substituted phthalonitrile **1.21** with 3 equiv. of 4,5-dioctyloxyphthalonitrile (**1.22**) in the presence of nickel acetate in *N,N*-dimethylaminoethanol (DMAE) to give the unsymmetrical phthalocyanine **1.23**. This compound could be purified readily

by silica gel column chromatography (Scheme 1.5). Upon treatment with dibenzylammonium salt, a self-assembled supramolecular structure **1.15** was formed in which the dibenzylammonium cations threaded through the crown ether moieties of the unsymmetrical phthalocyanines.^{8b}

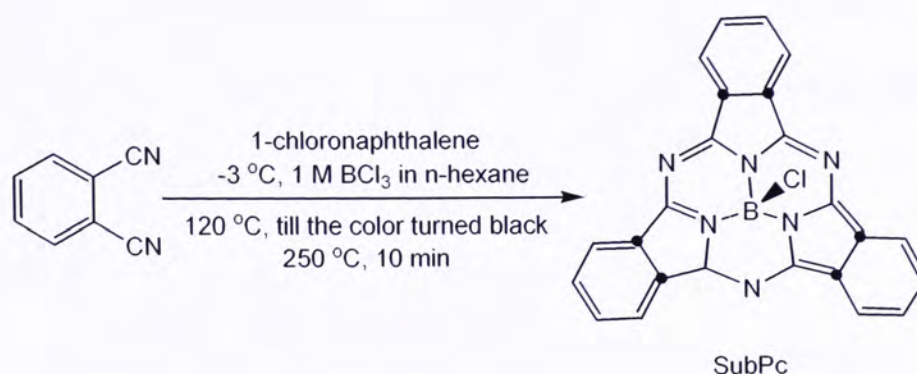


Scheme 1.5. Synthesis of nickel unsymmetrical phthalocyanine having a crown ether moiety for the formation of self-assembled supramolecular dimer.

In spite of the low selectivity of this statistical condensation, it is the most widespread method for preparing A₃B-type phthalocyanines, and satisfactory results can be achieved by a careful control of the reaction conditions.

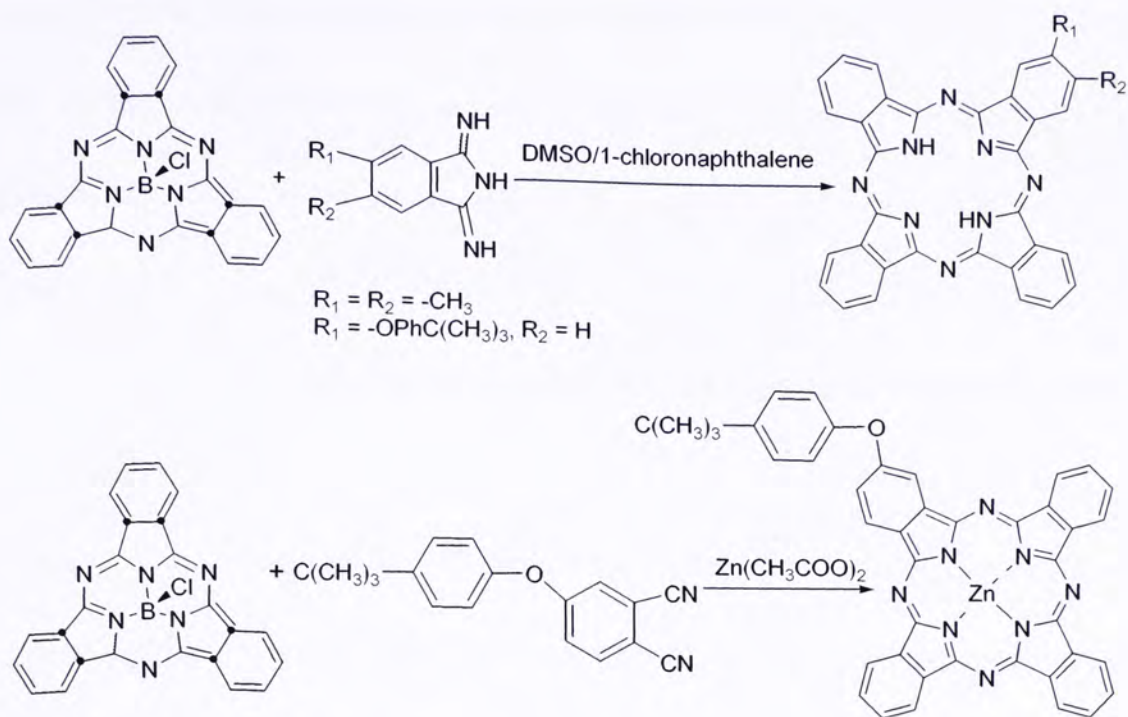
1.2.2 The Subphthalocyanine Approach

This method was developed in the late 1980s by Kobayashi and other researchers.^{15, 16} The reactions involve ring expansion of a subphthalocyanine (SubPc) core.^{17, 18} SubPc is composed of three isoindole subunits containing boron as the central atom. The macrocyclic complex contains an aromatic delocalized 14 π -electron system and a C_{3v} cone-shaped structure. This complex is usually synthesized in a high yield by reacting phthalonitriles with BCl_3 or other boron derivatives (Scheme 1.6).¹⁹



Scheme 1.6. Synthesis of a chloro-subphthalocyanine.

The A_3B phthalocyanines can be prepared by treating SubPc with a 1,3-diiminoisoindoline derivative or a differently substituted phthalonitrile, as shown in Scheme 1.7.¹⁷



Scheme 1.7. Selective synthesis of A_3B phthalocyanines via subphthalocyanines.

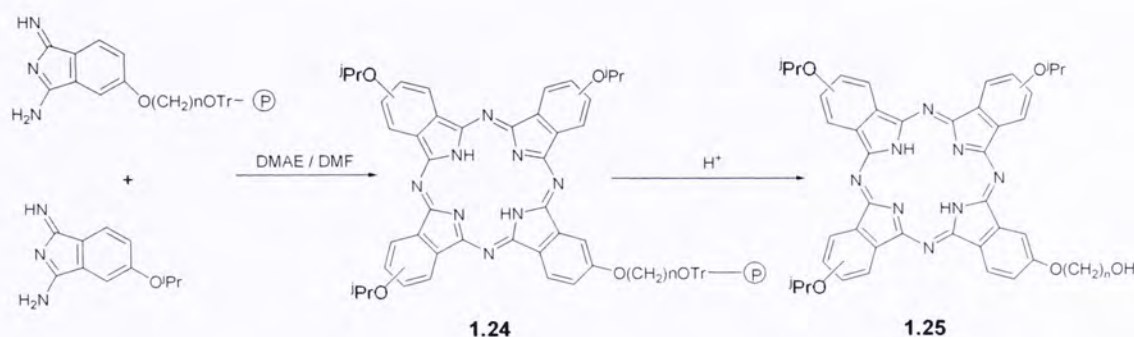
A theoretical study of the reactivity of SubPc toward the ring expansion reactions was performed by Kobayashi *et al.*^{18b} By calculating the bond energies of SubPc and compared with those of MgPc, it was found that no significant donation took place in the case of SubPc, while the total donating energy of lone pairs on pyrrole N to central Mg in MgPc was calculated to be $129 \text{ kJ}\cdot\text{mol}^{-1}$. The lack of electron donation in SubPc is attributed to the lack of electron-accepting orbitals in boron. Thus, the ring expansion reactions of SubPc might be caused to form the stable phthalocyanines. In addition, a structural change accompanying elimination of the axial ligand of SubPc (i.e., $\text{SubPc} \rightarrow \text{SubPc}^+ + \text{X}^-$) was considered from a shuttlecock-shaped form to a more

planar form, and the stabilization energy was about $100 \text{ kJ}\cdot\text{mol}^{-1}$. This indicated that the initial step of the ring expansion reaction consisted of a dehalogenation process. Furthermore, the enthalpy of the ring expansion reaction ($\text{SubPc} + \text{phthalonitrile} \rightarrow \text{Pc}$) was estimated to be $-113.64 \text{ kJ}\cdot\text{mol}^{-1}$, and this value suggested that the reaction was exothermic and apt to proceed without supplying substantial heat.

Although this method seems to be a logical approach to prepare “3+1” phthalocyanines, it is still highly dependent on the reactants and the experimental conditions. For example, addition of a metal salt to the reaction mixture may increase the yield of the desired unsymmetrical phthalocyanines.¹⁷ Occasionally, the SubPc undergoes fragmentation leading to the formation of a mixture of statistical products as in mixed cyclization.^{17, 18, 20} When a less reactive phthalonitrile was used instead of diiminoisoindoline (e.g. Scheme 1.7), the reaction gave a higher yield of phthalocyanines but the mixture contained a higher proportion of di-, tri-, and tetra-substituted phthalocyanines. Addition of a catalytic amount of DBU and pentanol and using a higher temperature increase the rate of the ring-opening reaction of the SubPc, favoring the formation of A_3B product.¹⁷ Overall speaking, owing to the low selectivity, this method is not a general methodology.

1.2.3 Synthesis on Polymeric Support

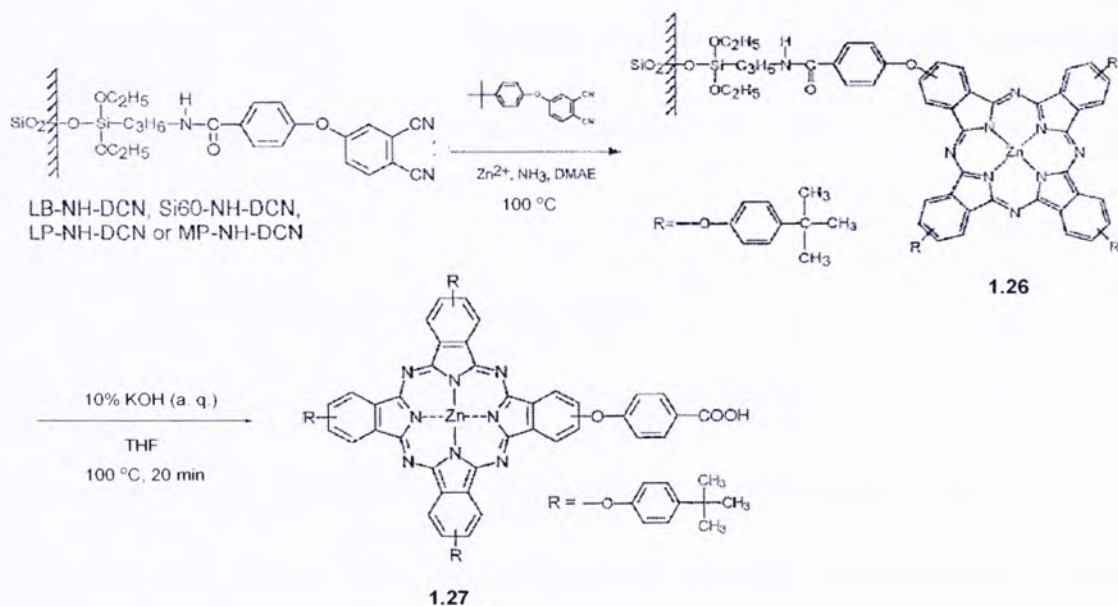
The preparation of A₃B phthalocyanines via a solid phase support was developed mainly by Leznoff *et al.*²¹ As shown in Scheme 1.8, a 1,3-diiminoisoindoline is finely linked to a polymer support. Cyclization of this insoluble polymer-bound precursor with a large excess of another unbound phthalonitrile or 1,3-diiminoisoindoline gives a polymer bound A₃B phthalocyanine (compound **1.24**). After removing of the soluble A₄ phthalocyanine by washing, the polymer bound A₃B phthalocyanine could be readily isolated. By treating it with an acid, the resulting A₃B product (compound **1.25**) can be finally liberated from the polymer to yield the desired product in *ca.* 20% (Scheme 1.8).^{21a}



Scheme 1.8. Synthesis of an A₃B phthalocyanine on polymeric support.

Apart from this polymer-bound method, Wöhrle *et al.* introduced modified silica gels as another kind of support for these solid-phase reactions.²² The phthalonitrile was bound to modified silica gels, then cyclized with

4-(4-*tert*-butylphenoxy)-phthalonitrile in the presence of a zinc(II) salt and NH_3 in DMAE at $100\text{ }^\circ\text{C}$. The insoluble crude product was filtered and washed with acetone and water in a Soxhlet apparatus until colorless to give a silica gel bound unsymmetric phthalocyanine **1.26**. The release of the desired A_3B phthalocyanine from this carrier was accomplished by alkaline hydrolysis in aqueous THF leading to the monocarboxy-substituted phthalocyanine **1.27** (Scheme 1.9).



Scheme 1.9. Synthesis of an A_3B phthalocyanine on silica gel support.

Although the polymer supported method appears to have some advantages in the selectivity and purification, this approach is limited to phthalonitriles or diiminoisoindolines bearing substituents that can easily react with the polymer and later be released from it. However, with the development

of the solid-phase technology and the wide variety of commercially available solid phases, this method may be a common route to prepare A_3B phthalocyanines in the future.

Among the three methods mentioned above for preparing unsymmetrically substituted A_3B type phthalocyanines, statistical condensation is still the most commonly used one. This approach has been applied in the synthesis of unsymmetrical subphthalocyanines.^{18a} The other two methods also have some selectivity and convenient purification procedures in some conditions, even though sometimes they cannot be controlled very well.

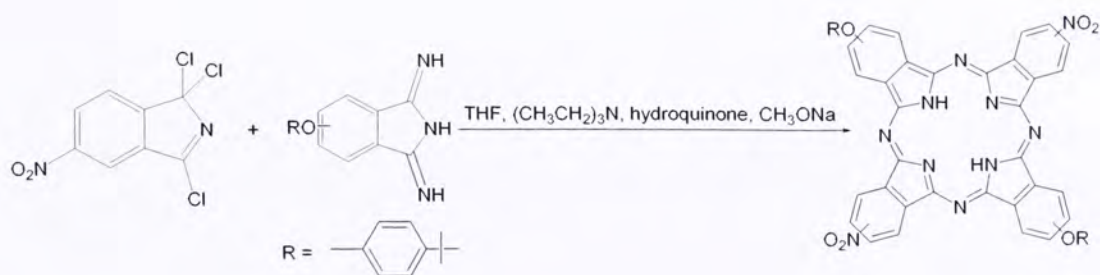
1.3 Synthesis of A_2B_2 Phthalocyanines

Both “opposite” (ABAB) and “adjacent” (AABB) type phthalocyanines have their special applications. For example, the “opposite” ones are good precursors to prepare ladder-type oligomers containing phthalocyanine units.²³ The “adjacent” analogues may function as second-order non-linear optical chromophores.²⁴ These compounds are also promising candidates in photodynamic therapy.^{6e, 25}

Despite these important applications, isolation of these two isomers from the statistical mixture is very difficult. Novel synthetic approaches are therefore required to prepare these phthalocyanines. Some of them are briefly described below.

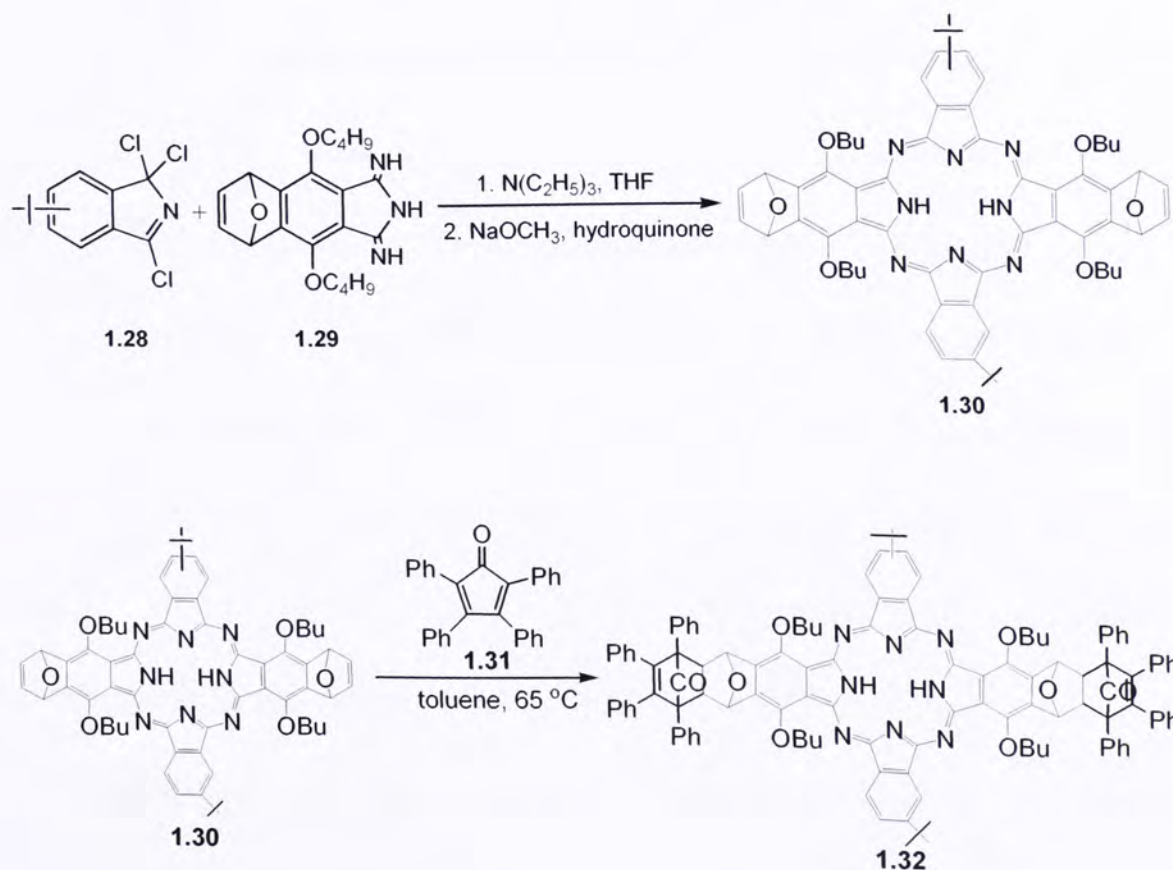
1.3.1 Preparation of Crosswise-Substituted Phthalocyanines (ABAB-type)

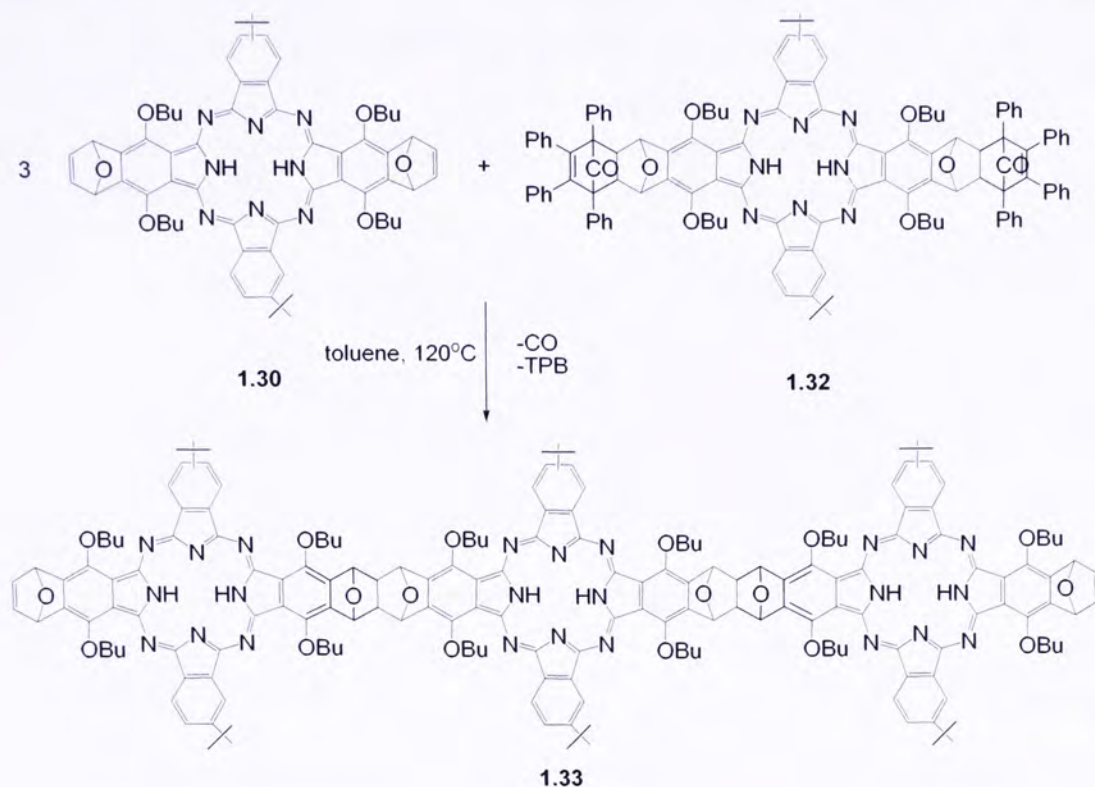
On the basis of a previously reported patent,²⁶ Young *et al.* reported a rather general method to prepare crosswise-substituted phthalocyanines. In this methodology, 1,3,3-trichloroisoidolines are treated with 1,3-diiminoisoidolines in a 1:1 molar ratio in the presence of a base and a reducing reagent. The ABAB-type phthalocyanine is formed via reductive coupling of the chloro-compound and the diiminoisoidoline derivative, Scheme 1.10 shows one of these examples.²⁷ By considering the experimental conditions and the stepwise nature of the synthetic procedures, the authors concluded that six of the nitrogen atoms in the phthalocyanine ring came from the diimino starting material without cleavage, while the other two nitrogen atoms were derived from the trichloro-compound. The yield of this compound was reported to be 48%,²⁷ but other researchers could only achieve a yield of 15 to 25%, with some AAAB phthalocyanines formed as by-products.^{23, 25a, 28}



Scheme 1.10. Selective synthesis of ABAB-type phthalocyanines via 1,3,3-trichloroisoidoline.

Hanack *et al.* employed this methodology to prepare the ABAB phthalocyanine **1.30**. The synthesis was carried out by condensation of diiminoisoindoline **1.29** with an excess of 6/7-*tert*-butyl-1,3,3-trichloroisoindoline **1.28**. Treatment of the resulting phthalocyanine **1.30** with tetracyclone (**1.31**) gave another ABAB phthalocyanine **1.32**. These *bis*diene- (compound **1.30**) and *bis*dienophile-type (compound **1.32**) phthalocyanines can be linked together by Diels-Alder reactions to form ladder-type oligomers (compound **1.33**), as shown in Scheme 1.11.²³ Some other ABAB-type phthalocyanines bearing sterically hindered substituents on the peripheral position have also been prepared in a similar manner.²⁹

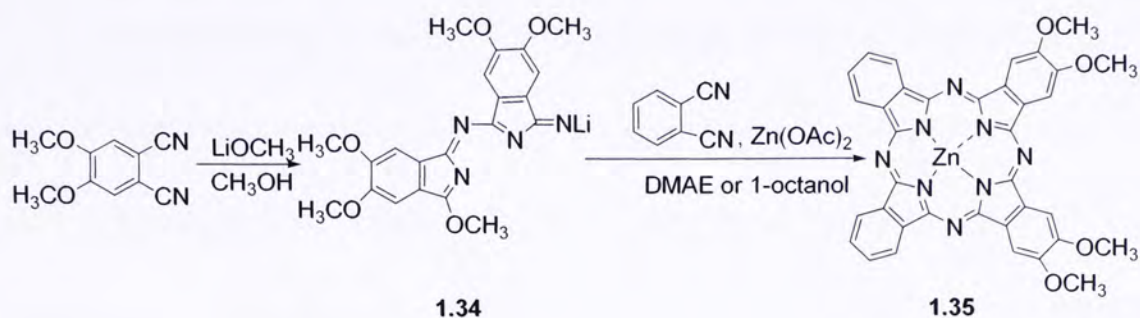




Scheme 1.11. Synthesis of a ladder-type trimer **1.33** based on *bisdiene*- and *bisdienophile*-type phthalocyanines.

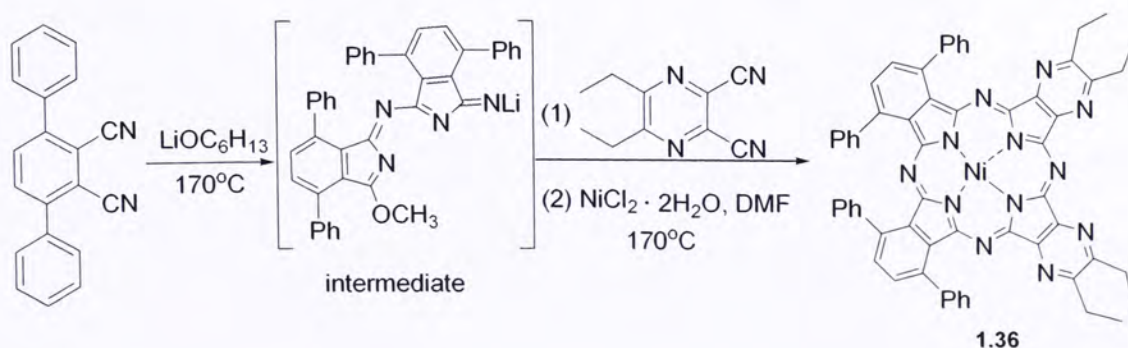
1.3.2 Preparation of “Adjacent” Phthalocyanines (AABB-type)

One of the new approaches to synthesize AABB phthalocyanines involves a “half-Pc” intermediate **1.34**.³⁰ As shown in Scheme 1.12, treatment of 4,5-dimethoxyphthalonitrile with lithium methoxide in methanol gives the “half-Pc” **1.34**. Further reaction of this intermediate with unsubstituted phthalonitrile in the presence of zinc(II) acetate in DMAE or 1-octanol leads to the formation of the AABB-type phthalocyanine **1.35** in a reasonably good yield of 28 % with few by-products.



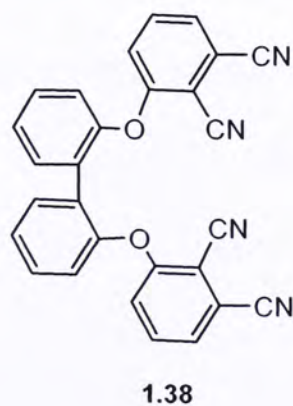
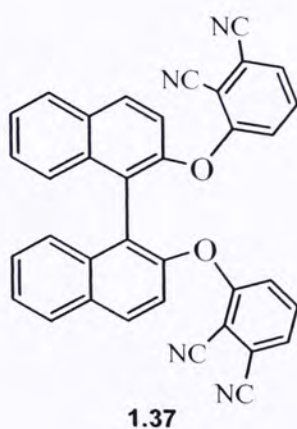
Scheme 1.12. Preparation of zinc “adjacent” AABB phthalocyanines including “half-Pc” intermediate.

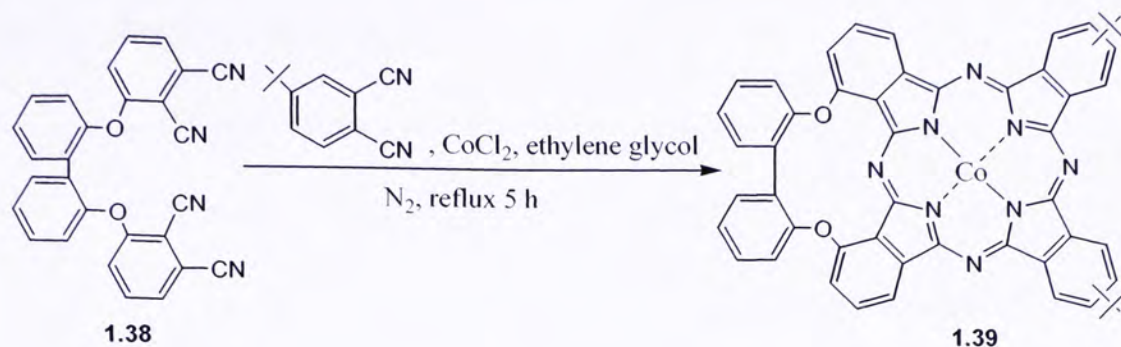
This approach has also been employed recently by Kobayashi and Fukuda to synthesize a donor-acceptor phthalocyanine.²⁴ By using 3,6-diphenylphthalonitrile and 2,3-dicyano-5,6-diethyl-1,4-pyrazine as starting materials, the reaction gives the adjacent phthalocyanine **1.36** via the “half-Pc” intermediate (Scheme 1.13). The yield of the desired AABB product is far above those of the other cyclized products.



Scheme 1.13. Synthesis of adjacently-fused donor-acceptor phthalocyanine.

An alternative synthetic pathway to AABB phthalocyanines involves the use of *bis*(phthalonitriles) linked by an appropriate bridging group, such as 2,2'-dihydroxy-1,1'-dinaphthyl (**1.37**).³¹ The steric constraint prevents the formation of opposite isomer during the cyclization. Additionally, the distance between the two phenoxy groups is close enough to facilitate intramolecular cyclization, avoiding the formation of oligomeric phthalocyanines. Treatment of these *bis*(phthalonitriles) with a differently substituted phthalonitrile can give "adjacent" phthalocyanines in a reasonably good yield. The interesting structures of "adjacent" phthalocyanines lead to intriguing spectroscopic and electrochemical properties. For example, Kobayashi *et al.* prepared the cobalt AABB phthalocyanine **1.39** with the biphenyl-linked *bis*(phthalonitrile) **1.38** (Scheme 1.14).³² This compound gave special spectroscopic properties, which were reasonably reproduced by molecular orbital calculations.





Scheme 1.14. Preparation of a cobalt AABB phthalocyanine using a biphenyl-linked *bis*(phthalonitrile).

1.4 Objectives of This Thesis

This project aims to prepare new phthalocyanines, in particular the unsymmetrical amphiphilic analogues, which can be used as photosensitizers for photodynamic therapy.

The first part of the work reports a modified statistical condensation method to prepare a series of A₃B phthalocyanines. The method uses the bulky 3,4,5-tris(dodecyloxy)phenylmethoxy group as a functional group to facilitate the purification after mixed cyclizations. This group can also be removed subsequently to give mono-hydroxy amphiphilic phthalocyanines.

In the second part, a series of zinc(II) phthalocyanines substituted with *N,N*-dimethylaminoethylsulfanyl groups will be described, including their synthesis, spectroscopic properties, and *in vitro* photodynamic activities.

1.5 References

1. (a) *Phthalocyanines - Properties and Applications*; Leznoff, C. C., Lever, A. B. P., Eds.; VCH: New York, 1989, Vol. 1; 1993, Vols. 2 and 3; 1996, Vol. 4. (b) McKeown, N. B. *Phthalocyanine Materials: Synthesis, Structure and Function*, Cambridge University Press: Cambridge, 1998.
2. (a) Li, D.; Ratner, M. A.; Marks, T. J. *J. Am. Chem. Soc.* **1988**, *110*, 1707. (b) Torres, T.; de la Torre, G.; García-Ruiz, J. *Eur. J. Org. Chem.* **1999**, 2323. (c) Maya, E. M.; García, C.; García-Frutos, E. M.; Vázquez, P.; Torres, T. *J. Org. Chem.* **2000**, *65*, 2733.
3. Guggenheim, E. A. *Trans. Faraday Soc.* **1949**, *45*, 714.
4. González-Cabello, A.; Vázquez, P.; Torres, T.; Guldi, D. M. *J. Org. Chem.* **2003**, *68*, 8635.
5. Ding, X.; Xu, H. *Sensors and Actuators B: Chem.* **2000**, *65*, 108.
6. (a) Michelsen, U.; Kliesch, H.; Schnurpfeil, G.; Sobbi, A. K.; Wöhrle, D. *Photochem. Photobiol.* **1996**, *64*, 694. (b) Hu, M.; Bresseur, N.; Yildiz, S. Z.; van Lier, J. E.; Leznoff, C. C. *J. Med. Chem.* **1998**, *41*, 1789. (c) Giuntini, F.; Nistri, D.; Chiti, G.; Fantetti, L.; Jori, G.; Roncucci, G. *Tetrahedron Lett.* **2003**, *44*, 515. (d) Cosimelli, B.; Roncucci, G.; Dei, D.; Fantetti, L.; Ferroni, F.; Ricci, M.; Spinelli, D. *Tetrahedron* **2003**, *59*, 10025. (e) Bonneau, S.; Morlière, P.; Brault, D. *Biochem. Pharmacol.* **2004**, *68*, 1443. (f) Lo, P. C.; Huang, J. D.; Cheng, D. Y. Y.; Chan, E. Y. M.; Fong, W. P.; Ko, W. H.; Ng, D. K. P. *Chem. Eur. J.* **2004**, *10*, 4831.

7. Makhseed, S.; Bumajdad, A.; Ghanem, B.; Msayib, K.; McKeown, N. B. *Tetrahedron Lett.* **2004**, *45*, 4865.
8. (a) Engelkamp, H.; Middelbeek, S.; Nolte, R. J. M. *Science* **1999**, *284*, 785. (b) Martínez-Díaz, M. V.; Rodríguez-Morgade, M. S.; Feiters, M. C.; van Kan, P. J. M.; Nolte, J. M.; Stoddart, J. F.; Torres, T. *Org. Lett.* **2000**, *2*, 1057. (c) Charvet, R.; Jiang, D.; Aida, T. *Chem. Commun.* **2004**, 2664.
9. *The Porphyrin Handbook*; Kadish, K. M., Smith, K. M., Guillard, R., Eds.: Academic Press, 2003, Vol. 15. Chap. 99.
10. de la Torre, G.; Claessens, C. G.; Torres, T. *Eur. J. Org. Chem.* **2000**, 2821.
11. Torres, T. *J. Porphyrins Phthalocyanines* **2000**, *4*, 325.
12. Chambrier, I.; Cook, M. J.; Russell, D. A. *Synthesis* **1995**, 1283.
13. (a) Schweikart, K.; Hanack, M. *Eur. J. Org. Chem.* **2000**, 2551. (b) Ozan, N.; Bekaroğlu, Ö *Polyhedron* **2003**, *22*, 819. (b) Kalkan, A.; Koca, A.; Bayır, Z. A. *Polyhedron* **2004**, *23*, 3155.
14. Martínez-Díaz, M. V.; Fender, N. S.; Rodríguez-Morgade, M. S.; Gómez-López, M.; Diederich, F.; Echegoyed, L.; Stoddart, J. F.; Torres, T. *J. Mater. Chem.* **2002**, *12*, 2095.
15. Ando, M.; Mori, Y. *56th Annual Meeting, Chemical Society of Japan*, Tokyo **1988**, Abstr. 3VA01. Ando, M.; Mori, Y. (Tokyo Ink Mfg. Co., Ltd.), Jpn. Kokai Tokkyo Koho JP 02 09, 882 [90 09, 882], **1990** [*Chem. Abstr.* **1990**, *113*, 25558c].

16. Kobayashi, N.; Kondo, R.; Nakajima, S.-I.; Osa, T. *J. Am. Chem. Soc.* **1998**, *120*, 12808.
17. Weitemeyer, A.; Kliesch, H.; Wöhrle, D. *J. Org. Chem.* **1995**, *60*, 4900.
18. (a) Ali, H.; Sim, S. K.; van Lier, J. E. *J. Chem. Res. (S)* **1999**, 496. (b) Kobayashi, N.; Ishizaki, T.; Ishii, K.; Konami, H. *J. Am. Chem. Soc.* **1999**, *121*, 9096. (c) Matlaba, P.; Nyokong, T. *Polyhedron* **2002**, *21*, 2463.
19. Meller, A.; Ossko, A. *Monatsh. Chem.* **1972**, *103*, 150.
20. Sastre, A.; del Rey, B.; Torres, T. *J. Org. Chem.* **1996**, *61*, 8591.
21. (a) Leznoff, C. C.; Hall, T. W. *Tetrahedron Lett.* **1982**, *23*, 3023. (b) Hall, T. W.; Greenberg, S.; McArthur, C. R.; Khouw, B.; Leznoff, C. C. *Nouv. J. Chim.* **1982**, *6*, 653. (c) Leznoff, C. C. *Can. J. Chem.* **2000**, *78*, 167.
22. Hirth, A.; Sobbi, A. K.; Wöhrle, D. *J. Porphyrins Phthalocyanines* **1997**, *1*, 275.
23. Hanack, M.; Stihler, P. *Eur. J. Org. Chem.* **2000**, 303.
24. Fukuda, T.; Kobayashi, N. *Chem. Lett.* **2002**, 866.
25. (a) Dabak, S.; Bekaroğlu, Ö. *J. Chem. Res. (S)* **1997**, *1*, 8. (b) Gantchev, T. G.; Ouellet, R. van Lier J. E. *Archives of Biochem. and Biophys.* **1999**, *366*, 21.
26. Idelson, E. M. U. S. Patent 4,061,654 **1977** [*Chem. Abstr.* **1977**, *88*,171797m].

27. Young, J. G.; Onyebuagu, W. *J. Org. Chem.* **1990**, *55*, 2155.
28. (a) Stihler, P.; Hauschel, B.; Hanack, M. *Chem. Ber.* **1997**, *130*, 801. (b) Dabak, S.; Bekâröglu, Ö *New J. Chem.* **1997**, *21*, 267.
29. (a) Kobayashi, N.; Ashida, T.; Osa, T. *Chem. Lett.* **1992**, 2031. (b) Yang, J.; Van De Mark, M. R. *J. Heterocyclic Chem.* **1995**, *32*, 1521. (c) Polley, R.; Linssen, T. G.; Stihler, P.; Hanack, M. *J. Porphyrins Phthalocyanines* **1997**, *1*, 169.
30. Nolan, K. J. M.; Hu, M.; Leznoff, C. C. *Synlett* **1997**, 593.
31. (a) Kobayashi, N. *Chem. Commun.* **1998**, 487. (b) Miwa, H.; Kobayashi, N. *Chem. Lett.* **1999**, 1303.
32. Kobayashi, N.; Miwa, H.; Nemykin, V. N. *J. Am. Chem. Soc.* **2002**, *124*, 8007.

Chapter 2 Synthesis, Characterization and in vitro Photodynamic Activities of Mono-Alkoxy and Hydroxy Zinc(II) Phthalocyanines

2.1 Introduction

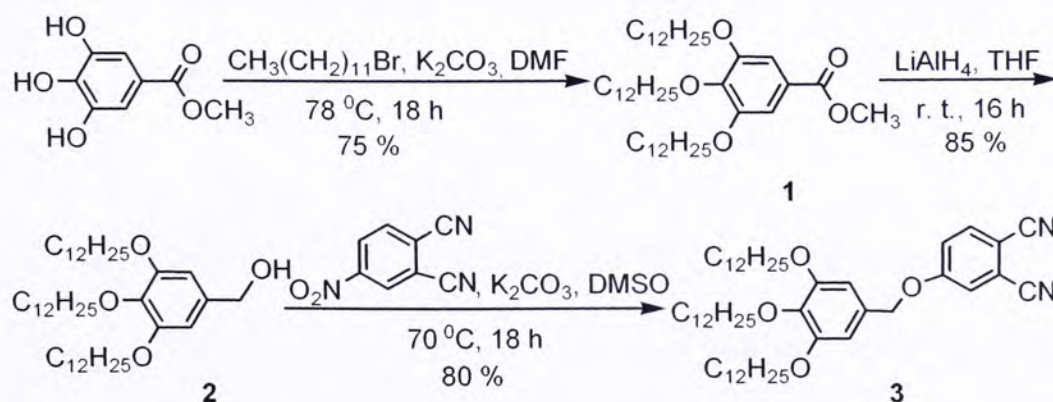
As introduced in previous chapter, unsymmetrical amphiphilic phthalocyanines with both hydrophilic and hydrophobic moieties are promising photosensitizers for photodynamic therapy.^{1,2} Hydroxy phthalocyanines, for example, have been shown to exhibit high *in vitro* photodynamic activities.³ However, the preparation and purification of these compounds are difficult due to their intrinsic aggregation behavior and the many undesirable side products formed during mixed cyclization.

In this chapter, a simplified procedure to synthesize mono-hydroxy amphiphilic zinc(II) phthalocyanine is reported. By using the phthalonitrile substituted with the bulky 3,4,5-tris(dodecyloxy)phenylmethoxy group, the unsymmetrical zinc(II) phthalocyanine formed in the mixed cyclization with an excess of unsubstituted phthalonitrile can be isolated readily. The bulky group can then be removed upon treatment with $\text{CF}_3\text{CO}_2\text{H}$ to give the mono-hydroxy zinc(II) phthalocyanine. This amphiphilic phthalocyanine exhibits a high *in vitro* photocytotoxicity. Attempts have also been made to prepare the halogenated analogues by performing mixed condensations of this bulky phthalonitrile and halogenated phthalonitriles. These compounds can be isolated

by high performance liquid chromatography (HPLC). The preparation and characterization of these compounds are also reported in this chapter.

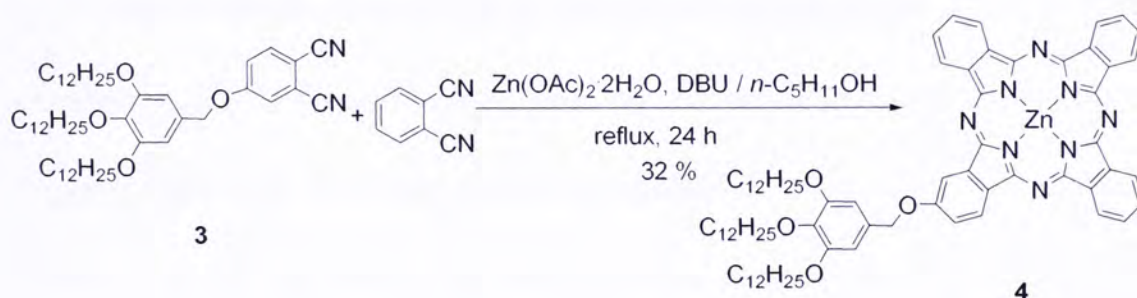
2.2 Preparation and Characterization of Unsymmetrical Zinc(II) Phthalocyanines Substituted with a 3,4,5-Tris(dodecyloxy)phenylmethoxy Group

In attempt to simplify the isolation of unsymmetrical phthalocyanines, phthalonitrile **3**, which contains a bulky 3,4,5-tris(dodecyloxy)phenylmethoxy group was first synthesized. As shown in Scheme 2.1, methyl gallate was treated with 1-bromododecane in the presence of K_2CO_3 in *N,N*-dimethylformamide (DMF) to give the trialkylated product **1**. Compound **1** was then reduced with lithium aluminum hydride in tetrahydrofuran (THF) to afford compound **2**,⁴ which was then coupled with 4-nitrophenaldehyde in the presence of K_2CO_3 in dimethyl sulfoxide (DMSO) to produce phthalonitrile **3** in good yield.⁵



Scheme 2.1. Synthesis of phthalonitrile **3** bearing a bulky 3,4,5-tris(dodecyloxy)phenylmethoxy group.

Mixed cyclization between phthalonitrile **3** and the unsubstituted phthalonitrile was performed in the presence of $\text{Zn}(\text{OAc})_2 \cdot 2\text{H}_2\text{O}$ and 1,8-diazabicyclo[5.4.0]undec-7-ene (DBU) in *n*-pentanol (Scheme 2.2). Different molar ratios of the two precursors were used in order to simplify the separation procedure and increase the yield of the desired “3+1” unsymmetrical phthalocyanine. It was found that a molar ratio of 1:9 for phthalonitrile **3** to the unsubstituted phthalonitrile was the best condition. The desired unsymmetrical phthalocyanine **4** was isolated readily in 32 % yield by silica gel column chromatography using THF/hexane (1:4, v/v) as eluent.



Scheme 2.2. Mixed cyclization between phthalonitrile **3** and the unsubstituted phthalonitrile.

The purity of this compound isolated by column chromatography was checked by HPLC by detecting the absorption at 669 nm, where the Q-band absorption of this phthalocyanine appears. As shown in Figure 2.1, the isolated compound was essentially pure.

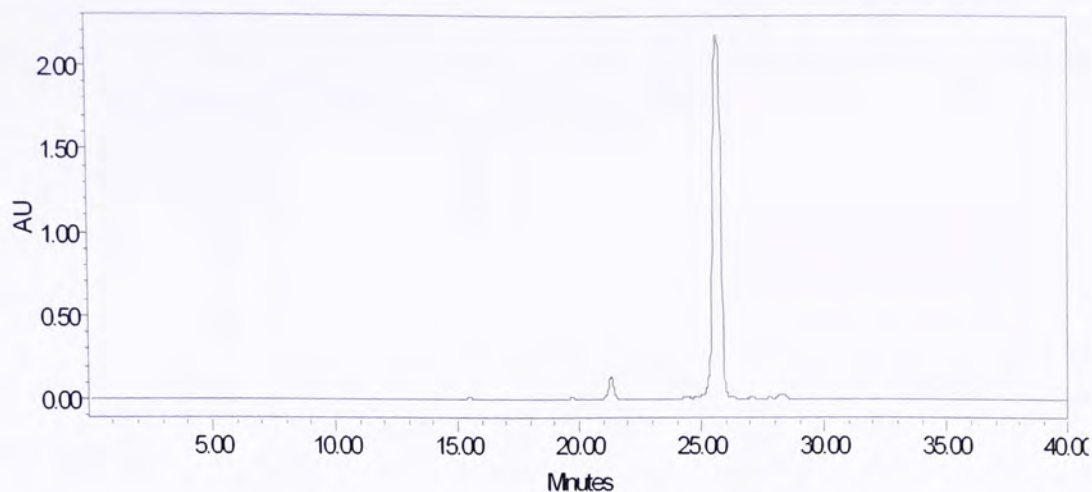


Figure 2.1. HPLC profile of phthalocyanine **4** by monitoring the absorption at 669 nm.

Due to the strong aggregation tendency of phthalocyanine **4**, its ^1H NMR spectrum in CDCl_3 showed several broad signals which were difficult to assign. Figure 2.2 shows its ^1H NMR spectrum in pyridine- d_5 . The singlet at δ 9.23 and doublet at δ 8.03 are due to the phthalocyanine α and β protons, respectively, adjacent to the substituent. The multiplets in the regions δ 9.61-9.66 and 8.24-8.28 can be assigned to the remaining α and β ring protons, respectively. The aryl ring protons and the OCH_2 protons of the substituent resonate as two singlets at δ 7.44 and 6.00, respectively. The remaining dodecyl chains give several multiplets at *ca.* δ 4.3 and in the region δ 0.8-2.1.

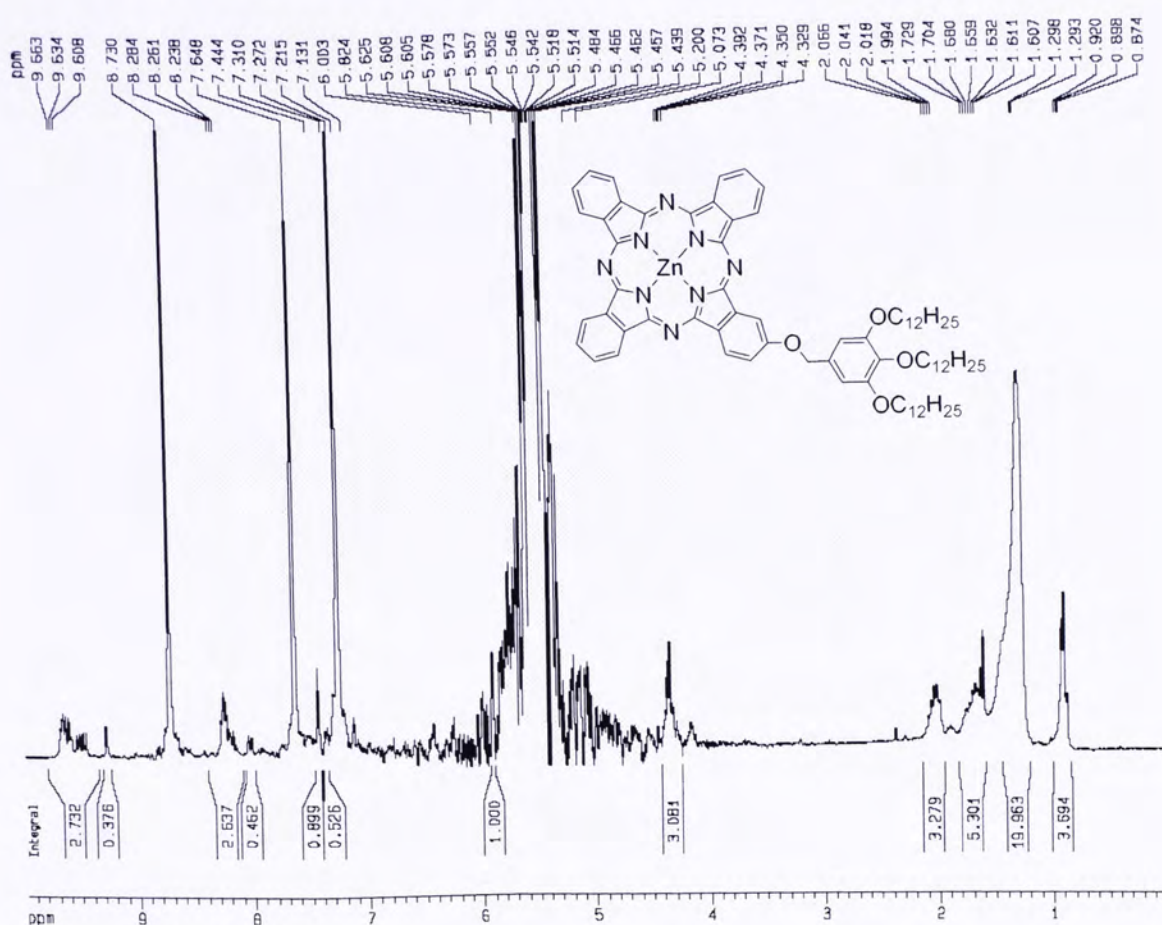


Figure 2.2. ^1H NMR spectrum of phthalocyanine **4** in pyridine- d_5 .

Figure 2.3 shows the absorption spectra of phthalocyanine **4** in THF. The sharp Q-band absorption at 669 nm is a typical π - π^* transition of metallophthalocyanines. The inset shows a plot of the Q-band absorbance at 669 nm versus the concentration of **4**. The linear relationship indicates that this absorption obeys the Lambert-Beer law, and the compound is essentially free from aggregation under these conditions. This is corroborated with the strong fluorescence emission at 675 nm upon excitation at 610 nm. The fluorescence quantum yield was found to be 0.34.⁶

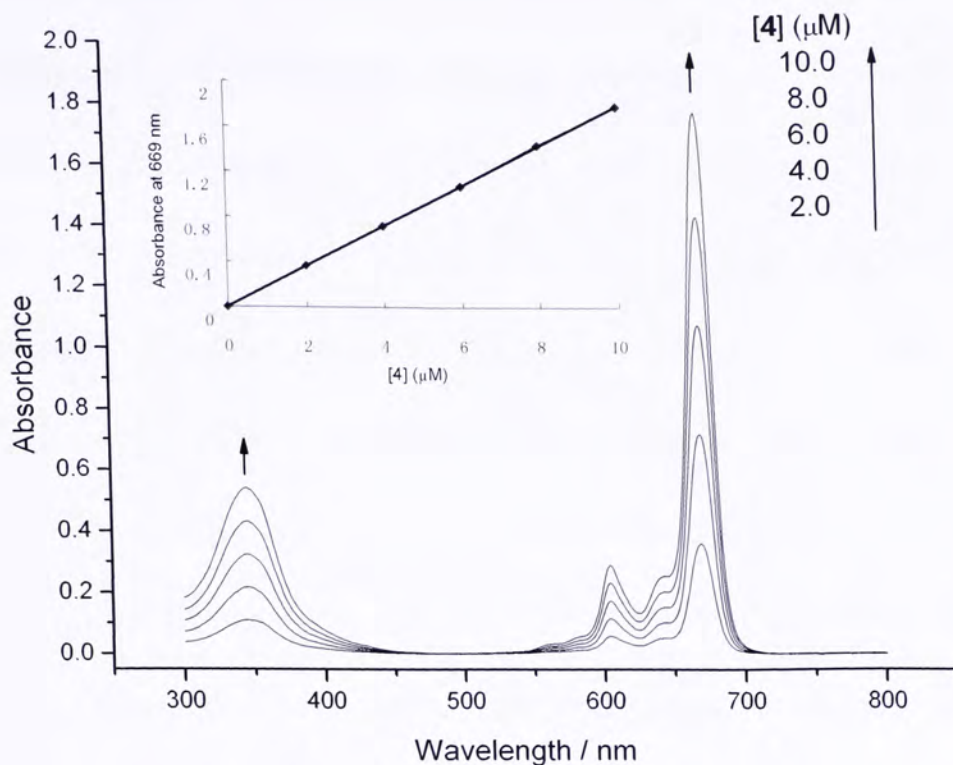


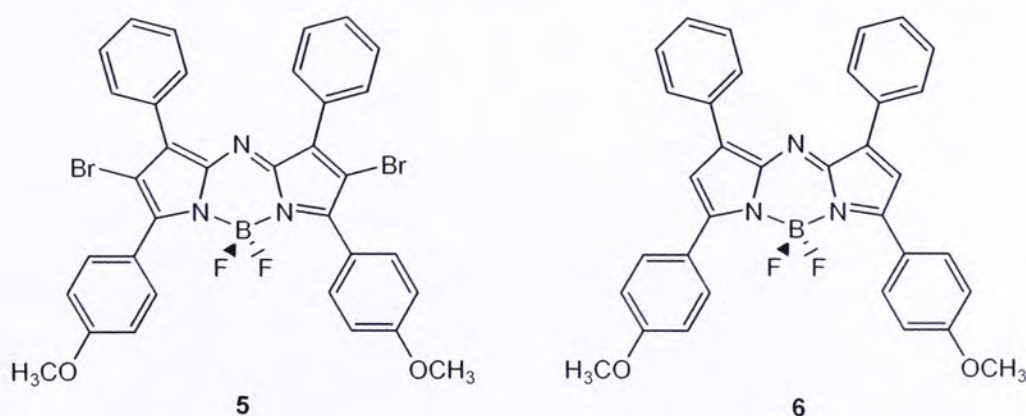
Figure 2.3. Electronic absorption spectra of **4** in THF in different concentrations.

The plot of the absorbance of the Q-band at 669 nm versus the concentration of **4** is given in the inset.

Compound **4** was also characterized with liquid-secondary ion mass spectrometry (L-SIMS). The spectrum showed an intense isotopic envelope peaking at m/z 1235.6798, which was in good agreement with the calculated value for MH^+ (1235.6762). The isotopic pattern also closely resembled to the simulated pattern.

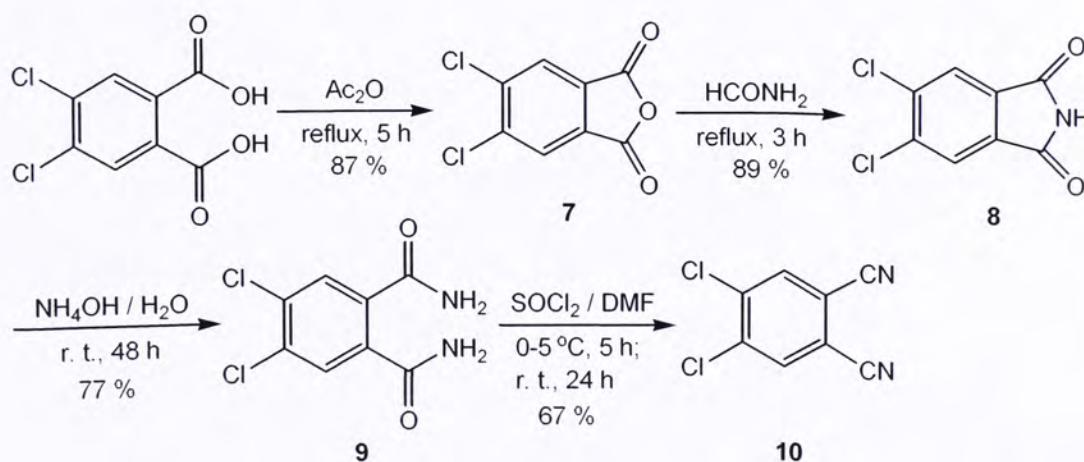
2.3 Preparation and Characterization of Halogenated Unsymmetrical Zinc(II) Phthalocyanines

One of the important applications of phthalocyanines is to be used as photosensitizers for photodynamic therapy (PDT). Singlet oxygen is the key cytotoxic agent in the photodynamic process. The efficiency of singlet oxygen generation is regulated by the intersystem crossing (ISC), which is a spin-forbidden electronic transition from a singlet to a triplet state. Introduction of heavy atoms is known to promote the ISC as a result of the heavy-atom effect.⁷ Halogen substituents, as heavy atoms, may therefore increase population of the excited triplet state of the photosensitizers and increase their singlet oxygen quantum yields. O'Shea *et al.* have reported a BF₂-chelated tetraarylazadipyrromethene with bromo substituents (compound **5**). This compound exhibits a very substantial heavy-atom effect, showing a 1000-fold higher *in vitro* photocytotoxicity than the non-brominated analogue **6**.⁸



For this reason, we also planned to synthesize halogenated unsymmetrical phthalocyanines and studied their heavy atom effects in PDT. To this end, several halogenated phthalonitrile precursors were first synthesized according to literature procedures with a minor modification.

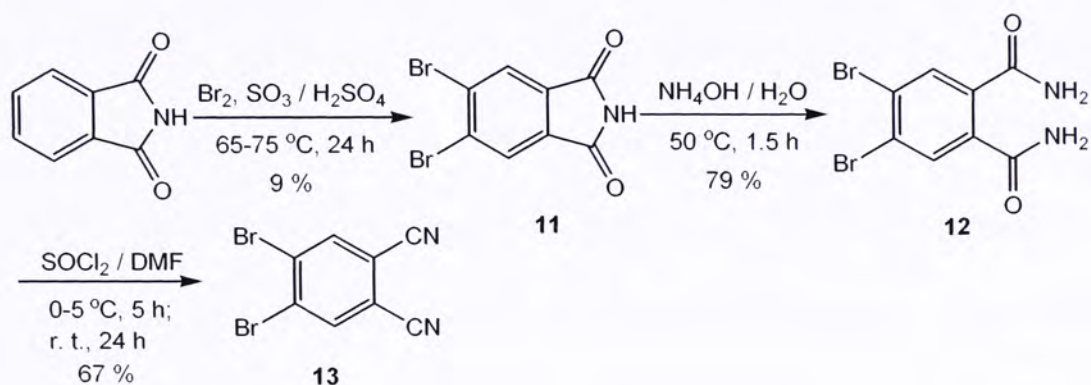
4,5-Dichlorophthalonitrile (**10**) was prepared from 4,5-dichlorophthalic acid in four steps as shown in Scheme 2.3.⁹ Dehydration with acetic anhydride, followed by the treatment with formamide gave the cyclic amide **8**. Compound **8** was then stirred in an ammonia solution to yield 4,5-dichlorophthalamide (**9**), which was then treated with thionyl chloride in DMF to give 4,5-dichlorophthalonitrile (**10**).



Scheme 2.3. Preparation of 4,5-dichlorophthalonitrile (**10**).

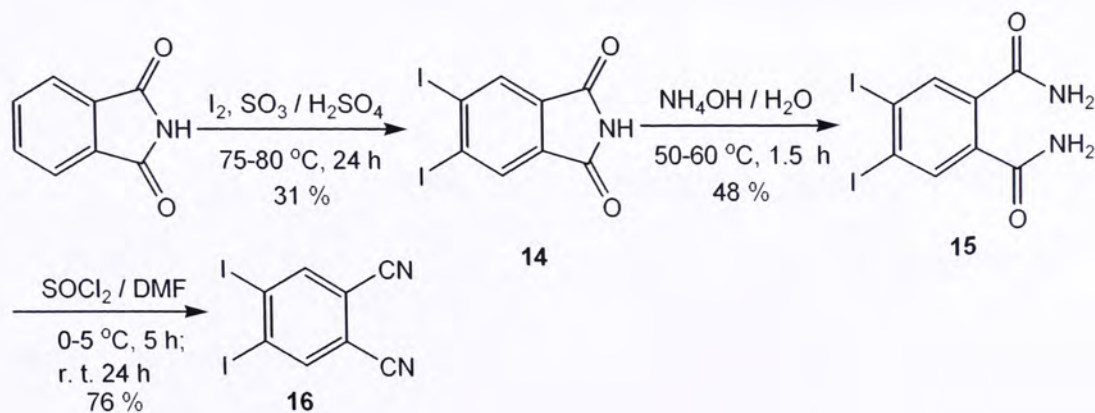
4,5-Dibromophthalonitrile (**13**) was synthesized by a modified literature procedure.¹⁰ Bromination of phthalimide in 20% fuming sulfuric acid gave compound **11**, which was then stirred in ammonia solution to give

4,5-dibromophthalamide (**12**). Upon treatment with thionyl chloride in DMF, compound **12** was converted to 4,5-dibromophthalonitrile (**13**) in satisfactory yield (Scheme 2.4).



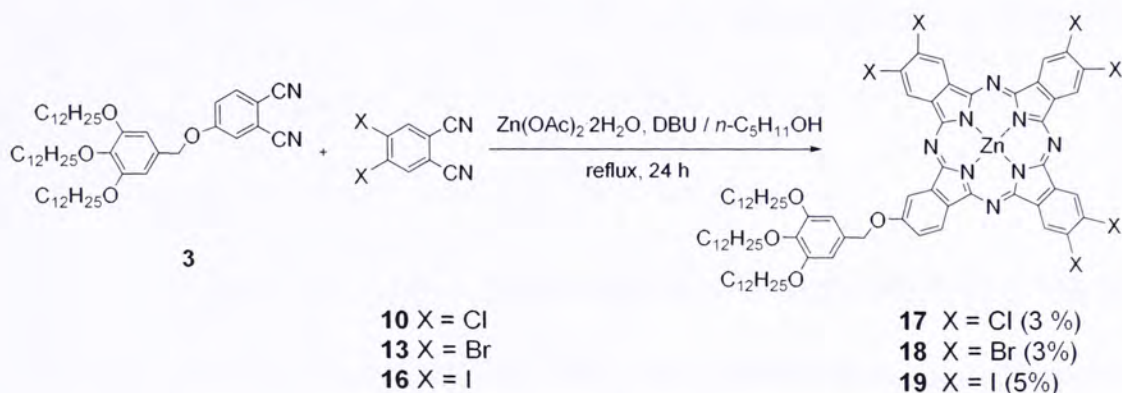
Scheme 2.4. Preparation of 4,5-dibromophthalonitrile (**13**).

4,5-Diiodophthalonitrile (**16**) was prepared similarly using iodine instead of bromine as one of the starting materials. As shown in Scheme 2.5, this compound was prepared in three steps.¹¹



Scheme 2.5. Preparation of 4,5-diiodophthalonitrile (**16**).

These halogenated phthalonitriles were then cyclized with the phthalonitrile **3** under the usual conditions (Scheme 2.6). After several attempts, it was found that a molar ratio of 1:3 for phthalonitrile **3** to the halogenated phthalonitrile could lead to a better result. Even so, purification by column chromatography was found to be difficult. Pure products could not be obtained. It is likely that the halogen substituents enhance the stacking of the phthalocyanines, reducing the separation efficiency. The desired halogenated unsymmetrical phthalocyanines **17-19** could however be isolated in trace amounts with the aid of HPLC using a C18 column with THF/H₂O as eluent. (This part of work was performed by Prof. Jiandong Huang in Fuzhou University.)



Scheme 2.6. Preparation of halogenated unsymmetrical phthalocyanines **17-19**.

The HPLC profiles of the purified products are shown in Figure 2.4, by monitoring the corresponding Q-band absorption. It can be seen that all the samples are essentially pure.

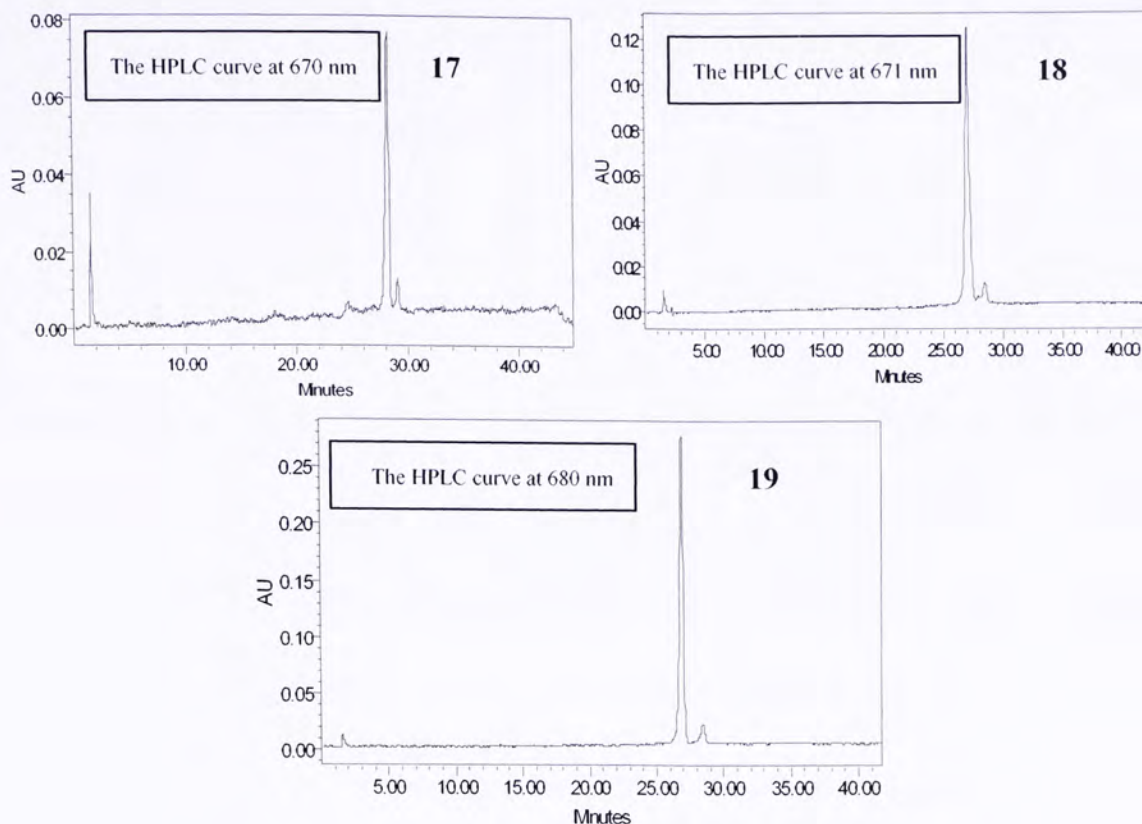


Figure 2.4. HPLC profiles of the halogenated unsymmetrical phthalocyanines **17-19**.

All these compounds display typical electronic absorption spectra of phthalocyanines (Figure 2.5). In THF, they show two strong absorptions at around 350 nm (B-band) and 670-680 nm (Q-band). The small splitting of the Q-band for **17** may be attributed to the lower symmetry of this compound. Based on these spectral features, it seems that all the three compounds are essentially non-aggregated in THF.

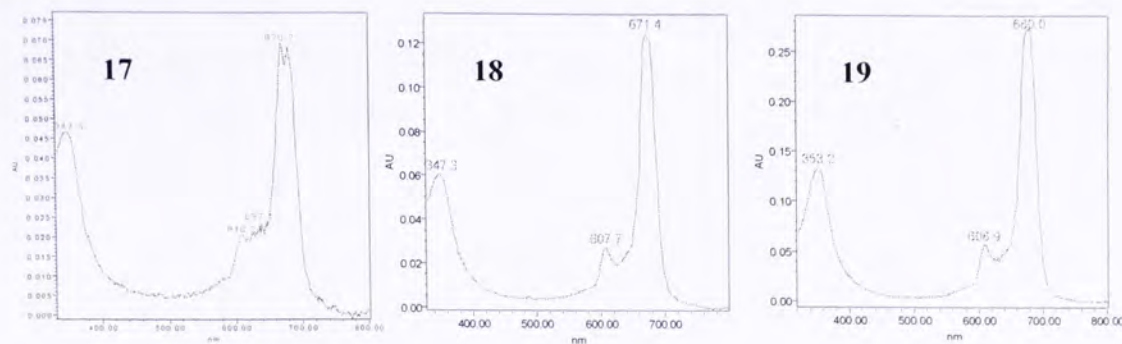


Figure 2.5. UV-visible spectra of unsymmetrical phthalocyanines **17-19** in THF.

For further characterization, ^1H NMR spectra of **17-19** were recorded in pyridine- d_5 . However, due to the poor solubility of the chlorinated phthalocyanine **17** in this solvent, satisfactory ^1H NMR spectrum could not be obtained. Figure 2.6 shows the ^1H NMR spectrum of the brominated analogue **18** in pyridine- d_5 . Again, due to the strong aggregation, some of the signals are broadened or even split. The phthalocyanine ring protons resonate as several broad signals at δ 8.0-9.6. The broad signal at δ 7.5 can be attributed to the two aryl protons of the substituent. The OCH_2 protons' signal at *ca.* δ 6 is split due to aggregation. The signals for the dodecyl chains appear as several broad signals at *ca.* δ 4.3 (for OCH_2) and 0.8-2.3 (for the remaining protons). The ^1H NMR spectrum of the iodinated analogue **19** is very similar to that of **18**, and can be assigned in a similar manner.

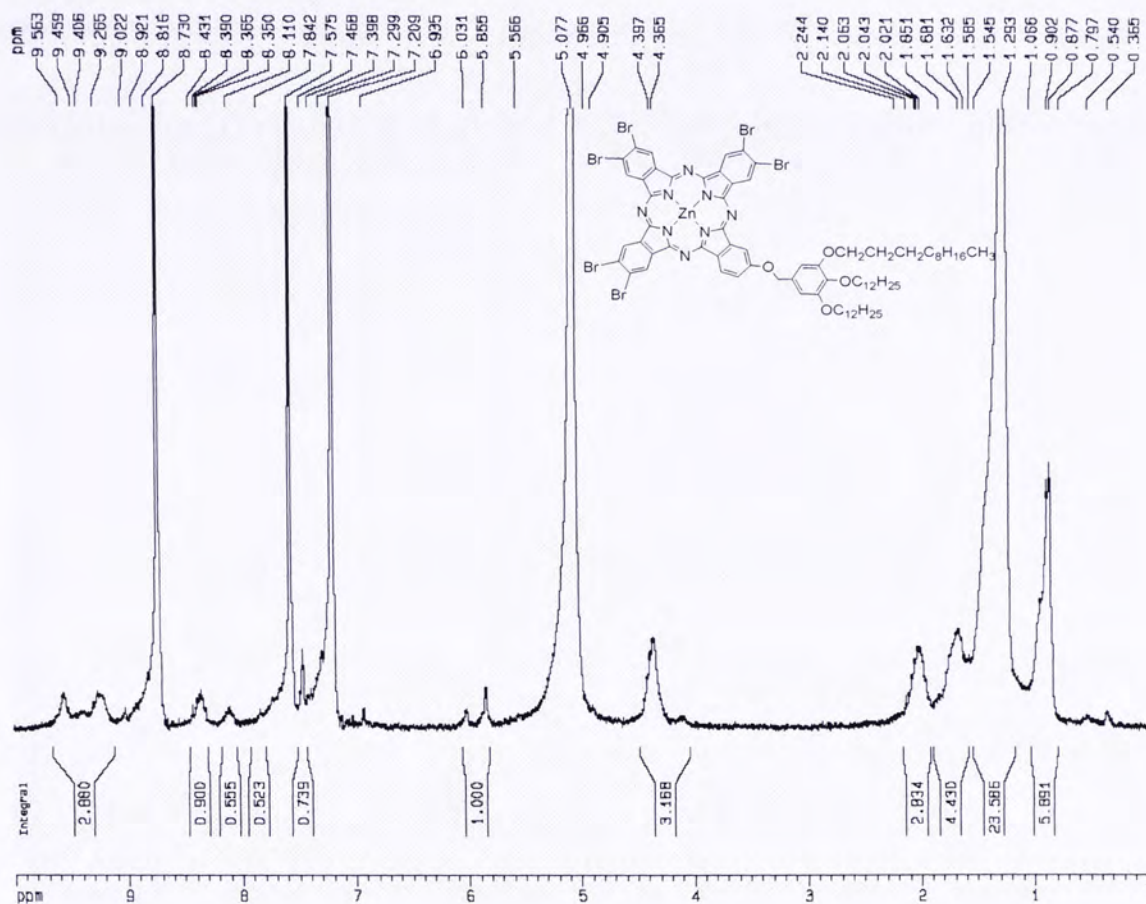


Figure 2.6. ¹H NMR spectrum of compound **18** in pyridine-*d*₅.

The MALDI-TOF mass spectrum of **17** showed an intense isotopic cluster peaking at m/z 800.3, which could be assigned to the fragment ion $[M-Ar]^+$, in which the bulky aryl group was removed. The molecular ion peak could not be found. The MALDI-TOF mass spectrum of **18** showed the clusters peaking at m/z 1471.5 and 826.1, which could be assigned to the fragments $[M-3Br]^+$ and $[M-3Br-Ar]^+$, respectively. The MALDI-TOF mass spectrum for the iodo analogue **19** was similar to that of **18**. In order to reveal the molecular ion, a softer ionization technique, namely electrospray ionization (ESI) was used. The ESI spectrum of **19** showed an intense isotopic envelope peaking at m/z

1990.0421, which was in good agreement with the calculated value for the molecular ion (1990.0483) (Figure 2.7). The isotopic pattern also closely resembled to the simulated pattern.

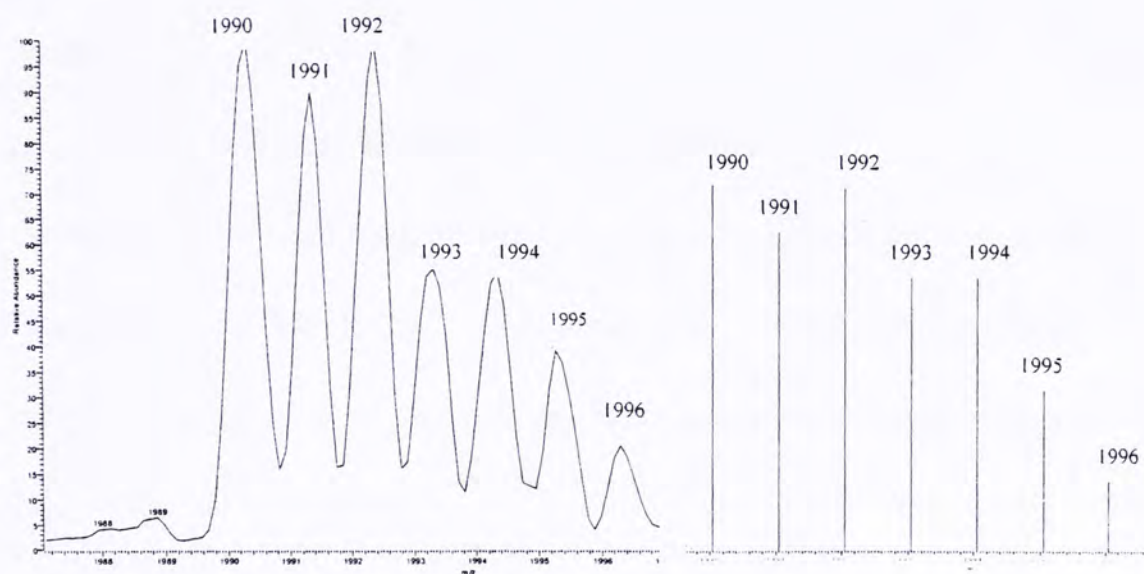
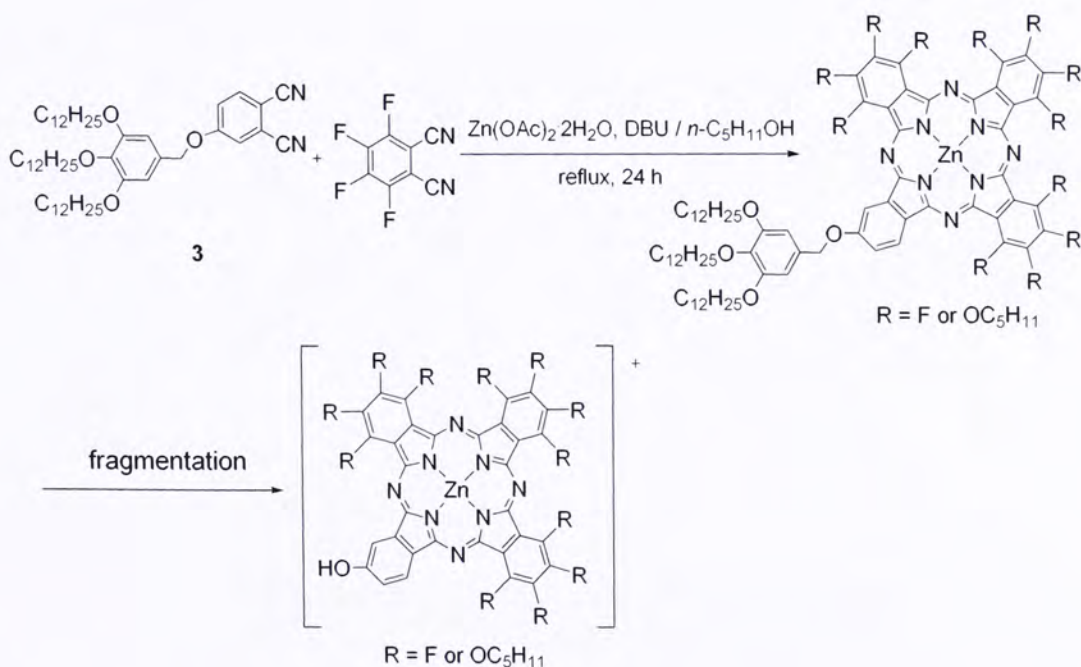


Figure 2.7. Molecular ion cluster of **19** shown in the MALDI-TOF mass spectrum (left). The corresponding simulated isotopic pattern is shown on the right.

Apart from the above halogenated phthalocyanines, we also tried to prepare an unsymmetrical fluorinated phthalocyanine by mixed condensation of phthalonitrile **3** and tetrafluorophthalonitrile in the presence of DBU and $\text{Zn}(\text{OAc})_2 \cdot 2\text{H}_2\text{O}$ in *n*-pentanol. Surprisingly, the MALDI-TOF mass spectrum of the product did not show the molecular ion M^+ of the expected product. Isotopic clusters peaking at m/z 1859 and 1216 were found instead. The former could be attributed to the fragment $[\text{M}-6\text{F}+6(\text{OC}_5\text{H}_{11})]^+$, in which six of the fluorine atoms were replaced with the pentyloxy group. The latter could be assigned to the

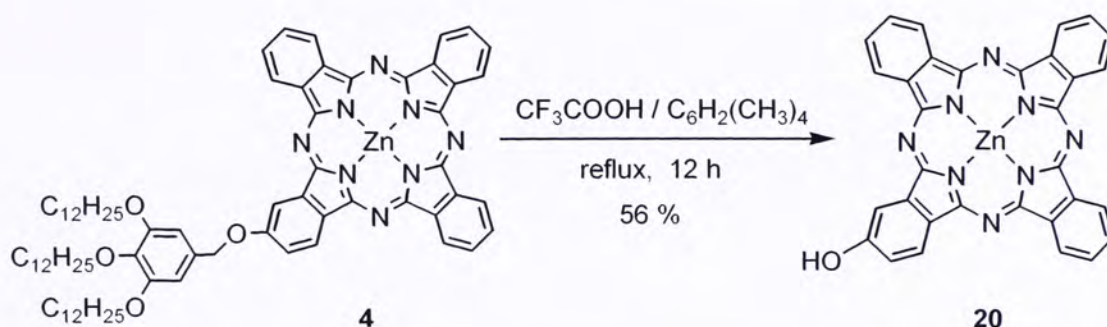
fragment $[M-6F+6(OC_5H_{11})-Ar]^+$, in which the bulky aryl group was further removed. Isotopic clusters which could be attributed to the fragments in which seven or eight of the fluorine atoms were replaced with the pentyloxy groups were also observed. It is likely that some of the fluoro groups are substituted with pentyloxy ions, generated from *n*-pentanol and DBU, either prior or after the cyclization. Scheme 2.7 shows a possible pathway leading to the formation of the fragments. Substitution of tetrafluorophthalonitrile with different alcohols in the presence of K_2CO_3 in DMF has been reported.¹² These reactions support one belief that substitution of some of the fluoro groups occurs under the reaction conditions.



Scheme 2.7. Mixed cyclization of **3** and tetrafluorophthalonitrile.

2.4 Preparation and Characterization of 2-Hydroxy Zinc(II) Phthalocyanine

The bulky group of the unsymmetrical zinc phthalocyanines **4** and **17-19** can in principle be removed to give the corresponding mono-hydroxy zinc phthalocyanines. However, due to the low yield of the halogenated phthalocyanines **17-19**, this deprotection reaction was only performed with the unsymmetrical phthalocyanine **4**. As shown in Scheme 2.8, treatment of **4** with trifluoroacetic acid (TFA) in the presence of tetramethylbenzene as a benzyl cation scavenger gave 2-hydroxy zinc(II) phthalocyanine (**20**) in satisfactory yield. The compound could be purified by column chromatography and had a pretty good solubility in THF, DMF, and DMSO.



Scheme 2.8. Preparation of 2-hydroxy zinc(II) phthalocyanine (**20**).

Figure 2.8 shows the ^1H NMR spectrum of phthalocyanine **20** in $\text{DMSO}-d_6$. The hydroxyl proton signal appears as a broad signal at δ 10.72. The phthalocyanine ring protons b, c, and d resonate as a doublet of doublet at δ

7.65, a doublet at δ 9.12, and a slightly broad signal at δ 8.66, respectively. The remaining multiplets at δ 9.1-9.3 and 8.1-8.2 are due to the remaining α and β phthalocyanine ring protons.

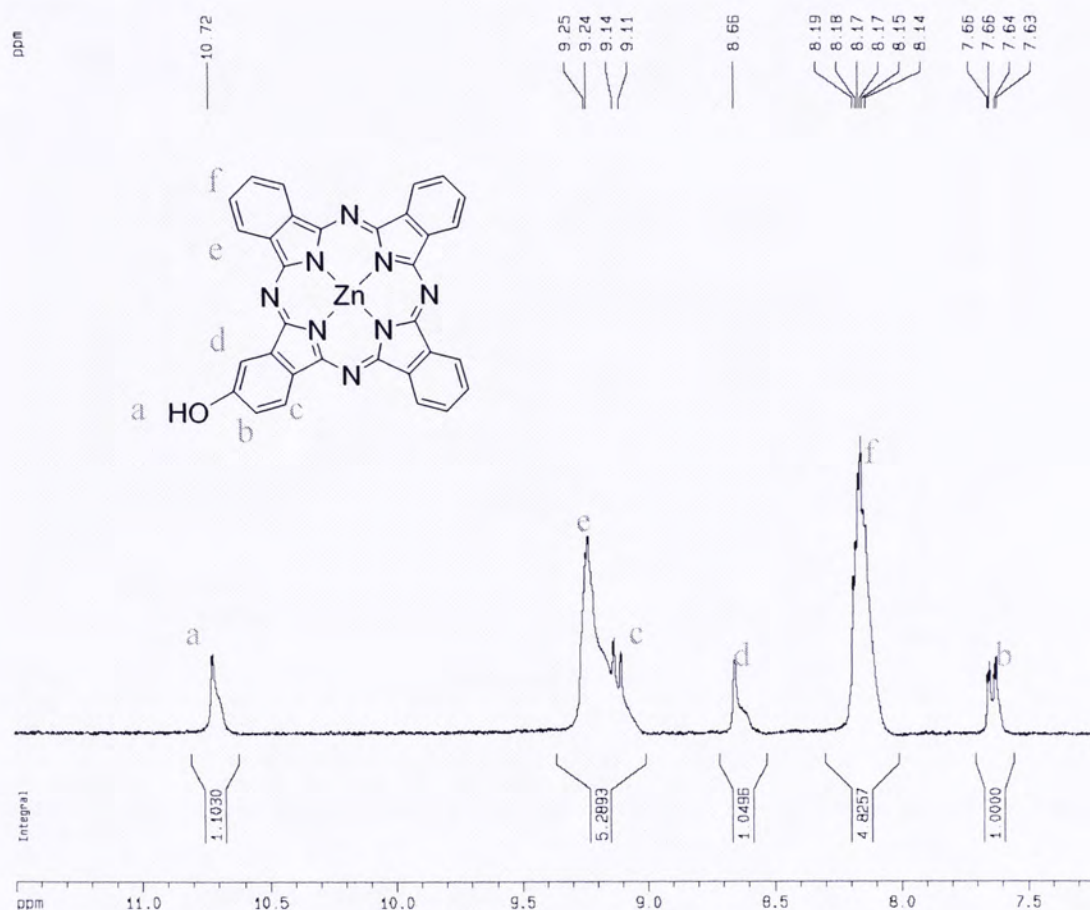


Figure 2.8. ¹H NMR spectrum of compound **20** in DMSO-*d*₆.

Figure 2.9 shows the UV-visible and fluorescence spectra of compound **20** in THF. The absorption spectrum shows a very sharp Q-band at 667 nm and a B-band at 342 nm. Upon excitation at 610 nm, this compound gives a very strong fluorescence emission at 681 nm. The fluorescence quantum yield was calculated to be 0.17. These spectral features indicate that this compound is

essentially non-aggregated in nature. This is extremely important for a photosensitizer in photodynamic therapy as aggregation provides an efficient nonradiative energy relaxation pathway, greatly shortening the excited state lifetimes.¹³

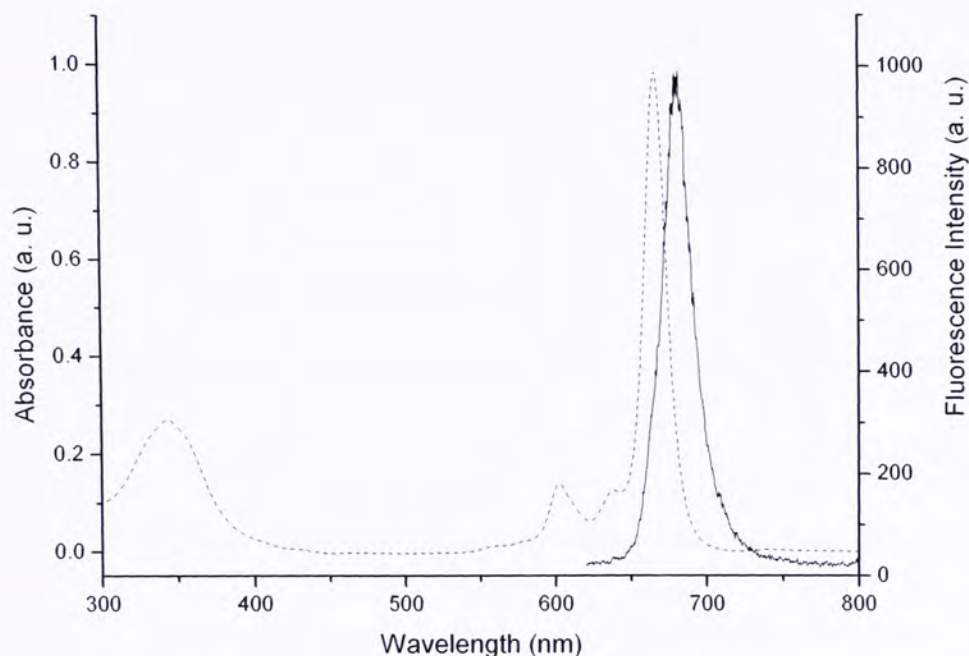


Figure 2.9. UV-visible (---) and fluorescence (—) spectra of 2-hydroxy zinc(II) phthalocyanine (**20**) in THF.

Figure 2.10 shows the MALDI-TOF mass spectrum of compound **20**, which displays an intense isotopic cluster assigned to the molecular ion. The good agreement of the relative abundance of the isotopic cluster with the simulated spectrum of M^+ , as shown in the inset, provides a strong evidence for the identity of this compound.

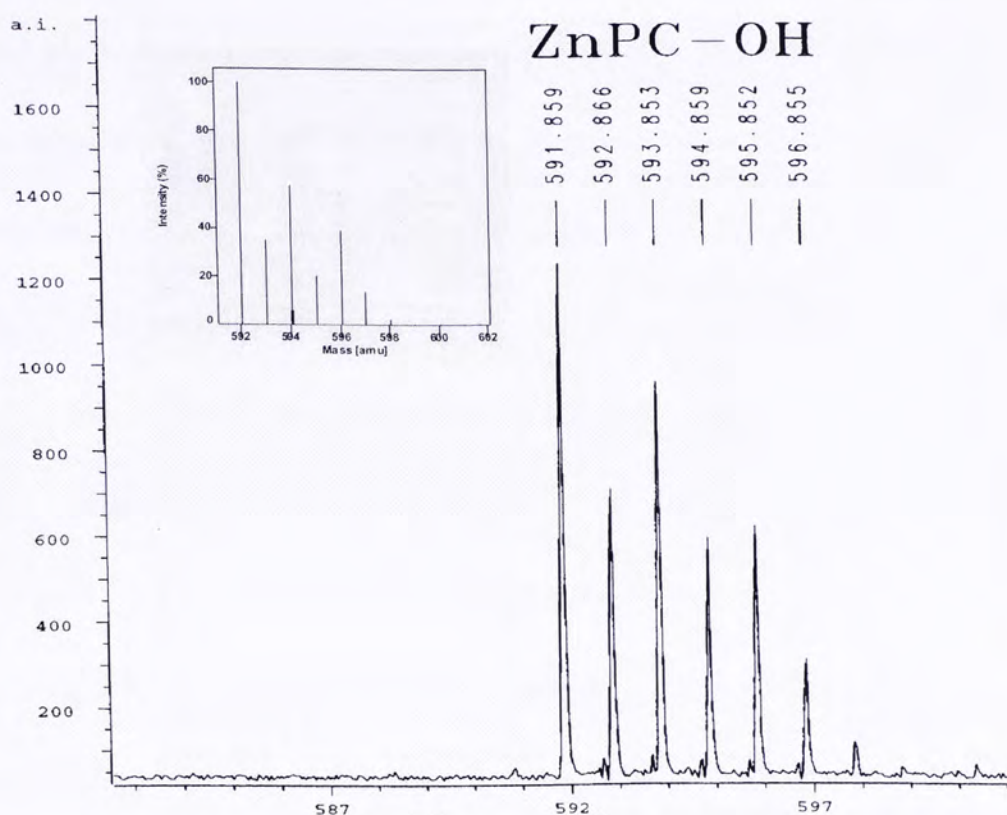


Figure 2.10. The MALDI-TOF mass spectrum of 2-hydroxy zinc(II) phthalocyanine (**20**). The simulated spectrum of the molecular ion is shown in the inset.

2.5 Introduction of Photodynamic Therapy (PDT)

Before reporting the photodynamic activity of 2-hydroxy zinc(II) phthalocyanine, a brief introduction of photodynamic therapy (PDT) is given below.

Photodynamic therapy has emerged to be a promising treatment for a range of cancer and age-related macular degeneration. It involves three individually non-toxic components, namely a photosensitizer, light, and oxygen, that are combined to cause cellular and tissue damage.² Figure 2.11 shows the

general photophysical mechanisms involved in photodynamic therapy.¹⁴ Upon exposure to light, the photosensitizer at its ground state is excited to the singlet excited state ($^1\text{Sen}^*$). The lifetime of this species is very short. It immediately interacts with surroundings leading to photobleaching or turns to the excited triplet state ($^3\text{Sen}^*$) via intersystem crossing (ISC). Then the triplet photosensitizer undergoes an electron transfer with oxygen molecule to give superoxide radicals (Type I mechanism), or transfers its energy to oxygen producing singlet oxygen (Type II mechanism). Both of these reactive oxygen species are cytotoxic to tumor cells, but the Type II mechanism is considered to be predominant in the photodynamic processes, and singlet oxygen plays a key role in PDT. The efficiency of singlet oxygen production can be determined empirically by the singlet-oxygen quantum yield (Φ_{Δ}), which describes the number of singlet oxygen molecules formed per photon of energy absorbed.² Therefore, the lifetime of the triplet photosensitizer and the quantum yield of singlet oxygen are significantly related to photodynamic efficiencies.¹⁵

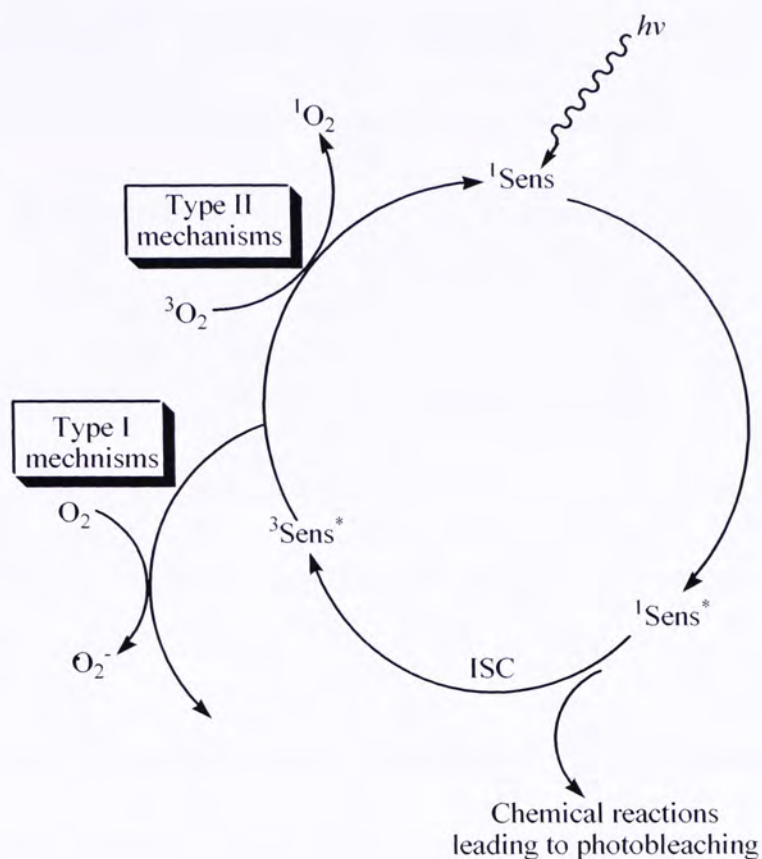


Figure 2.11. General photophysical mechanisms involved in photodynamic therapy.

Apart from the traditional porphyrin- or chlorin-type photosensitizers, phthalocyanines have been studied extensively as second-generation photosensitizers.¹⁶ They usually exhibit a strong absorption peak (Q-band) in the region of 680-780 nm (with a molar extinction coefficient in the range of $10^5 \text{ M}^{-1} \text{ cm}^{-1}$) resulting in better light penetration into skin and tissue.¹⁷ In addition, their long triplet lifetimes and high singlet oxygen quantum yields also make them promising candidates for photodynamic therapy.¹⁸

Unsymmetrical phthalocyanines with an amphiphilic character have some

advantages for use in photodynamic therapy. The cellular uptake and intracellular localization mostly depend on the hydrophobic and hydrophilic properties of photosensitizers.¹⁹ Because of the unique polarity, amphiphilic compounds usually have a better cellular uptake^{3,20} and can localize to the hydrophobic-hydrophilic interfaces in membranes and proteins.²¹ Amphiphilicity can also affect the degree to which a compound aggregates which, in turn, can influence the photophysical properties of a photosensitizer.¹⁶

2.6 In vitro Photodynamic Activities of 2-Hydroxy Zinc(II) Phthalocyanine

The *in vitro* photosensitizing activities of the amphiphilic compound **20** in Cremophor EL emulsion were investigated against two different cell lines, namely HT29 colon cancer cells and HepG2 human hepatocarcinoma cells. This part of the work was done by Pui-Chi Lo in our group and Prof. Jiandong Huang in Fuzhou University. Figure 2.12 shows the effect of **20** on HT29 cells. It can be seen that the compound is essentially non-toxic at concentration lower than 1 μM in the absence of light. Upon exposure to light, the compound exhibits a very high photocytotoxicity. The IC_{50} value, defined as the dye concentration required to kill 50 % of the cells, is about 0.13 μM . A similar result was obtained for HepG2 cells, as shown in Figure 2.13. The corresponding IC_{50} value is *ca.* 0.25 μM .

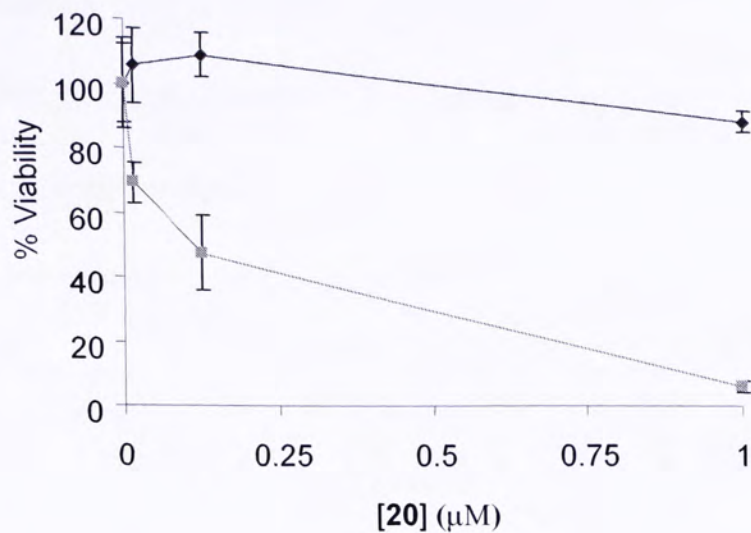


Figure 2.12. Effect of compound **20** against HT29 colon cells in the absence (♦) and presence (■) of light. For the latter, the cells were illuminated with a red light ($\lambda > 610$ nm, 40 mW cm^{-2} , 48 J cm^{-2}). Data are expressed as mean \pm SD ($n = 3$).

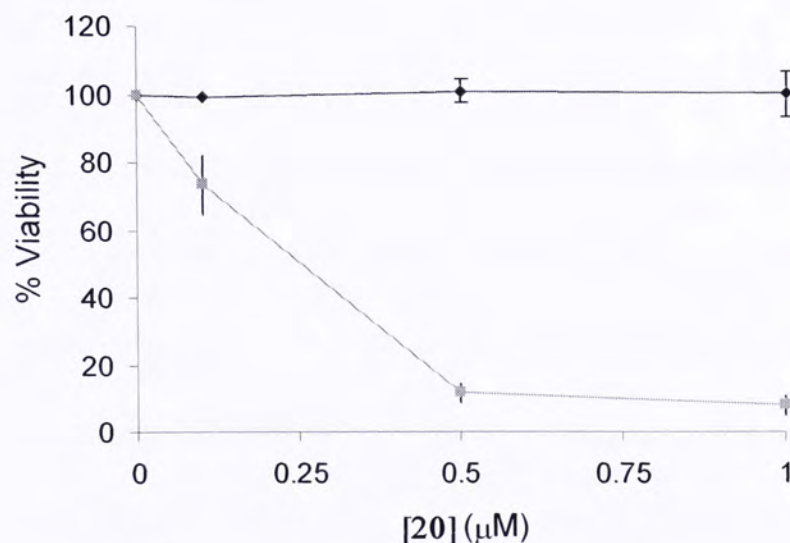


Figure 2.13. Effect of compound **20** against HepG2 human hepatocarcinoma cells in the absence (♦) and presence (■) of light. For the latter, the cells were illuminated with a red light ($\lambda > 610$ nm, 40 mW cm^{-2} , 48 J cm^{-2}). Data are expressed as mean \pm SD ($n = 3$).

2.7 Conclusion

By using phthalonitrile **3**, which has the bulky 3,4,5-tris(dodecyloxy)phenylmethoxy group in the mixed cyclization with unsubstituted phthalonitrile, the unsymmetrical “3+1” zinc(II) phthalocyanine has been prepared and separated readily. However, the halogenated analogues are difficult to be purified probably due to the lower solubility and higher aggregation tendency in common organic solvents. This bulky group can then be removed to produce 2-hydroxy zinc(II) phthalocyanine. This mono-hydroxy phthalocyanine shows a high *in vitro* photocytotoxicity against HT29 colon cancer cells and HepG2 human hepatocarcinoma cells.

2.8 Experimental Section

General remarks. DMF and DMSO were distilled from BaO under reduced pressure. 1-Pentanol was distilled from sodium under reduced pressure. THF was distilled from sodium benzophenone ketyl. Chromatographic purification was performed on silicon gel columns (Macherey Nagel, 70-230 mesh) with the indicated eluents unless otherwise stated. All other reagents and solvents were of reagent grade and used as received. ¹H NMR spectra were recorded with a Bruker DPX 300 spectrometer (300 MHz) in deuterated solutions. Spectra were referenced internally by using the residual solvent resonances ($\delta = 7.26$ ppm for CDCl₃, $\delta = 2.49$ ppm for DMSO-*d*₆, $\delta = 8.73, 7.58, 7.21$ ppm for pyridine-*d*₅) relative to SiMe₄. HPLC separation was performed under these

conditions: C18 column 4.6 × 250 mm; Temperature: 30 °C; Detection: 250-800 nm; Mobile phase: H₂O and THF; Flow rate: 1 mL/min; 0-30 min: linear gradient from 40 % to 100 % THF; 30-40 min: 100 % THF. UV-visible and steady-state fluorescence spectra were taken on a CARY 5G UV/Vis/NIR spectrophotometer and a Hitachi F-4500 spectrofluorometer, respectively. Fluorescence quantum yields (Φ_f) were determined by the following equation with unsubstituted zinc(II) phthalocyanine (ZnPc) in 1-chloronaphthalene as the reference,

$$\Phi_{sample} = \frac{F_{sample} \times A_{ref} \times n_{sample}^2}{F_{ref} \times A_{sample} \times n_{ref}^2} \times \Phi_{ref}$$

where F , A , and n are the measured fluorescence (area under the fluorescence spectra), the absorbance at 610 nm, and the refractive index of the solvent, respectively; the subscripts “sample” and “ref” denote the sample and the reference, respectively, and $\Phi_{ref} = 0.30$ for ZnPc in 1-chloronaphthalene.⁶ Liquid-secondary ion (LSI) and electrospray ionization (ESI) mass spectra were recorded on a Thermo Finnigan MAT95XL mass spectrometer. 3-Nitrobenzyl alcohol was used as the matrix for L-SIMS. MALDI-TOF mass spectra were recorded on a Bruker APEX47e ultra-high resolution Fourier transformation ion cyclotron resonance (FT-ICR) mass spectrometer with α -cyano-4-hydroxycinnamic acid as a matrix.

Synthesis of methyl 3,4,5-tris(dodecyloxy)benzoate (1).⁴ To a solution of methyl gallate (2.8 g, 15 mmol) in DMF (100 mL) was added K₂CO₃ (23 g, 0.18 mol). The mixture was stirred at 80 °C under N₂ for 1 h, then

1-bromododecane (14 g, 0.55 mol) was added. The resulting mixture was heated at 80 °C under a N₂ atmosphere with stirring for 17 h. TLC analysis (hexane/EtOAc, 7:3, v/v) indicated that the reaction was completed. The solvent was then removed under reduced pressure. The residue was dissolved in H₂O (80 mL) and extracted with EtOAc (60 mL × 3). The combined organic fractions were then dried over anhydrous MgSO₄, filtered, and rotary-evaporated. The crude product was recrystallized from EtOAc to give a white solid (7.8 g, 75 %). ¹H NMR (CDCl₃): δ 7.25 (s, 2 H, Ar-H), 3.95-4.05 (m, 6 H, -CH₂), 3.89 (s, 3 H, -CH₃), 1.65-1.85 (m, 6 H, -CH₂), 1.40-1.52 (m, 6 H, -CH₂), 1.15-1.40 (m, 24 H, -CH₂), 0.82-0.92 (m, 9 H, -CH₃).

Synthesis of 3,4,5-tris(dodecyloxy)phenylmethyl alcohol (2).⁴ To a solution of LiAlH₄ (1.7 g, 44 mmol) in THF (50 mL) at 0 °C was added dropwise a solution of **1** (7.6 g, 11 mmol) in THF (50 mL) with stirring. The mixture was then stirred at room temperature overnight. After cooling to 0 °C, the mixture was slowly quenched with a mixture of EtOH and H₂O (20 mL, 1:1, v/v). The precipitate was filtered off and washed with THF. The filtrate was dried with anhydrous MgSO₄ and the solvent was rotary-evaporated. The crude product was purified by column chromatography with EtOAc/hexane (1:4, v/v) as eluent (R_f = 0.55). The solvent was rotary-evaporated to give a white solid (6.2 g, 85 %). ¹H NMR (CDCl₃): δ 6.55 (s, 2 H, Ar-H), 4.59 (d, *J* = 6.0 Hz, 2 H, -CH₂), 3.87-4.00 (m, 6 H, -CH₂), 1.70-1.80 (m, 6 H, -CH₂), 1.40-1.52 (m, 6 H, -CH₂), 1.16-1.28 (m, 24 H, -CH₂), 0.80-0.92 (m, 9 H, -CH₃).

Synthesis of 4-(3,4,5-tris(dodecyloxy)phenylmethoxy)phthalonitrile

(3).⁵ A mixture of the alcohol **2** (3.8 g, 5.7 mmol), 4-nitrophthalonitrile (1.5 g, 8.6 mmol), and K₂CO₃ (3.9 g, 28 mmol) in DMSO (60 mL) was heated at 70 °C for 18 h. The mixture was then poured into ice-water and extracted with CH₂Cl₂ (150 mL × 3). The combined extracts was rotary-evaporated, then chromatographed with EtOAc/hexane (1:4, v/v) as eluent (R_f = 0.87). The white product was recrystallized from CH₂Cl₂/hexane (1:5, v/v) (3.5 g, 78 %). ¹H NMR (CDCl₃): δ 7.71 (d, *J* = 9.0 Hz, 1 H, Ar-H), 7.33 (d, *J* = 3.0, 1 H, Ar-H), 7.23 (d, *J* = 3.0, 1 H, Ar-H), 6.56 (s, 2 H, Ar-H), 5.03 (s, 2 H, -CH₂), 3.92-4.02 (m, 6 H, -CH₂), 1.70-1.86 (m, 6 H, -CH₂), 1.52-1.65 (m, 6 H, -CH₂), 1.16-1.40 (m, 24 H, -CH₂), 0.82-0.96 (m, 9 H, -CH₃).

Synthesis of unsymmetrical zinc(II) phthalocyanine 4. A mixture of phthalonitrile **3** (0.40 g, 0.51 mmol), phthalonitrile (0.59 g, 4.6 mmol), DBU (0.76 mL, 5.1 mmol), and Zn(OAc)₂·2H₂O (0.28 g, 1.3 mmol) was stirred in refluxing *n*-pentanol (10 mL) for 24 h. The solvent was then removed *in vacuo* and the residue was purified by column chromatography with THF/hexane (1:4, v/v) as eluent (R_f = 0.45). The solvent was evaporated to give the product as a green oil (0.20 g, 32 %). ¹H NMR (pyridine-*d*₅): δ 9.61-9.66 (brs, 6 H, Ar-H), 9.23 (s, 1 H, Ar-H), 8.24-8.28 (brs, 6 H, Ar-H), 8.03 (d, *J* = 6.0 Hz, 1 H, Ar-H), 7.44 (s, 2 H, Ar-H), 7.33 (d, *J* = 6.0 Hz, 1 H, Ar-H), 6.00 (s, 2 H, -CH₂), 4.33-4.37 (m, 6 H, -CH₂), 1.99-2.07 (m, 6 H, -CH₂), 1.61-1.76 (m, 6 H, -CH₂), 1.29-1.30 (m, 24 H, -CH₂), 0.82-0.92 (m, 9 H, -CH₃). HRMS (L-SIM): *m/z* calcd. for C₇₅H₉₄N₈O₄Zn

[MH⁺] 1235.6762, found 1235.6798. UV-Vis (THF): λ_{\max} (log ϵ) = 669 (5.25), 604 (4.46), 345 (4.73) nm. Fluorescence quantum yield: $\Phi_f = 0.34$.

Synthesis of 5,6-dichloro-1,3-isobenzofurandione (7).⁹ A mixture of 4,5-dichlorophthalic acid (30 g, 0.13 mol) and Ac₂O (50 mL) was heated under reflux for 5 h. After cooling, the precipitate was filtered and extensively washed with ether. The white product was dried in vacuum (24 g, 87 %).

Synthesis of 4,5-dichlorophthalimide (8).⁹ A solution of **7** (22 g, 0.10 mol) in HCONH₂ (30 mL) was refluxed for 3 h. After cooling, the precipitate was filtered and washed with H₂O. The light yellow product was dried in vacuum (19 g, 89 %).

Synthesis of 4,5-dichlorophthalamide (9).⁹ Compound **8** (22 g, 0.10 mol) was stirred in 25 % NH₄OH (300 mL) at room temperature for 24 h. 33 % NH₄OH (100 mL) was then added and stirring was continued for 24 h. The precipitate was filtered and washed with H₂O. The light yellow product was dried in vacuum (18 g, 77 %). ¹H NMR (DMSO-*d*₆): δ 7.88 (s, 2 H, -NH), 7.70 (s, 2 H, Ar-H), 7.50 (s, 2 H, -NH).

Synthesis of 4,5-dichlorophthalonitrile (10).⁹ At 0 °C, SOCl₂ (35 mL) was added to freshly distilled DMF (50 mL). After stirring for 2 h, compound **9** (10 g, 43 mmol) was added. The mixture was stirred at 0-5 °C for 5 h, and then at room temperature overnight. The mixture was then poured into ice water. The precipitate formed was filtered and washed with H₂O. The crude product was recrystallized twice from MeOH, and then dried in vacuum (5.5 g, 67 %).

^1H NMR (CDCl_3): δ 7.93 (s, Ar-H).

Synthesis of 4,5-dibromophthalimide (11).¹⁰ To a solution of phthalimide (15 g, 0.10 mol) in 20 % fuming sulfuric acid (90 mL) were added bromine (10 mL, 0.20 mol) and a little iodine as catalyst at 0 °C. The mixture was heated to 65-75 °C and stirred for 24 h. At the end of the reaction, air was bubbled through the solution to remove unreacted bromine. The mixture was then poured into 400g of ice, and the resulting suspension was extracted with EtOAc (150 mL \times 5). The combined organic solution was sequentially washed with H_2O (200 mL \times 2), a 2% solution of K_2CO_3 (200 mL), a saturated solution of $\text{Na}_2\text{S}_2\text{O}_3$ (150 mL), and H_2O (200 mL). The solution was then dried over anhydrous MgSO_4 and rotary-evaporated. The resulting product was recrystallized from acetone to give white crystals (2.8 g, 9 %). ^1H NMR ($\text{DMSO}-d_6$): δ 11.58 (s, 1 H, -NH), 8.12 (s, 2 H, Ar-H).

Synthesis of 4,5-dibromophthalamide (12).¹⁰ A mixture of **11** (8.1 g, 27 mmol) and conc. aqueous NH_3 (80 mL) was stirred at 50-60 °C for 1.5 h. After cooling, the precipitate was filtered and washed with ice-cold water and methanol. The resulting white solid was dried in vacuum (6.8 g, 79 %). ^1H NMR ($\text{DMSO}-d_6$): δ 7.88 (s, 2 H, -NH), 7.79 (s, 2 H, Ar-H), 7.48 (s, 2 H, -NH).

Synthesis of 4,5-dibromophthalonitrile (13).¹⁰ At 0 °C, SOCl_2 (25 mL) was added to freshly distilled DMF (50 mL). After stirring for 2 h, compound **12** (6.7 g, 21 mmol) was added. The mixture was stirred at 0-5 °C for 5 h, and then at room temperature overnight. The mixture was then poured into ice water.

The precipitate formed was filtered and washed with H₂O. The crude product was recrystallized twice from EtOH to give white crystals which were dried *in vacuo* (4.0 g, 67 %). ¹H NMR (CDCl₃): δ 8.06 (s, Ar-H).

Synthesis of 4,5-diiodophthalimide (14).¹¹ To a solution of phthalimide (15 g, 0.10 mol) in 20 % fuming sulfuric acid (60 mL) was added iodine (25 g, 0.10 mol). The mixture was heated to 75-80 °C and stirred for 24 h. The mixture was then poured into 400 g of ice, and the resulting suspension was filtered off using a funnel with a glass frit. The solid was washed with H₂O (200 mL × 2), a 2% solution of K₂CO₃ (200 mL), a saturated solution of Na₂S₂O₃ (150 mL), and H₂O (200 mL), and then dried *in vacuo*. The solid was extracted with acetone (750 mL) in a Soxhlet extractor for 48 h. After cooling, the precipitate formed was filtered off, and then H₂O (100 mL) was added to the filtrate. The solution was concentrated to 500 mL by rotary evaporator, and cooled to give bright-yellow precipitate. The precipitate was filtered and dried *in vacuo* to give a bright-yellow solid as pure product (9.4 g, 24 %). The filtrate was then concentrated to 100 mL by rotary evaporator. After cooling, the precipitate was filtered off and subjected to column chromatography with EtOAc/CHCl₃ (1:4, v/v) as eluent (R_f = 0.67) to give the product as a white solid (2.7 g, 7 %). ¹H NMR (DMSO-*d*₆): δ 11.43 (s, 1 H, -NH), 8.24 (s, 2 H, Ar-H).

Synthesis of 4,5-diiodophthalamide (15).¹¹ A mixture of **14** (12 g, 30 mmol) and conc. aqueous NH₃ (140 mL) was stirred at 50-60 °C for 1.5 h. After cooling, the precipitate was filtered and washed with ice-cold water and

methanol. The resulting white solid was dried in vacuum (6.0 g, 48 %). ^1H NMR ($\text{DMSO-}d_6$): δ 7.90 (s, 2 H, Ar-H), 7.84 (s, 2 H, -NH), 7.41 (s, 2 H, -NH).

Synthesis of 4,5-diiodophthalonitrile (16).¹¹ At 0 °C, SOCl_2 (8 mL) was added to freshly distilled DMF (10 mL). After stirring for 2 h, compound **15** (3.8 g, 9.1 mmol) was added. The mixture was stirred at 0-5 °C for 5 h, and then at room temperature overnight. The mixture was then poured into ice water. The precipitate formed was filtered and washed with H_2O . The crude product was recrystallized twice from EtOH to give white crystals which were dried *in vacuo* (2.6 g, 76 %). ^1H NMR (CDCl_3): δ 8.22 (s, Ar-H).

General procedure for the preparation of halogenated unsymmetrical zinc(II) phthalocyanines 17-19. A mixture of phthalonitrile **3** (0.10 g, 0.13 mmol), the halogenated phthalonitrile (0.38 mmol), $\text{Zn}(\text{OAc})_2 \cdot 2\text{H}_2\text{O}$ (0.29 g, 0.13 mmol), and DBU (0.8 mL, 0.51 mmol) was stirred in refluxing *n*-pentanol (3 mL) for 24 h. After cooling, the solvent was removed *in vacuo* and the mixture was subjected to column chromatography.

Chlorinated unsymmetrical zinc(II) phthalocyanine 17. The crude product was first purified by column chromatography with THF/hexane (1:9, v/v) as eluent. After eluting with THF/hexane (1:9, v/v), some impurity was eluted out. The crude product remained on the top of the silica gel column was then isolated with THF/hexane (1:4, v/v) as eluent. By checking with TLC, the portions with R_f values from 0.73 to 0.11 were collected. After removing the solvent by rotary evaporator, the mixture was further isolated by HPLC eluting

with THF/H₂O in different ratios as eluents at a rate of 1mL/min. The solution was rotary-evaporated to give the resulting green product (0.056 g, 3 %). MS (MALDI-TOF) isotopic clusters peaking at m/z 800.3 {calcd. for [C₃₂H₁₀N₈O₄Cl₆Zn]⁺ ([M-Ar]⁺) 800.58}.

Brominated unsymmetrical zinc(II) phthalocyanine 18. The crude product was first purified by column chromatography with THF/hexane (1:9, v/v) as eluent. After eluting with THF/hexane (1:9, v/v), some impurity was removed. The crude product remained on the top of the silica gel column was then isolated with THF/hexane (1:4, v/v) as eluent. By checking with TLC, the portions with R_f values from 0.82 to 0.22 were collected. The solution was rotary-evaporated, and then the mixture was further isolated by HPLC eluting with THF/H₂O in different ratios as eluents at a rate of 1mL/min. The solvent was rotary-evaporated to give the resulting green product (0.066 g, 3 %). ¹H NMR (pyridine-*d*₅): δ 9.45-9.78 (brs, 2 H, Ar-H), 9.41 (s, 1 H, Ar-H), 9.12-9.35 (brs, 2 H, Ar-H), 8.36-8.52 (brs, 2 H, Ar-H), 8.11 (s, 1 H, Ar-H), 7.84 (s, 1 H, Ar-H), 7.47 (s, 2 H, Ar-H), 5.86 (s, 2 H, -CH₂), 4.00-4.65 (m, 6H, -CH₂), 1.94-2.42 (m, 6 H, -CH₂), 1.62-1.85 (m, 6 H, -CH₂), 1.10-1.62 (m, 24 H, -CH₂), 0.80-1.10 (m, 9 H, -CH₃). MS (MALDI-TOF) isotopic clusters peaking at m/z 1471.5 {calcd. for [C₇₅H₈₈N₈O₄Br₃Zn]⁺ ([M-3Br]⁺) 1470.67}, 826.1 {calcd. for [C₃₂H₁₀N₈O₁Br₃Zn]⁺ ([M-3Br-Ar]⁺) 827.58}.

Iodinated unsymmetrical zinc(II) phthalocyanine 19. The crude product was first purified by column chromatography with THF/hexane (1:9, v/v)

as eluent. After eluting with THF/hexane (1:9, v/v), some impurity was removed. The crude product remained on the top of the silica gel column was then isolated with THF/hexane (1:4, v/v) as eluent. By checking with TLC, the portions with R_f values from 0.76 to 0.22 were collected. The solvent was rotary-evaporated, and then the mixture was further isolated by HPLC eluting with THF/H₂O in different ratios as eluents at a rate of 1 mL/min. The solution was rotary-evaporated to give the resulting green product (0.13 g, 5 %). ¹H NMR (pyridine-*d*₅): δ 9.72-9.98 (brs, 2 H, Ar-H), 9.37 (s, 1 H, Ar-H), 9.01-9.22 (brs, 2 H, Ar-H), 8.42-8.62 (brs, 2 H, Ar-H), 8.10 (s, 1 H, Ar-H), 7.74 (s, 1 H, Ar-H), 7.47 (s, 2 H, Ar-H), 5.84 (s, 2 H, -CH₂), 4.02-4.52 (m, 6 H, -CH₂), 1.85-2.25 (m, 6 H, -CH₂), 1.56-1.85 (m, 6 H, -CH₂), 1.08-1.56 (m, 24 H, -CH₂), 0.80-1.08 (m, 9 H, -CH₃). MS (MALDI-TOF) isotopic clusters peaking at m/z 1614.0 {calcd. for [C₇₅H₉₁N₈O₄I₃Zn]⁺ ([M-3I]⁺) 1614.67}, 971.6 {calcd. for [C₃₂H₁₃N₈O₁I₃Zn]⁺ ([M-3I-Ar]⁺) 971.58}. HRMS (ESI): m/z calcd. for C₇₅H₈₈N₈O₄Zn [M]⁺ 1990.0483, found 1990.0421.

Synthesis of 2-hydroxy zinc(II) phthalocyanine 20. A mixture of phthalocyanine **4** (0.27 g, 0.22 mmol), tetramethylbenzene (TMB) (0.03 g, 0.22 mmol), and trifluoroacetic acid (TFA) (15 mL, 0.22 mmol) was refluxed for 12 h. After cooling to room temperature, the mixture was evaporated under reduced pressure. The residue was purified by column chromatography with THF/hexane (1:4, v/v) as eluent to remove the unreacted phthalocyanine **4**. The product remained on the top of the silica gel column was then eluted with

THF/hexane (1:1, v/v) ($R_f = 0.62$). The solution was rotary-evaporated to give the product as a green solid (0.33 g, 56 %). $^1\text{H NMR}$ ($\text{DMSO-}d_6$): δ 10.72 (s, 1 H, OH), 9.12-9.30 (m, 6 H, Ar-H), 9.13 (d, $J = 4.5$ Hz, 1 H, Ar-H), 8.65 (d, $J = 3.0$ Hz, 1 H, Ar-H), 8.02-8.22 (m, 6 H, Ar-H), 7.65 (dd, $J = 3.0$ Hz, 1 H, Ar-H). MS (MALDI-TOF) isotopic clusters peaking at m/z 593.853 {calcd. for $[\text{C}_{32}\text{H}_{16}\text{N}_8\text{O}_1\text{Zn}]^+$ 593.91}.

***In vitro* studies.** Phthalocyanines were first dissolved in DMF (1.5 mM) and the solutions were diluted to 80 μM with a *ca.* 0.01 M aqueous solution of Cremophor EL (Sigma, 0.47 g in 100 mL of H_2O). The solutions were filtered with a 0.45 μM filter, then diluted with the medium to appropriate concentrations.

The HT29 human colon carcinoma cells (from ATCC) were maintained in Dulbecco's modified Eagle's medium (DMEM) (Invitrogen, cat no. 10313-021) supplemented with fetal calf serum (10 %), penicillin-streptomycin (100 units/mL and 100 g/mL, respectively), L-glutamine (2 mM) and transferrin (10 g/mL). The HepG2 human hepatocarcinoma cells were maintained in RPMI medium 1640 (Invitrogen) supplemented with 10 % fetal calf serum (Invitrogen). About 3×10^4 (for HT29) or 2×10^4 (for HepG2) cells per well in these media were inoculated in 96-multiwell plates and incubated overnight at 37 $^\circ\text{C}$ in a humidified 5 % CO_2 atmosphere.

The cells were rinsed with PBS and incubated with the above phthalocyanine solutions (100 μL) for 2 h under the same conditions. The cells were then rinsed again with PBS and re-fed with the growth medium (100 μL)

before being illuminated at ambient temperature. The light source consisted of a 300 W halogen lamp, a water tank for cooling, and a color glass filter (Newport) cut-on 610 nm. The fluence rate ($\lambda > 610$ nm) was 40 mW cm^{-2} . An illumination of 20 min led to a total fluence of 48 J cm^{-2} .

Cell viability was determined by means of the colorimetric MTT assay.²² After illumination, the cells were incubated at $37 \text{ }^\circ\text{C}$ under 5 % CO_2 overnight. An MTT (Sigma) solution in PBS ($50 \text{ }\mu\text{L}$, 3 mg mL^{-1}) was added to each well followed by incubation for 2 h under the same environment. A solution of sodium dodecyl sulfate (Sigma) in 0.04 M HCl (aq) ($50 \text{ }\mu\text{L}$, 10 % by weight) was then added to each well. The plate was incubated in a $60 \text{ }^\circ\text{C}$ oven for 30 min, then *iso*-propanol ($80 \text{ }\mu\text{L}$) was added to each well. The plate was agitated on a Bio-Rad microplate reader at ambient temperature for 20 s before the absorbance at 540 nm at each well was taken. The average absorbance of the blank wells, which did not contain the cells, was subtracted from the readings of the other wells. The cell viability was then determined by the equation: Cell Viability (%) = $[\sum(A_i/A_{\text{control}} \times 100)]/n$, where A_i is the absorbance of the i th data ($i = 1, 2, \dots, n$), A_{control} is the average absorbance of the control wells, in which the phthalocyanine was absent, and $n (= 3)$ is the number of the data points.

2.9 References

1. Ali, H.; van Lier, J. E. *Chem. Rev.* **1999**, *99*, 2379.
2. MacDonald, I. J.; Dougherty, T. J. *J. Porphyrins Phthalocyanines* **2001**, *5*,

- 105.
3. Hu, M.; Brasseur, N.; Yildiz, S. Z.; van Lier, J. E.; Leznoff, C. C. *J. Med. Chem.* **1998**, *41*, 1789.
 4. Hammond, S. R.; Zhou, W.; Gin, D. L. *Liquid Crystals* **2002**, *29*, 1151.
 5. Poon, K.; Liu, W.; Chan, P.; Yang, Q.; Chan, T. D.; Mak, T. C. W.; Ng, D. K. P. *J. Org. Chem.* **2001**, *66*, 1553.
 6. Austin, M.; Gouterman, M. *Bioinorg. Chem.* **1978**, *9*, 28.
 7. Turro, N. J. In *Modern Molecular Photochemistry*; University Science Books; Sausalito, CA, 1991; pp 191.
 8. Gorman, A.; Killoran, J.; O'Shea, C.; Kenna, T.; Gallagher, W. M.; O'Shea, D. F. *J. Am. Chem. Soc.* **2004**, *126*, 10619.
 9. Wöhrle, D.; Eskes, M.; Shigehara, K.; Yamada, A. *Synthesis* **1993**, 194.
 10. Leznoff, C. C.; Li, Z.; Isago, H.; D'Ascanio, A. M.; Terekhov, D. S. *J. Porphyrins Phthalocyanines* **1999**, *3*, 406.
 11. Terekhov, D. S.; Nolan, K. J. M.; McArthur, C. R.; Leznoff, C. C. *J. Org. Chem.* **1996**, *61*, 3034.
 12. (a) Eberhardt, W.; Hanack, M. *Synthesis* **1997**, 95. (b) Tian, M.; Wada, T.; Sasabe, H. *J. Heterocyclic Chem.* **1997**, *34*, 171.
 13. Howe, L.; Zhang, J. Z. *J. Phys. Chem. A* **1997**, *101*, 3207.
 14. Milgrom, L.; MacRobert, S. *Chem. Brit.* May **1998**, 45.
 15. *Photosensitization of Porphyrins and Phthalocyanines* Okura, I. Kodansha: Tokyo; GB Publisher **2000**, Chap. 5.

16. van Lier, J. E.; Ali, H. *Chem. Rev.* **1999**, *99*, 2379.
17. Wilson, B. C.; Jeeves, W. P. in *Photomedicine* Ben-Hur, E.; Rosenthal, I. CRC Press, Boca Ration, FL. **1987**, Vol.2, p 127.
18. Jori, G. *J. Photochem. Photobiol. A. Chem.* **1992**, *62*, 371.
19. (a) Berg, K.; Bommer, J. C.; Winkelman, J. W.; Moan, J. *Photochem. Photobiol.* **1990**, *52*, 775. (b) Boyle, R. W.; Dolphin, D. *Photochem. Photobiol.* **1996**, *64*, 469. (c) MacDonald, I. J.; Morgan, J.; Bellnier, D. A.; Paszkiewicz, G. M.; Whitaker, J. E.; Litchfield, D. J.; *et al.* *Photochem. Photobiol.* **1999**, *70*, 789.
20. (a) Michelsen, U.; Kliesch, H.; Schnurpfeil, G.; Sobbi, A. K.; Wöhrle, D. *Photochemistry and Photobiology* **1996**, *64(4)*, 694. (b) Bonneau, S.; Morlière, P.; Brault, D. *Biochemical Pharmacology* **2004**, *68*, 1443.
21. (a) Margaron, P.; Gergoire, M.; Scasnar, V.; *et al.* *Photochem. Photobiol.* **1996**, *63*, 217. (b) Chatterjee, S. R.; Srivastava, T. S.; Kamat, J. P.; Devasagayam, T. P. A. *Mol. Cell. Biochem.* **1997**, *166*, 25.
22. MTT = 3-(4,5-dimethyl-2-thiazolyl)-2,5-diphenyl-2*H*-tetrazolium bromide. Tada, H.; Shiho, O.; Kuroshima, K.; Koyama, M.; Tsukamoto, K. *J. Immunol. Methods* **1986**, *93*, 157.

Chapter 3 Synthesis, Characterization and in vitro Photodynamic Activities of Phthalocyanines Containing N,N-Di- methylaminoethylsulfanyl Substituents

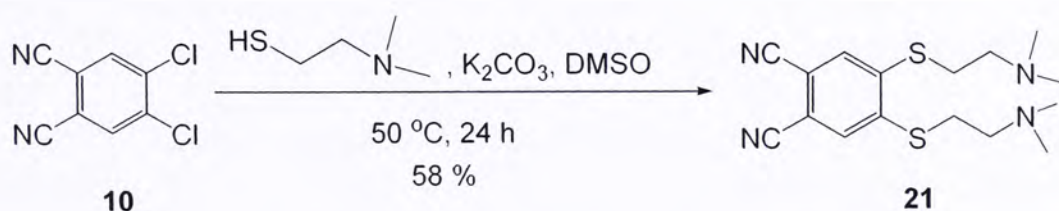
3.1 Introduction

For the application in photodynamic therapy, the photosensitization efficiency and intracellular localization of photosensitizers strongly depend on the structure, the amphiphilic character, and aggregation behavior of the photosensitizer in biological media.¹ The charge of the photosensitizer also plays an important role.² Some comparative studies of three differently charged (anionic, neutral, and cationic) zinc(II) phthalocyanines have shown that cationic phthalocyanines are usually more effective,³ which may be due to their higher singlet oxygen quantum yields and better tumor-localizing properties.⁴ Additionally, amphiphilic properties may facilitate the cellular uptake and excretion after treatment, which are also important in photodynamic therapy.⁵ The 2-hydroxy zinc(II) phthalocyanine reported in the previous chapter, for example, exhibits a high photocytotoxicity. There are relatively few reports on amphiphilic phthalocyanines bearing positively charged substituents for photodynamic therapy. In this chapter, the synthesis of a series of zinc(II) phthalocyanines substituted with *N,N*-dimethylaminoethylsulfanyl groups is reported. The spectroscopic properties and *in vitro* photobiological activities of

these compounds together with their methylated analogues are also reported herein.

3.2 Preparation and Characterization of Octasubstituted Phthalocyanines

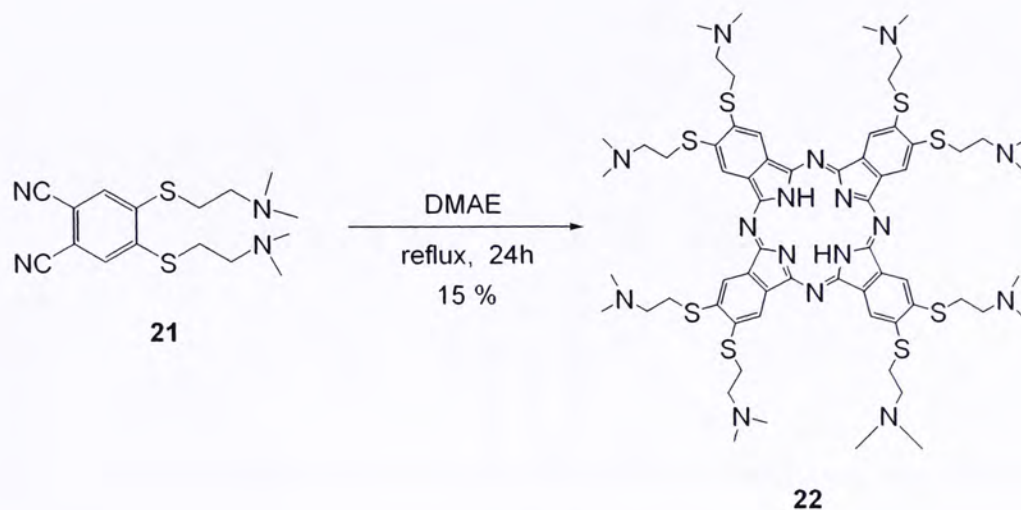
To prepare these compounds, the precursor 4,5-bis-(2-dimethylaminoethylsulfanyl)phthalonitrile (**21**) was first synthesized according to literature procedure with a slight modification.⁶ Treatment of 4,5-dichlorophthalonitrile with *N,N*-dimethylaminoethanethiol in the presence of K_2CO_3 in DMSO at 50 °C gave the product **21** (Scheme 3.1). The yield of the product is relatively higher than that obtained in DMF as used in the literature (45 %).



Scheme 3.1. Preparation of 4,5-bis-(2-dimethylaminoethylsulfanyl)-phthalonitrile (**21**).

Scheme 3.2 shows the synthetic route for the octakis-(2-dimethylaminoethylsulfanyl)phthalocyanine (**22**).⁶ Treatment of the dinitrile

21 in refluxing DMAE for 24 h gave the desired product which could be purified by column chromatography on a neutral alumina column.



Scheme 3.2. Synthesis of octakis(2-dimethylaminoethylsulfanyl)phthalocyanine (**22**).

Figure 3.1 shows the ^1H NMR spectrum of compound **22** in CDCl_3 . The aromatic protons of the phthalocyanine ring resonate as a broad signal at δ 8.71. The signals for the substituents appear as two triplets at δ 3.58 (for SCH_2) and 3.00 (for NCH_2), and a singlet at δ 2.54 (for CH_3). The inner NH protons, signal could not be observed due to the exchange with residual water in the solution.

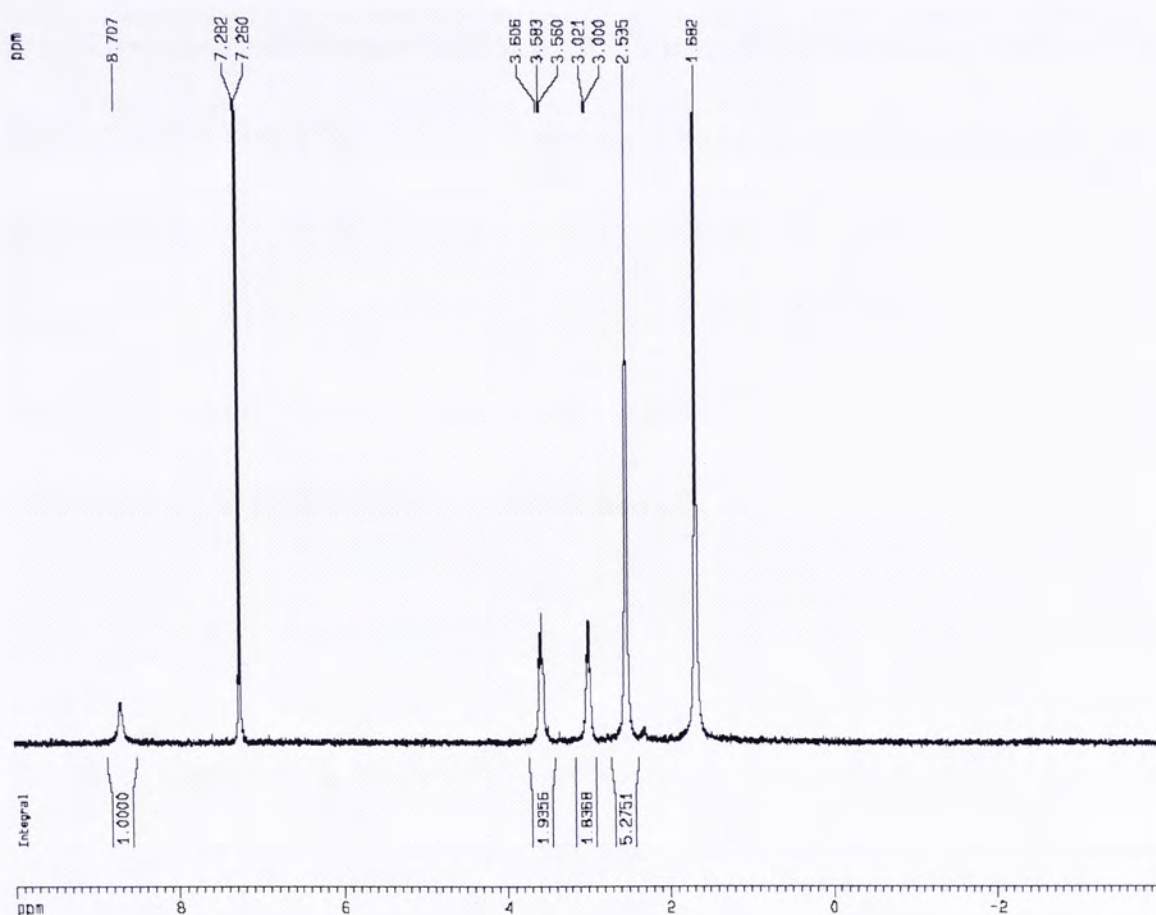


Figure 3.1. ^1H NMR spectrum of compound **22** in CDCl_3 .

Compound **22** was also characterized by $^{13}\text{C}\{^1\text{H}\}$ NMR spectrometry. The spectrum showed four singlets at δ 148.0 (for C-N), 139.8 (for CH), 132.9 (for C), and 120.3 (for C-S) for the phthalocyanine ring, and three other signals at δ 58.2 (for SCH_2), 45.5 (for NCH_3), and 31.5 (for NCH_2) for the substituents.

Figure 3.2 shows the absorption spectra of **22** in CHCl_3 in different concentrations. The compound gives typical absorptions of metal-free phthalocyanines, including two Q bands at 699 and 731 nm, two vibronic bands at 636 and 667 nm, a $n \rightarrow \pi^*$ transition at 450 nm, and a split Soret band at 332 and 359 nm. The Q bands are significantly red-shifted compared with those of other β -substituted phthalocyanines.⁷ The inset shows a plot of the Q-band absorbance

at 731 nm versus the concentration of **22**. The linear relationship indicates that this absorption obeys the Lambert-Beer law, and the compound is essentially free from aggregation in this organic solvent. Upon excitation at 630 nm, this compound gave a weak fluorescence emission at 733 nm with a quantum yield of 0.13. It is likely that the amino groups reductively quench the singlet excited state,⁸ leading to the weak fluorescence emission.

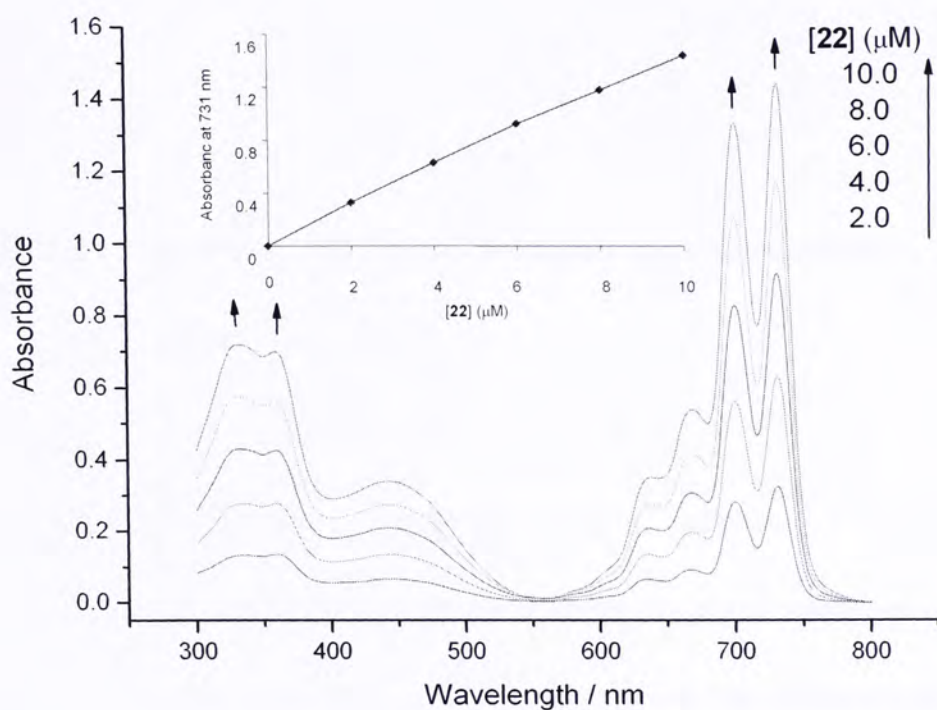
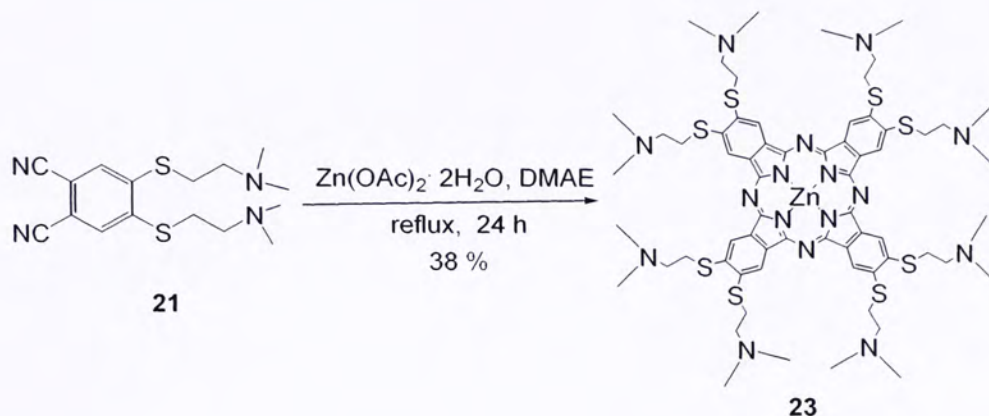


Figure 3.2. Electronic absorption spectra of **22** in CHCl_3 in different concentrations. The plot of the absorbance of the Q-band at 731 nm versus the concentration of **22** is given in the inset.

The zinc(II) phthalocyanine **23** was prepared by a similar procedure with the addition of zinc(II) acetate dihydrate (Scheme 3.3). Compared with the metal-free analogue, this metallated derivative was prepared in a higher yield.

The yield was also higher than that obtained by using DMF as the solvent (26 %).⁶



Scheme 3.3. Synthesis of octakis(2-dimethylaminoethylsulfanyl) zinc(II) phthalocyanine (**23**).

To reduce the aggregation tendency, a drop of pyridine-*d*₅ was added to a CDCl₃ solution of **23** for NMR measurement. The ¹H NMR spectrum is shown in Figure 3.3. The broad signal at δ 9.08 is attributed to the phthalocyanine ring protons. The remaining triplets at δ 3.58 (for SCH₂) and 2.98 (for NCH₂), and the singlet at δ 2.73 (for CH₃) are due to the substituents. The ¹³C{¹H} NMR spectrum also showed the expected signals which are consistent with the structure.

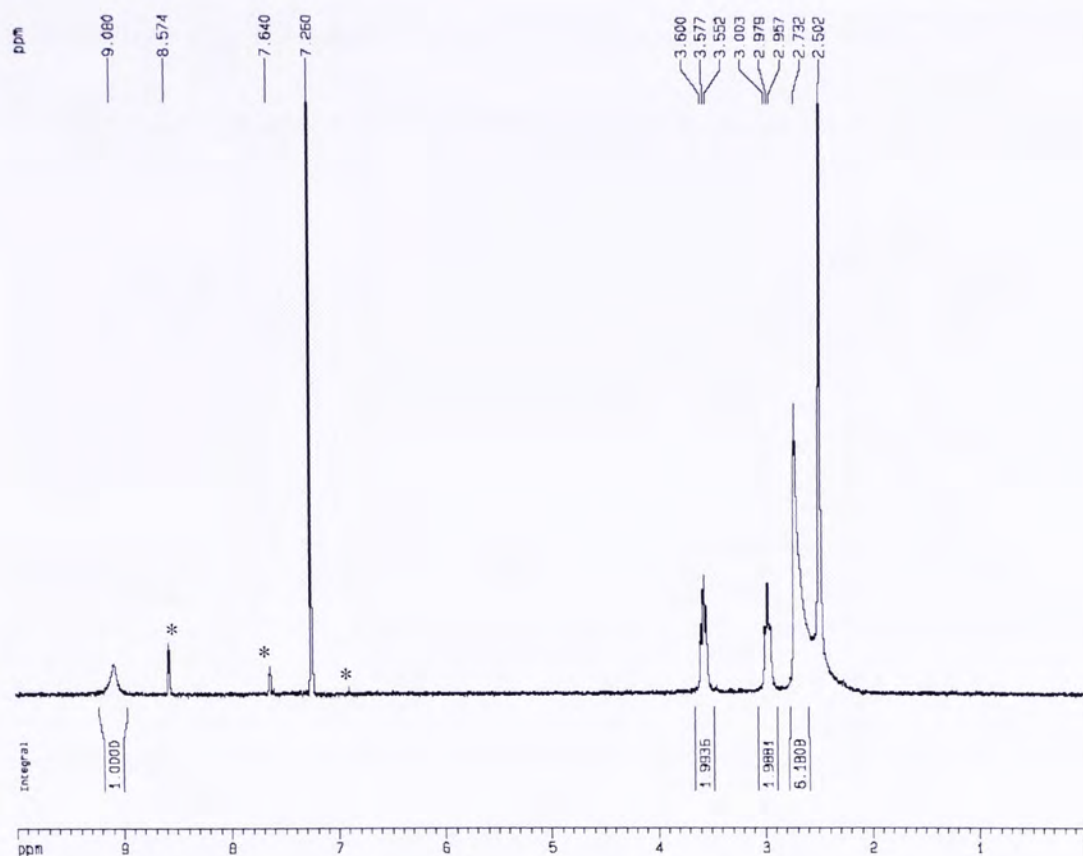


Figure 3.3. ^1H NMR spectrum of compound **23** in CDCl_3 with a drop of pyridine- d_5 . The asterisk indicates the signals of pyridine- d_5 .

Figure 3.4 shows the UV-vis spectra of phthalocyanine **23** in DMF in different concentrations. The absorption at 706 nm (Q-band) is attributed to the π - π^* transition from the highest occupied molecular orbital (HOMO) to the lowest unoccupied molecular orbital (LUMO) of the Pc^{2-} ring. The other absorption in the UV region at 380 nm (Soret band) arises from the transition from a deeper π level to LUMO.⁹ A vibronic band at 634 nm was also observed. The linear plot of the absorbance of the Q band versus the dye concentration shown in the inset indicates that the compound is free from aggregation in DMF. Upon excitation at 630 nm, the compound emitted at 712 nm. The fluorescence

quantum yield was calculated to be 0.13. The weak fluorescence was probably due to the amino groups which partially quench the singlet excited state.⁸

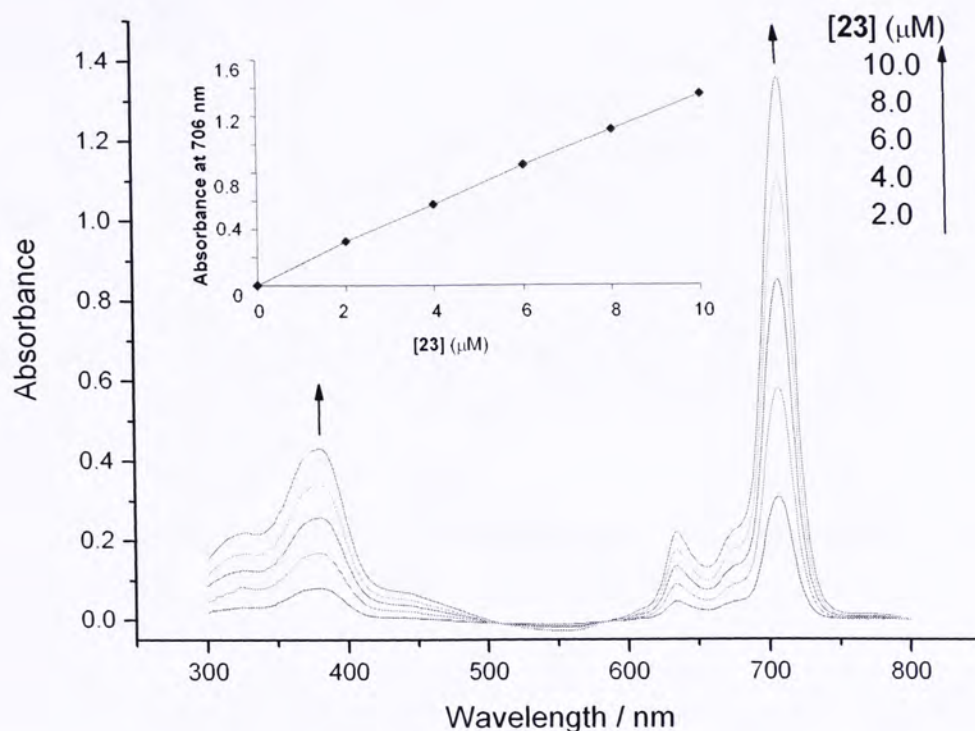
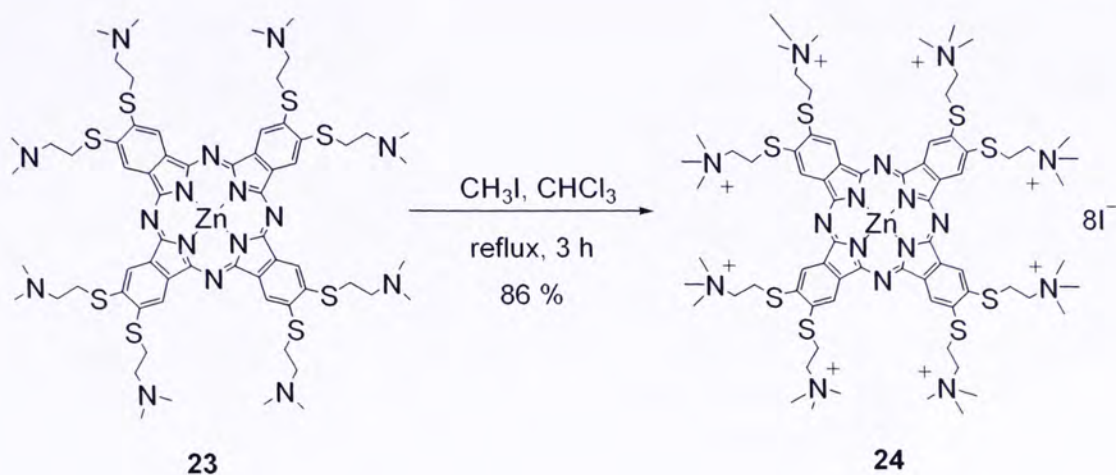


Figure 3.4. Electronic absorption spectra of **23** in DMF in different concentrations. The plot of the absorbance of the Q-band at 706 nm versus the concentration of **23** is given in the inset.

Compound **23** was methylated with methyl iodide in refluxing chloroform (Scheme 3.4). After cooling to room temperature, the resulting green precipitate was filtered off, washed with chloroform, and dried to give the cationic phthalocyanine **24** in high yield. The compound was also characterized with various spectroscopic methods including ^1H and ^{13}C NMR, and UV-vis spectroscopy.



Scheme 3.4. Synthesis of octacationic phthalocyanine **24**.

3.3 Characterization of Disubstituted Amphiphilic Zinc(II) Phthalocyanines

For comparison, the unsymmetrical amphiphilic zinc(II) phthalocyanines **25-27** were synthesized by Dr. Wubiao Duan in our group. Compound **25** was prepared by a mixed cyclization of phthalonitrile **21** and the unsubstituted phthalonitrile in the presence of $\text{Zn}(\text{OAc})_2 \cdot 2\text{H}_2\text{O}$ and DBU in *n*-pentanol, while compounds **26** and **27** were prepared by methylation and pentylation of **25** with the corresponding alkyl iodide in *N*-methyl-2-pyrrolidinone (NMP). The spectroscopic characterization of these compounds was performed by the author and the data are reported below.

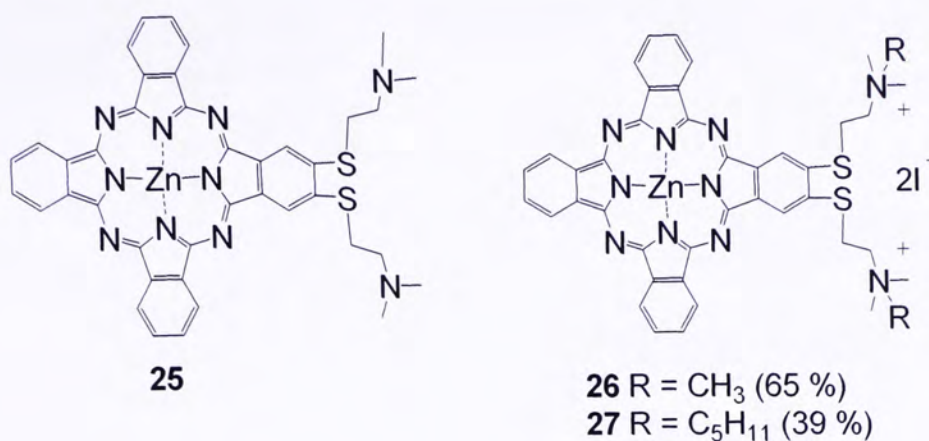


Figure 3.5 shows the ^1H NMR spectrum of **25** in $\text{DMSO-}d_6$. The singlet at δ 8.73 can be attributed to the phthalocyanine ring protons adjacent to the substituents. Because of the lower symmetry in this molecule, the other aromatic β - and α -protons of the unsubstituted isoindole units are split to several signals at *ca.* δ 8.1-8.2 and 9.0-9.3, respectively. The signals for the substituents appear as two triplets at δ 3.56 (for SCH_2) and 2.88 (for NCH_2) together with a singlet at δ 2.45 (for CH_3).

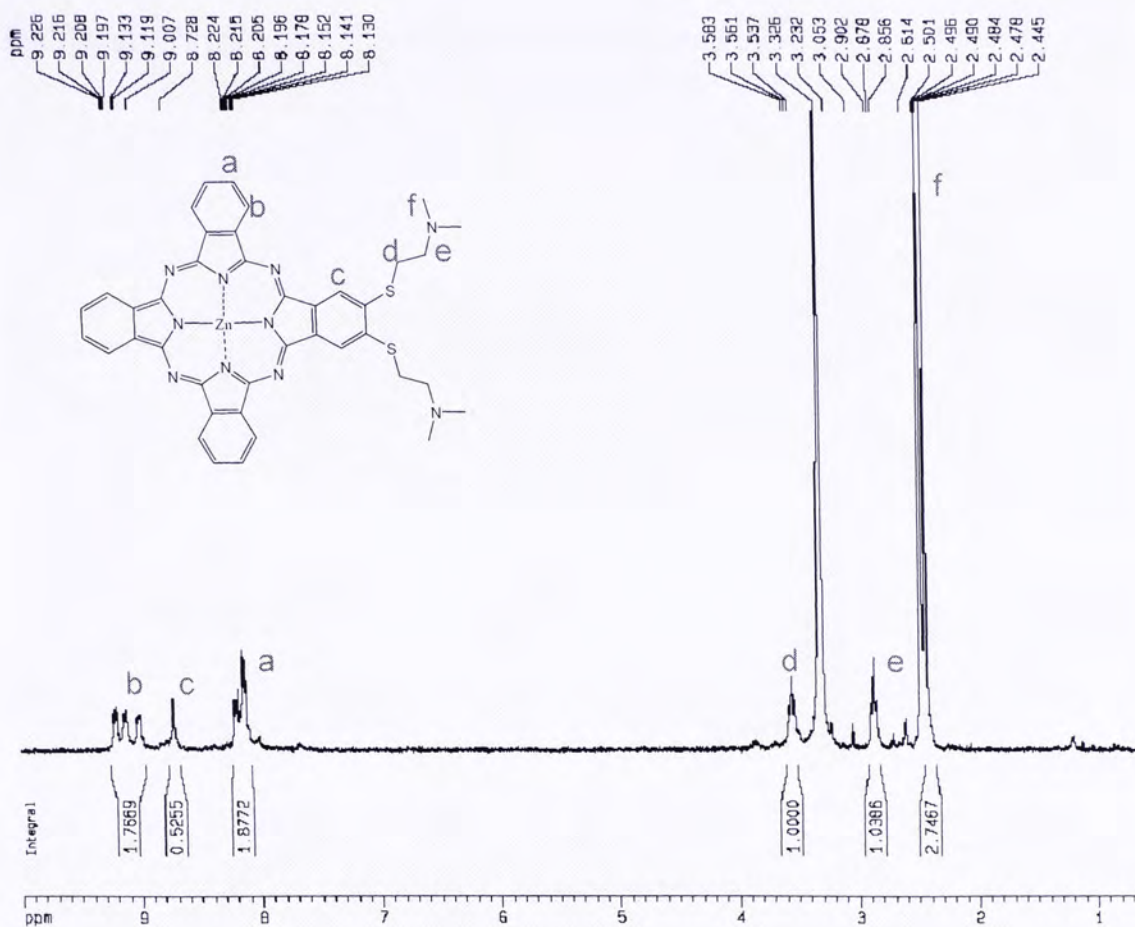


Figure 3.5. ^1H NMR spectrum of **25** in $\text{DMSO}-d_6$.

Figure 3.6 shows the absorption spectra of phthalocyanine **25** in DMF in different concentrations. In contrast to the octasubstituted analogue, the Q-band of this compound is not particularly red-shifted. It shows a sharp Q-band at 680 nm and a Soret band at 345 nm together with a vibronic band at 612 nm. The corresponding molar absorptivity was calculated to be 5.28, 4.73, and 4.50, respectively. The inset shows a plot of the Q-band absorbance versus the concentration of **25**. Again, a linear relationship was observed, indicating that the compound is essentially free from aggregation under these conditions. This is corroborated with the strong fluorescence emission at 687 nm upon excitation at 610 nm. The fluorescence quantum yield was calculated to be 0.27, which is

significantly higher than that of the symmetrical analogue **23**.

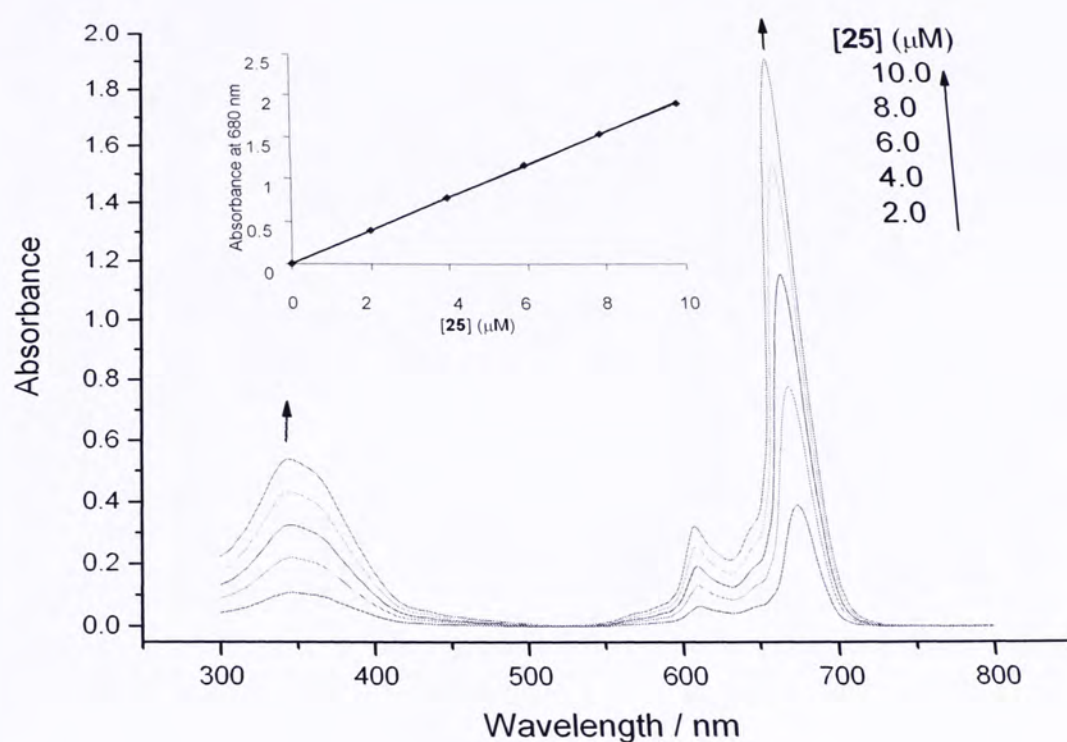


Figure 3.6. Electronic absorption spectra of **25** in DMF in different concentrations. The plot of the absorbance of the Q-band at 680 nm versus the concentration of **25** is given in the inset.

The ^1H NMR spectrum of the pentylated compound **27** in $\text{DMSO-}d_6$ is shown in Figure 3.7. The two multiplets at *ca.* δ 8.2-8.3 (6 H) and 9.3-9.4 (8 H) are due to the phthalocyanine β and α ring protons, respectively. The alkyl proton signals of the substituents appear as several triplets or singlet as assigned in Figure 3.7.

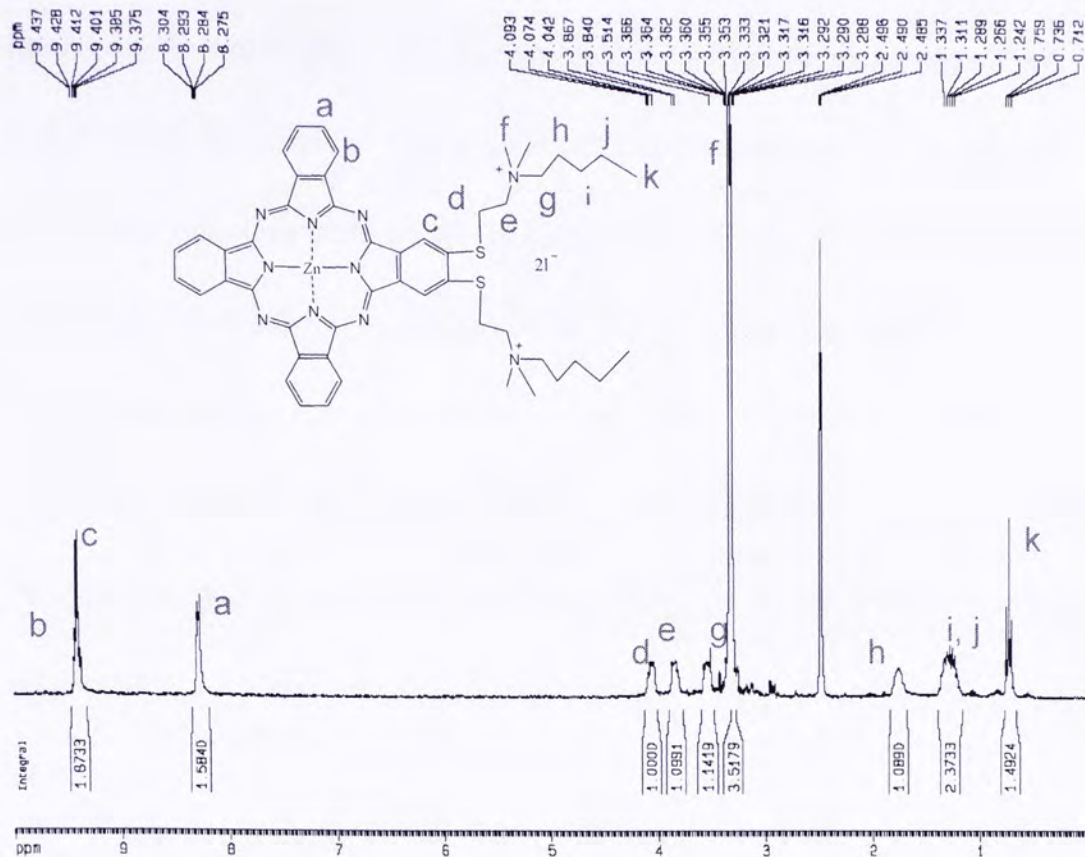


Figure 3.7. ^1H NMR spectrum of **27** in $\text{DMSO-}d_6$.

The $^{13}\text{C}\{^1\text{H}\}$ NMR spectrum of **27** in $\text{DMSO-}d_6$ showed 14 carbon signals for the phthalocyanine ring. The missing two signals might be overlapped with some of these signals. The spectrum also showed 7 other signals for the substituents. It is believed that the signal at δ 21.9 contains two overlapping signals.

The electronic absorption and photophysical properties of compounds **23-27** are summarized in Table 3.1. From this table, it can be seen that the absorptions of the octasubstituted zinc(II) phthalocyanines **23** and **24** are significantly red-shifted compared with those of the disubstituted analogues **25-27**. For example, the Q-band absorption of phthalocyanine **23** is red-shifted by 32 nm

compared with that of **25**. The disubstituted zinc(II) phthalocyanines **25-27** have stronger fluorescence than the octasubstituted counterparts. For instance, the fluorescence quantum yield of **25** is twice as large as that of **23**. It is similar for compounds **26** and **24**. In addition, the singlet oxygen quantum yields of the disubstituted phthalocyanines are also larger than those of the octasubstituted analogues. These results show that the disubstituted phthalocyanines **25-27** have better photophysical properties and may serve as better photosensitizers for photodynamic therapy.

Table 3.1. Electronic absorption and photophysical data for zinc(II) phthalocyanines **23-27** in DMF.

Compound	λ_{max} (nm) (log ϵ)	λ_{em} (nm)	Φ_{f}^c	Φ_{Δ}^d
23	380 (4.64), 634 (4.34), 706 (5.13)	712 ^a	0.13	0.13
24	384 (4.71), 631 (4.38), 704 (5.15)	709 ^a	0.15	0.19
25	345 (4.73), 612 (4.50), 680 (5.28)	687 ^b	0.27	0.50
26	352 (4.76), 611 (4.51), 681 (5.28)	688 ^b	0.25	0.26
27	349 (4.70), 612 (4.47), 682 (5.24)	688 ^b	0.26	0.29

^a Excited at 630 nm. ^b Excited at 610 nm. ^c With reference to ZnPc with $\Phi_{\text{f}} = 0.30$ in 1-chloronaphthalene. ^d With reference to ZnPc with $\Phi_{\Delta} = 0.56$ in DMF.¹⁰

3.4 *In vitro* Photodynamic Activities

The *in vitro* photodynamic activities of compounds **23-27** in Cremophor EL emulsion were investigated against HepG2 human hepatocarcinoma cell lines. The photoactivity of **25-27** was also studied toward two other cell lines, namely HT29 and T84 human colorectal adenocarcinoma. This part of the work was done by Pui-Chi Lo in our group.

Figure 3.8 shows the effect of phthalocyanine **23** on HepG2 cells. It can be seen that this compound is essentially noncytotoxic at the concentration lower than 8 μM in the absence of light. Upon exposure to light, it is slightly photocytotoxic. The IC_{50} value, defined as the dye concentration required to kill 50 % of the cells, is *ca.* 4.6 μM . The cationic zinc phthalocyanine **24** has a much higher photocytotoxicity and gives a much lower IC_{50} value (0.09 μM) (Figure 3.9). Hence, the cationic phthalocyanine **24** is much more efficient than the neutral analogue in *in vitro* photodynamic activities under these conditions.

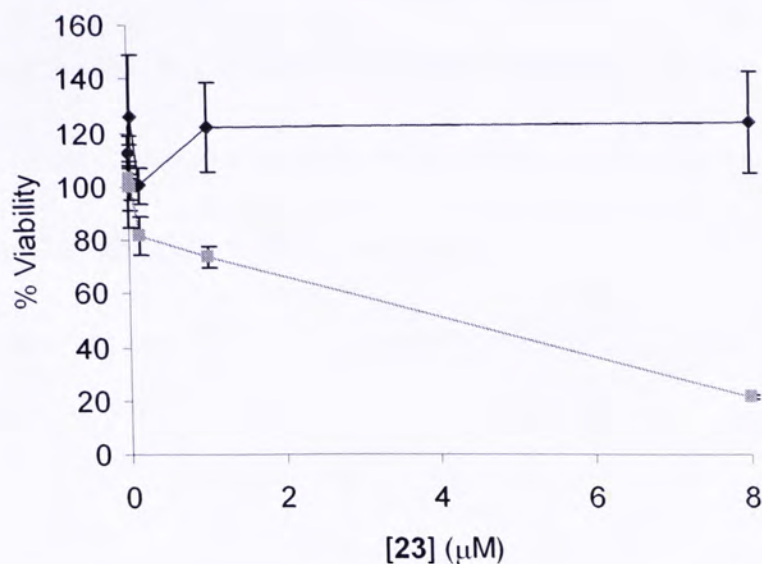


Figure 3.8. Effect of compound **23** against HepG2 human hepatocarcinoma cells in the absence (◆) and presence (■) of light. For the latter, the cells were illuminated with a red light ($\lambda > 610$ nm, 40 mW cm^{-2} , 48 J cm^{-2}). Data are expressed as mean \pm SD ($n = 1$).

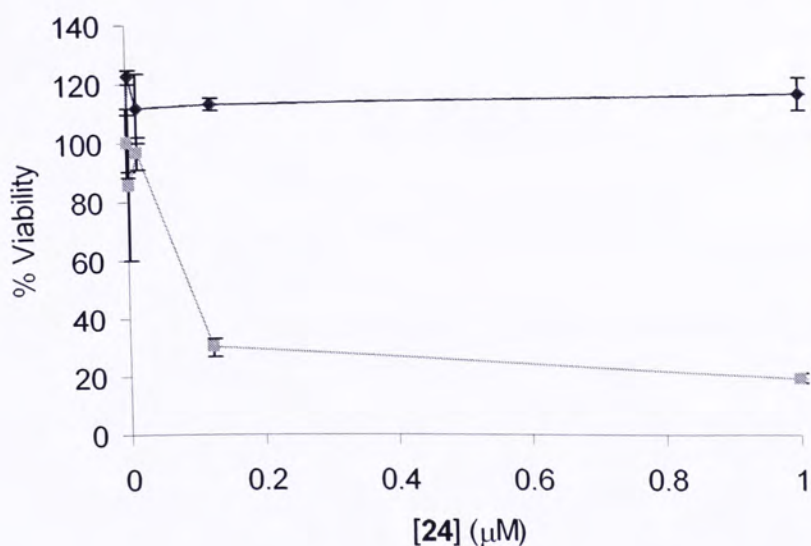


Figure 3.9. Effect of compound **24** against HepG2 human hepatocarcinoma cells in the absence (◆) and presence (■) of light. For the latter, the cells were illuminated with a red light ($\lambda > 610$ nm, 40 mW cm^{-2} , 48 J cm^{-2}). Data are expressed as mean \pm SD ($n = 1$).

Compared with the octasubstituted phthalocyanines, the disubstituted phthalocyanine **25** also has a very high PDT efficiency against HepG2 cells (Figure 3.10). The IC_{50} value is down to $0.07 \mu\text{M}$. The corresponding values for the amphiphilic zinc(II) phthalocyanines **26** and **27** are 0.20 and $0.33 \mu\text{M}$, respectively, showing that the disubstituted neutral phthalocyanine **25** has the highest photodynamic activities toward HepG2 cells (Table 3.2).

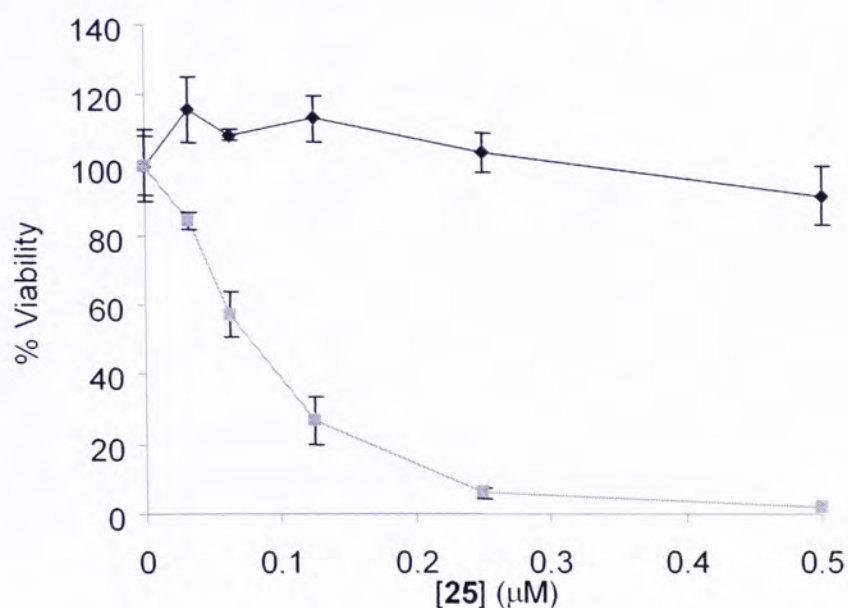


Figure 3.10. Effect of compound **25** against HepG2 human hepatocarcinoma cells in the absence (◆) and presence (■) of light. For the latter, the cells were illuminated with a red light ($\lambda > 610 \text{ nm}$, 40 mW cm^{-2} , 48 J cm^{-2}). Data are expressed as mean \pm SD ($n = 1$).

The photoactivity of compounds **25-27** against HT29 and T84 human colon adenocarcinoma was also examined. The IC_{50} values are also summarized in Table 3.2. It can be seen that all the three compounds are also photocytotoxic

against these two cell lines. The IC_{50} values are as low as $0.07 \mu\text{M}$.

Table 3.2. Comparison of the IC_{50} values of zinc(II) phthalocyanines **23-27** against HepG2, HT29 and T84.

Compound	IC_{50} (μM) ^a		
	for HepG2	for HT29	for T84
23	4.6	—	—
24	0.09	—	—
25	0.07	0.17	0.12
26	0.20	0.09	0.13
27	0.33	0.18	0.19

^a Defined as the dye concentration required to kill 50 % of the cells.

3.5 Conclusion

By using the precursor 4,5-bis-(2-dimethylaminoethylsulfanyl)-phthalonitrile, the octasubstituted metal-free and zinc(II) phthalocyanines as well as the corresponding disubstituted zinc(II) phthalocyanines have been prepared and characterized. The corresponding *N*-methylated and *N*-pentylated analogues have also been synthesized. Compared with the octasubstituted phthalocyanines, the disubstituted analogues have larger fluorescence quantum yields and singlet oxygen quantum yields. The *in vitro* photodynamic activities of all the zinc(II) phthalocyanines have been evaluated against three different cell lines. The

amphiphilic disubstituted phthalocyanines are particularly potent giving IC_{50} values as low as $0.07 \mu\text{M}$.

3.5 Experimental Sections

General remarks. Experimental details regarding solvent purification and instrumentations have been described in the previous chapter. In addition, DMAE was distilled from K_2CO_3 under reduced pressure. Chromatographic purification was performed on silica gel columns (Macherey Nagel, 70–230 mesh) or neutral alumina columns (70-230 mesh ASTM) with the indicated eluents unless otherwise stated. ^{13}C NMR spectra were recorded with a Bruker DPX 300 spectrometer (300 MHz) in deuterium solutions. Spectra were referenced internally by using the residual solvent resonances ($\delta = 77.0$ ppm for CDCl_3 , $\delta = 39.7$ ppm for $\text{DMSO-}d_6$). Singlet oxygen quantum yields (Φ_Δ) were measured by the method of chemical quenching of 1,3-diphenylisobenzofuran (DPBF) described by Wöhrle et al.,¹⁰ except that the absolute light intensity of our system was not determined. All measurements were performed in DMF and referenced to ZnPc ($\Phi_\Delta = 0.56$). Elemental analysis was performed by Madac, Brunel Science Centre (UK).

Synthesis of 4,5-bis-(2-dimethylaminoethylsulfanyl)phthalonitrile (21).⁶ A mixture of 4,5-dichlorophthalonitrile (**10**) (0.21 g, 1.1 mmol) and 2-dimethylaminoethanethiol hydrochloride (0.48 g, 3.4 mmol) in DMSO (12 mL) was stirred at 50°C , and then K_2CO_3 (0.74 g, 5.4 mmol) was added in several

portions in the period of 30 min. After stirring at 50 °C for 24 h, the mixture was cooled to room temperature and poured into ice-water. The precipitate formed was filtered and washed with H₂O. The crude product was dried *in vacuo* and subjected to column chromatography with MeOH/CH₂Cl₂ (1:9, v/v) as eluent ($R_f = 0.93$). A white crystalline product was obtained after rotary-evaporation the solution (0.21 g, 58 %). ¹H NMR (CDCl₃): δ 7.47 (s, 2 H, Ar-H), 3.13 (t, $J = 7.5$ Hz, 4 H, S-CH₂), 2.66 (t, $J = 6.0$ Hz, 4 H, N-CH₂), 2.29 (s, 12 H, N-CH₃). HRMS (FAB): m/z calcd. for C₁₆H₂₂N₄S₂ [MH⁺] 335.1359, found 335.1365.

Synthesis of octakis(2-dimethylaminoethylsulfanyl)phthalocyanine (22).⁶ A solution of the precursor **21** (0.20 g, 0.60 mmol) in DMAE (1 mL) was refluxed under N₂ for 24 h. After cooling to room temperature, the green product was filtered off, washed with H₂O, and dried *in vacuo*. The crude product was purified by column chromatography on a neutral alumina column with EtOH/CHCl₃ (1:10, v/v) as eluent ($R_f = 0.89$) to give a green solid (0.03 g, 15 %). ¹H NMR (CDCl₃): δ 8.71 (s, 8 H, Ar-H), 3.58 (t, $J = 6.0$ Hz, 16 H, S-CH₂), 3.00 (t, $J = 6.0$ Hz, 16 H, N-CH₂), 2.54 (s, 48 H, N-CH₃), -2.65 to -1.90 (brs, 2 H, NH, exchangeable). ¹³C{¹H} NMR (CDCl₃): δ 148.0 (C-N), 139.8 (CH), 133.0 (C), 120.3 (C-S), 67.7 (CH₂-S), 45.5 (CH₃-N), 31.5 (CH₂-N). UV-Vis (CHCl₃): λ_{\max} (log ϵ) = 332 (4.86), 359 (4.85), 636 (4.54), 667 (4.73), 699 (5.12), 731 (5.16) nm. Fluorescence quantum yield: $\Phi_f = 0.13$.

Synthesis of octakis(2-dimethylaminoethylsulfanyl) zinc(II) phthalocyanine (23).⁶ A mixture of the precursor **21** (0.20 g, 0.60 mmol) and

Zn(OAc)₂·2H₂O (0.03 g, 0.15 mmol) in DMAE (1.0 mL) was refluxed under N₂ for 24 h. After cooling to room temperature, a MeOH/H₂O mixture (20 mL, MeOH : H₂O = 1:1, v/v) was added to precipitate the product. The precipitate was filtered off, washed with H₂O, then chromatographed on a neutral alumina column with EtOH/CHCl₃ (1:10, v/v) as eluent (R_f = 0.84). The product was isolated as a dark green solid (0.08 g, 38 %). ¹H NMR (CDCl₃): δ 9.08 (s, 8 H, Ar-H), 3.58 (t, *J* = 6.0 Hz, 16 H, S-CH₂), 2.98 (t, *J* = 6.0 Hz, 16 H, N-CH₂), 2.73 (s, 48 H, N-CH₃). ¹³C{¹H} NMR (CDCl₃): δ 152.0 (C-N), 138.5 (CH), 135.6 (C), 121.0 (C-S), 58.1 (CH₂-S), 45.3 (CH₃-N), 31.5 (CH₂-N). UV-Vis (DMF): λ_{max} (log ε) = 380 (4.64), 634 (4.34), 706 (5.13) nm. Fluorescence quantum yield: Φ_f = 0.13. Singlet oxygen quantum yield: Φ_Δ = 0.13.

Synthesis of octakis(2-trimethylammoniumethylsulfanyl) zinc(II) phthalocyanine octaiodide (24).⁶ A mixture of **23** (0.07 g, 0.05 mmol) and methyl iodide (0.07 g, 0.50 mmol) in CHCl₃ (2.0 mL) was refluxed under N₂ for 3 h. After cooling to room temperature, the green precipitate formed was filter off and washed with CHCl₃. The green solid collected was then dried *in vacuo* (0.11 g, 86 %). ¹H NMR (DMSO-*d*₆): δ 9.53 (s, 8 H, Ar-H), 4.07 (t, *J* = 4.2 Hz, 16 H, S-CH₂), 3.95 (t, *J* = 4.5 Hz, 16 H, N-CH₂), 3.41 (s, 72 H, N-CH₃). ¹³C{¹H} NMR (CDCl₃): δ 153.1 (C-N), 137.0 (two overlapping signals, CH and C), 123.1 (C-S), 63.6 (CH₂-S), 52.9 (CH₃-N), 26.6 (CH₂-N). UV-Vis (DMF): λ_{max} (log ε) = 384 (4.71), 631 (4.38), 704 (5.15) nm. Fluorescence quantum yield: Φ_f = 0.15. Singlet oxygen quantum yield: Φ_Δ = 0.19.

Characterization of 2,3-(*N,N*-dimethylaminoethylsulfanyl) zinc(II) phthalocyanine (25). ^1H NMR (DMSO- d_6): δ 9.01-9.23 (m, 6 H, Ar-H), 8.73 (s, 2 H, Ar-H), 8.13-8.22 (m, 6 H, Ar-H), 3.56 (t, $J = 6.0$ Hz, 4 H, S-CH₂), 2.88 (t, $J = 6.0$ Hz, 4 H, N-CH₂), 2.45 (s, 12 H, N-CH₃). $^{13}\text{C}\{^1\text{H}\}$ NMR (DMSO- d_6): δ 152.4, 151.4 (C-N); 137.8, 134.8 (CH); 129.3 (C), 122.4 (CH), 119.3 (C-S), 57.9 (CH₂-S), 45.3 (CH₃-N), 30.9 (CH₂-N). UV-Vis (DMF): λ_{max} (log ϵ) = 345 (4.73), 612 (4.50), 680 (5.28) nm. Fluorescence quantum yield: $\Phi_f = 0.27$. Singlet oxygen quantum yield: $\Phi_\Delta = 0.50$. Elemental analysis calcd (%) for C₄₀H₃₄N₁₀S₂Zn·2H₂O: C 58.56, H 4.68, N 17.08, S 7.82, Zn 7.97; found: C 58.50, H 4.01, N 16.70, S 7.18, Zn 7.64. HRMS (FAB): m/z calcd. for C₄₀H₃₄N₁₀S₂Zn [MH⁺] 783.1774, found 783.1746.

Characterization of 2,3-(*N,N*-trimethylammoniumethylsulfanyl) zinc(II) phthalocyanine diiodide (26). ^1H NMR (DMSO- d_6): δ 9.34-9.44 (m, 8 H, Ar-H), 8.21-8.31 (m, 6 H, Ar-H), 4.05 (t, $J = 6.0$ Hz, 4 H, S-CH₂), 3.89 (t, $J = 6.0$ Hz, 4 H, N-CH₂), 3.38 (s, 18 H, N-CH₃). $^{13}\text{C}\{^1\text{H}\}$ NMR (DMSO- d_6): δ 153.2 151.4 (C-N); 138.1, 136.1 (CH); 130.0 (C, two overlapping signals); 122.7 (CH), 121.6 (C-S), 63.6 (CH₂-S), 52.8 (CH₃-N), 25.7 (CH₂-N). UV-Vis (DMF): λ_{max} (log ϵ) = 352 (4.76), 611 (4.51), 681 (5.28) nm. Fluorescence quantum yield: $\Phi_f = 0.25$. Singlet oxygen quantum yield: $\Phi_\Delta = 0.26$. Elemental analysis calcd (%) for C₄₂H₄₀N₁₀S₂I₂Zn·3H₂O: C 44.95, H 4.14, N 12.48, S 5.72, I 22.61, Zn 5.83; found: C 44.76, H 3.64, N 12.78, S 6.03.

Characterization of 2,3-(*N,N*-dimethylpentylammoniumethylsulfanyl)

zinc(II) phthalocyanine diiodide (27). ^1H NMR (DMSO- d_6): δ 9.35-9.43 (m, 8 H, Ar-H), 8.27-8.30 (m, 6 H, Ar-H), 4.05 (t, $J = 4.8$ Hz, 4 H, S-CH₂), 3.85 (t, $J = 4.5$ Hz, 4 H, N-CH₂), 3.52 (t, $J = 4.5$ Hz, 4 H, N-CH₂), 3.32 (s, 12 H, N-CH₃), 1.70-1.86 (m, 4 H, -CH₂), 1.20-1.52 (m, 8 H, -CH₂-CH₂), 0.74 (t, $J = 6.9$ Hz, 6 H, -CH₃). $^{13}\text{C}\{^1\text{H}\}$ NMR (DMSO- d_6): δ 152.9, 151.0 (C-N); 138.0, 136.1 (CH); 129.7 (C, two overlapping signals), 122.6 (CH), 121.7 (C-S), 63.5 (CH₂-S), 61.7 (CH₂ of pentyl group), 50.5 (CH₃ of pentyl group), 28.2 (CH₂ of pentyl group), 25.7 (CH₂-N), 21.9 (CH₂ of pentyl, two overlapping signals), 13.9 (CH₃-N). UV-Vis (DMF): λ_{max} (log ϵ) = 349 (4.70), 610 (4.47), 682 (5.24) nm. Fluorescence quantum yield: $\Phi_f = 0.26$. Singlet oxygen quantum yield: $\Phi_\Delta = 0.29$.

***In vitro* studies.** Phthalocyanines **23-27** were first dissolved in DMF (1.5 mM) and the solutions were diluted to 80 μM with a *ca.* 0.01 M aqueous solution of Cremophor EL (Sigma, 0.47 g in 100 mL of H₂O). The solutions were filtered with a 0.45 μM filter, then diluted with the medium to appropriate concentrations.

The human hepatocarcinome HepG2 were maintained in RPMI medium 1640 (Invitrogen) supplemented with 10 % fetal calf serum (Invitrogen). The HT29 human colon carcinoma cells (from ATCC) were maintained in Dulbecco's modified Eagle's medium (DMEM) (Invitrogen, cat no. 10313-021) supplemented with fetal calf serum (10 %), penicillin-streptomycin (100 units/mL and 100 g/mL, respectively), L-glutamine (2 mM) and transferrin (10 g/mL). The T84 cells (also

from ATCC) were grown in DMEM/F-12 supplemented with fetal calf serum (10 %) and penicillin-streptomycin (100 units/mL and 100 g/mL, respectively). About 2×10^4 (for HepG2), 3×10^4 (for HT29) or 4×10^4 (for T84) cells per well in these media were inoculated in 96-multiwell plates and incubated overnight at 37 °C in a humidified 5 % CO₂ atmosphere.

The cells were rinsed with PBS and incubated with the above phthalocyanine solutions (100 µL) for 2 h under the same conditions. The cells were then rinsed again with PBS and re-fed with the growth medium (100 µL) before being illuminated at ambient temperature. The light source consisted of a 300 W halogen lamp, a water tank for cooling, and a color glass filter (Newport) cut-on 610 nm. The fluence rate ($\lambda > 610$ nm) was 40 mW cm⁻². An illumination of 20 min led to a total fluence of 48 J cm⁻².

Cell viability was determined by means of the colorimetric MTT assay.¹¹ After illumination, the cells were incubated at 37 °C under 5 % CO₂ overnight. An MTT (Sigma) solution in PBS (50 µL, 3 mg mL⁻¹) was added to each well followed by incubation for 2 h under the same environment. A solution of sodium dodecyl sulfate (Sigma) in 0.04 M HCl (aq) (50 µL, 10 % by weight) was then added to each well. The plate was incubated in a 60 °C oven for 30 min, then *iso*-propanol (80 µL) was added to each well. The plate was agitated on a Bio-Rad microplate reader at ambient temperature for 20 s before the absorbance at 540 nm at each well was taken. The average absorbance of the blank wells, which did not contain the cells, was subtracted from the readings of the other

wells. The cell viability was then determined by the equation: Cell Viability (%) = $[\sum(A_i/A_{\text{control}} \times 100)]/n$, where A_i is the absorbance of the i th data ($i = 1, 2, \dots, n$), A_{control} is the average absorbance of the control wells, in which the phthalocyanine was absent, and n (= 1 or 3) is the number of the data points.

3.6 References

1. (a) Berg, K.; Bommer, J. C.; Winkelman, J. W.; Moan, J. *Photochem. Photobiol.* **1990**, *52*, 775. (b) Boyle, R. W.; Dolphin, D. *Photochem. Photobiol.* **1996**, *64*, 469. (c) MacDonald, I. J.; Morgan, J.; Bellnier, D. A.; Paszkiewicz, G. M.; Whitaker, J. E.; Litchfield, D. J.; et al. *Photochem. Photobiol.* **1999**, *70*, 789.
2. Ball, D. J.; Mayhew, S.; Wood, S. R.; Griffiths, J.; Vernon, D. I.; Brown, S. B. *Photochem. Photobiol.* **1999**, *69*, 390.
3. Wood, S. R.; Brown, S. B. *Proc. SPIE Int. Soc. Opt. Eng.* **1995**, 2625.
4. (a) Verlhac, J. B.; Gaudemer, A.; Kraljic, I. *Nouv. J. Chim.* **1984**, *8*, 401. (b) Wöhrle, D.; Iskandar, N.; Grashew, G.; Sinn, H.; Friedrich, E. A.; Maier-Borst, W.; Stern, J.; Schlag, P. *Photochem. Photobiol.* **1990**, *51*, 351. (c) Villanueva, A.; Jori, G. *Cancer Lett.* **1993**, *73*, 59. (d) Villanueva, A. *Photochem. Photobiol. B Biol.* **1993**, *18*, 295.
5. MacDonald, I. J.; Dougherty, T. J. *J. Porphyrins Phthalocyanines* **2001**, *5*, 105-129.
6. Gürsoy, S.; Cihan, A.; Koçak, M. B.; Bekaroğlu, Ö. *Monatshefte für*

- Chemie* **2001**, *132*, 813-819.
7. (a) Plater, M. J.; Jeremiah, A.; Bourhill, G. *J. Chem. Soc., Perkin Trans.* **2002**, *1*, 91. (b) Kernag, C. A.; McGrath, D. V. *Chem. Commun.* **2003**, 1048.
8. Daraio, M. E.; Völker, A.; Aramendía, P. F.; San Román, E. *Langmuir*, **1996**, *12*, 2932.
9. Ahsen, V.; Yilmazer, E.; Ertaş, M.; Bekaroğlu, Ö. *J. Chem. Soc. Dalton Trans.* **1988**, 401.
10. Spiller, W.; Kliesch, H.; Wöhrle, D.; Hackbarth, S.; Röder, B.; Schnurpfeil, G. *J. Porphyrin Phthalocyanines*, **1998**, *2*, 145.
11. MTT = 3-(4,5-dimethyl-2-thiazolyl)-2,5-diphenyl-2*H*-tetrazolium bromide. Tada, H.; Shiho, O.; Kuroshima, K.; Koyama, M.; Tsukamoto, K. *J. Immunol. Methods* **1986**, *93*, 157.

CUHK Libraries



004279278